

# The *Spitzer* Local Volume Legacy Survey: Infrared Imaging and Photometry for 258 Nearby Galaxies

D.A. Dale<sup>1</sup>, S.A. Cohen<sup>1</sup>, L.C. Johnson<sup>1</sup>, M.D. Schuster<sup>1</sup>, M. Block<sup>2</sup>, C.W. Engelbracht<sup>2</sup>,  
A. Begum<sup>3</sup>, D. Calzetti<sup>4</sup>, J.J. Dalcanton<sup>5</sup>, J.G. Funes<sup>6</sup>, A. Gil de Paz<sup>7</sup>, K.D. Gordon<sup>8</sup>,  
B.D. Johnson<sup>9</sup>, R.C. Kennicutt<sup>3,2</sup>, J.C. Lee<sup>10</sup>, S. Sakai<sup>11</sup>, E.D. Skillman<sup>12</sup>, L. van Zee<sup>13</sup>,  
F. Walter<sup>14</sup>, D.R. Weisz<sup>12</sup>, B. Williams<sup>5</sup>, S.-Y. Wu<sup>4</sup>, Y. Wu<sup>15</sup>

## ABSTRACT

The project description and near-, mid-, and far-infrared flux properties are presented for the Local Volume Legacy survey, a *Spitzer Space Telescope* legacy program built upon a foundation of *GALEX* ultraviolet and ground-based H $\alpha$  imaging of 258 galaxies within 11 Mpc. The Local Volume Legacy survey covers an unbiased, representative, and statistically robust sample of nearby star-forming galaxies, exploiting the highest extragalactic spatial resolution achievable with *Spitzer*. As a result of its approximately volume-limited nature, LVL augments previous *Spitzer* observations of present-day galaxies (such as from SINGS, the *Spitzer* Infrared Nearby Galaxies Survey) with improved sampling of the low-luminosity dwarf galaxy population. The collection of LVL galaxies shows a large spread in mid-infrared colors, likely due to the conspicuous deficiency of PAH emission from low-metallicity galaxies. Conversely, the far-infrared tightly tracks the total infrared, with a dispersion in their flux ratio of order 0.1 dex.

---

<sup>1</sup>Department of Physics and Astronomy, University of Wyoming, Laramie, WY 82071; ddale@uwyo.edu

<sup>2</sup>Steward Observatory, University of Arizona, Tucson, AZ 85721

<sup>3</sup>Institute of Astronomy, University of Cambridge, Cambridge CB3 0HA, United Kingdom

<sup>4</sup>Astronomy Department, University of Massachusetts, Amherst, MA 01003

<sup>5</sup>Department of Astronomy, University of Washington, Seattle, WA 98195

<sup>6</sup>Vatican Observatory Research Group, Steward Observatory, University of Arizona, Tucson, AZ 85721

<sup>7</sup>Departamento de Astrofísica, Universidad Complutense, Madrid, E-28040, Spain

<sup>8</sup>Space Telescope Science Institute, 3700 San Martin Drive, Baltimore, MD 21218

<sup>9</sup>Department of Astronomy, Columbia University, New York, NY 10027

<sup>10</sup>Carnegie Observatories, 813 Santa Barbara Street, Pasadena, CA 91101

<sup>11</sup>Division of Astronomy and Astrophysics, University of California, Los Angeles, CA 90095

<sup>12</sup>Astronomy Department, University of Minnesota, Minneapolis, MN 55455

<sup>13</sup>Department of Astronomy, Indiana University, Bloomington, IN 47405

<sup>14</sup>Max Planck Institut für Astronomie, Königstuhl 17, 69117 Heidelberg, Germany

<sup>15</sup>Astronomy Department, Cornell University, Ithaca, NY 14853

In terms of the relation between infrared-to-ultraviolet ratio and ultraviolet spectral slope, the LVL sample is shifted to redder colors than the standard correlation for starburst galaxies. Theoretical models suggest that the amplitude of deviations from the starburst relation corresponds to the age of the stellar populations that dominate the ultraviolet/optical luminosities.

*Subject headings:* surveys — galaxies: photometry — infrared: galaxies

## 1. Introduction

The goal of the *Spitzer* Local Volume Legacy (LVL) survey<sup>1</sup> is to fill a vital niche in existing multi-wavelength surveys of present-day galaxies with a statistically robust, approximately volume-complete study of our nearest star-forming neighbors. Although star formation rates based on *GALEX*, *Spitzer*, and ground-based data are being collected for thousands of galaxies (and hundreds of thousands via the Sloan Digital Sky Survey), most of these datasets are derived from flux-limited samples, and thus suffer from the well-known biases against low-mass, low surface brightness systems. Multi-wavelength datasets that include such systems (e.g., SINGS (Kennicutt et al. 2003) and LITTLE THINGS (Hunter et al. 2009)) only provide representative samplings of the overall galaxy population, and are thus not suitable for studies that demand datasets which are true to the statistics rendered by volume-limited sampling.

We have chosen to directly address this problem by completing *Spitzer* infrared imaging for a tiered sample of 258 galaxies which consolidates the strengths of two existing volume-limited surveys. ANGST, the ACS Nearby Galaxies Survey Treasury (Dalcanton et al. 2007), includes all 69 known galaxies outside the Local Group within 3.5 Mpc and with  $|b| > 20^\circ$ , plus an extension to the M 81 group. ANGST augments existing deep HST imaging with new observations to provide complete stellar photometry with homogeneous depth. 11HUGS, the 11 Mpc H $\alpha$  and Ultraviolet Galaxy Survey, provides *GALEX* ultraviolet (Lee et al. 2009) and ground-based H $\alpha$  imaging (Kennicutt et al. 2008) of all known star-forming galaxies within 11 Mpc,  $m_B < 15.5$  mag and  $|b| > 30^\circ$ . These limits were selected to include a large enough volume to probe a diverse cross-section of morphologies and star formation properties (e.g., Lee et al. 2007), but still ensure completeness in the parent galaxy catalogs from which the sample was drawn. Statistical tests and comparison with blind all-sky H I surveys show that the catalog completeness is excellent ( $>95\%$ ) within these limits (Lee et al. 2009). The conjoined surveys are highly complementary. ANGST provides complete coverage within its volume, including all galaxy morphologies and the lowest mass galaxies. Conversely, 11HUGS covers a 30 times larger volume, and therefore offers a broader coverage of the star-forming galaxy population as a whole, including a 10 magnitude range in optical luminosity, a  $10^5$  range in star formation rates, and a 2 dex span in metallicity.

---

<sup>1</sup><http://www.ast.cam.ac.uk/IOA/research/lvls>

Thus, LVL provides the most complete census to date of dust and recent star formation in the Local Volume. The data include (i)  $H\alpha$  emission, which traces massive O star formation, (ii) ultraviolet emission, which traces O as well as longer-lived B stars, and (iii) infrared emission, which constrains how much of the energy produced by stars is absorbed and re-radiated by dust. This redundancy of star formation rate tracers provides not only robust, extinction-corrected star formation rates for an approximately volume-limited sample, it also constrains the temporal behavior of bursty star formation since the ultraviolet and  $H\alpha$  emission probe activity over timescales (of  $\sim 100$  Myr and  $< 5 - 10$  Myr, respectively) which flank the expected duration of starburst episodes. Crucial constraints on the old stellar population content of the galaxies can also be provided by mid-infrared luminosities. Public data releases of our multi-wavelength imaging have begun through the NASA/IPAC Infrared Science Archive<sup>2</sup> (IRSA), with expected completion of data product deliveries by the end of 2009.

Principal science issues to be addressed by the LVL team include: constraining the physical mechanisms underlying dust heating and understanding correlations between infrared emission, dust content and global galaxy properties; establishing the primary factors which influence polycyclic aromatic hydrocarbon (PAH) emission and evaluating the robustness of PAH emission as a star formation rate indicator, particularly at low metallicities and high specific star formation rates; and probing the temporal variation of star formation as a function of global properties, with special focus on the dwarf galaxy population that dominates the sample. In this paper, we present 2MASS near-infrared and *Spitzer* mid- and far-infrared flux densities for the LVL sample, which will form the basis for many of the analyses presented in subsequent papers. Section 2 describes the sample, Section 3 reviews the observational and data processing programs, Section 4 covers details of the integrated aperture photometry, Section 5 presents initial results based on the photometry, and Section 6 summarizes our work.

## 2. The Sample

As described above, the Local Volume Legacy sample is a compilation of 258 galaxies, which includes (i) galaxies from the ANGST program—69 known galaxies outside the Local Group with  $D < 3.5$  Mpc and  $|b| > 20^\circ$ , plus an extension to the M 81 group, and (ii) galaxies in the 11HUGS sample—an unbiased set of  $m_B < 15.5$  mag S-Irr galaxies from the larger, and more representative, 11 Mpc volume which is visible above the Galactic Plane ( $|b| > 30^\circ$ ). These limits define the ranges over which the parent samples are known to be relatively complete, and the selection of galaxies leverages LVL’s new *Spitzer* observations on already-available multi-wavelength imaging. A schematic illustration of LVL’s tiered volume coverage is shown in Figure 1.

The LVL sample, along with some general properties, are given in Table 1. Approximately

---

<sup>2</sup><http://ssc.spitzer.caltech.edu/legacy/lvlhistory.html>

half (53%) of the LVL galaxies have spiral morphology, 38% are irregulars, 8% are S0 galaxies, and there is a single elliptical (Figure 2). For comparison, SINGS has larger fractions of non-spiral morphologies, with 63% spiral, 17% irregular, 12% S0, and 8% elliptical morphologies. Since the origination of this project, four LVL galaxies have new distances which place them outside of 11 Mpc: UGC 00521, UGC 06782, IC 2049, and UGC 7321. Though the observations for these four systems are presented here, these galaxies will not be included in future, LVL sample-wide studies. This is an inherent difficulty with efforts to construct a volume-limited sample. The membership of the sample will be necessarily fluid until accurate distance and photometric measurements are available for all of the galaxies that are within the volume and around its periphery.

### 3. Observational Strategy and Data Processing

#### 3.1. New *Spitzer* IRAC 3.6, 4.5, 5.8, and 8.0 $\mu\text{m}$ Data

New *Spitzer* IRAC (Fazio et al. 2004) observations were obtained for 180 LVL galaxies. The IRAC observing strategy follows that of SINGS, which shows that stellar and small grain dust emission is typically detected out to the optical radius at a surface brightness level of  $\sim 0.01\text{--}0.1 \text{ MJy sr}^{-1}$  (Regan et al. 2006; Dale et al 2000). For galaxies smaller than the IRAC field of view ( $D_{25} \leq 300''$ ) the Astronomical Observing Requests (AORs) were constructed using four dithered 30 s integrations. For larger galaxies a mosaicking strategy with  $\sim$ half-array spatial offsets was used, with the sizes of the mosaic ‘cores’ tailored to the optical size of each galaxy. Two sets of IRAC maps were obtained for each source to enable asteroid removal and to enhance map sensitivity and redundancy. Combining all eight 30 s frames thus results in a net integration per pixel of 240 s (and 120 s around the  $\sim 2\text{!}5$ -wide mosaic peripheries). Since each source was observed in all IRAC channels, ample sky coverage is automatically provided by the non-overlapping nature of the two IRAC imagers.

The BCD data used for post-pipeline processing are from the S18 pipeline version (*should be true by submission time!*). The multi-epoch, multiple-pointing IRAC observations for each galaxy are combined into one single mosaic for each band using the MOPEX mosaicking software. Additional post-BCD processing includes: distortion corrections, rotation of the individual frames (for multi-epoch observations), bias structure and bias drift corrections, image offset determinations via pointing refinements from the SSC pipeline (MOPEX’s default), detector artifact removal, constant-level background subtraction, and image resampling to  $0\text{!}75$  pixels using drizzling techniques. The drizzling slightly improves the final PSF over the native one; the full-width half maxima are  $\sim 1\text{!}6$  in the shorter wavelength channels and  $\sim 1\text{!}9$  at  $8 \mu\text{m}$ . The final images are in units of  $\text{MJy sr}^{-1}$  and have the average sky level removed; sky values are estimated via several “blank” regions located near but beyond the target galaxy emission.

In cases where exceptionally bright target sources saturated or entered the non-linear regime of the detector during the 30 second exposure, additional 1.2 s images are used to allow for recovery

of this data. Pixels affected by these issues, typically in the 5.8 and 8.0  $\mu\text{m}$  frames, are flagged by MOPEX during processing. Correction begins by creating a mosaic of the 1.2 s exposures interpolated onto the same pixel grid as the original mosaic. A difference image is then created from the two mosaics and any residual, systematic difference in the background sky levels is removed. Pixels in the difference image valued at 1 MJy  $\text{sr}^{-1}$  or higher are flagged (routinely regions of  $\sim 400$  contiguous pixels) and these pixels in the long integration mosaic are replaced by their short integration counterparts. The nuclear regions for the following galaxies were affected by saturation: NGC 0253, NGC 2903, NGC 3031, NGC 3034 (at all IRAC wavelengths), NGC 3351, NGC 3593, NGC 3627, NGC 4258, NGC 5195, and NGC 5253.

### 3.2. New *Spitzer* MIPS 24, 70, and 160 $\mu\text{m}$ Data

New *Spitzer* MIPS (Rieke et al. 2004) observations were obtained for 201 LVL galaxies. Galaxies were imaged in all three MIPS bands centered at 24, 70, and 160  $\mu\text{m}$ , using the highly successful scan mapping strategy employed in the SINGS project. The scan mode was used even on galaxies small enough to fit within the array field of view, because achieving adequate background measurements for extended targets in photometry mode is less efficient than the scan mode. Each map was executed at the medium scan rate, and includes multiple scan legs tailored to the size of the galaxy and half-array offsets between scan legs. Each galaxy was mapped twice, with the maps separated by 10-40 days to allow time for asteroids to move out of the field. This second map was performed in the reverse direction (the “backward mapping” mode), with offsets in the cross-scan and in-scan directions. Taken together, these mapping strategies ensure that each point on the galaxy is scanned over in two different directions, which aids reduction of array artifacts on both Si:As and Ge:Ga arrays. The in-scan offset ensures that Ge:Ga stimflashes do not occur at the same point in both maps and thereby improves the calibration. The integration time per point is 160, 80, and 16 s at 24, 70, and 160  $\mu\text{m}$ , respectively.

The pixel scale of the MIPS mosaics is wavelength-dependent:  $1''.5$ ,  $4''.5$ , and  $9''.0$  at 24, 70, and 160  $\mu\text{m}$ , respectively. The MIPS images are processed with the MIPS Data Analysis Tool (DAT; Gordon et al. 2005), supplemented by custom scripts for the specific data reduction and mosaicking of extended sources. The latter include: at 24  $\mu\text{m}$ , readout offset correction, array-averaged background subtraction, and exclusion of the first five images in each scan leg due to boost frame transients. At 70 and 160  $\mu\text{m}$ , the custom scripts include a pixel-dependent background subtraction for each map to remove residual detector drifts and background cirrus and zodiacal emission. This method of reduction was used for all the SINGS galaxies as well as very large MIPS/GTO galaxies (M 31, M 33, M 101, etc.).

Finally, a correction for 70  $\mu\text{m}$  non-linearity effects is included in the data processing. A correction of the form

$$f_{\text{true}}^{70\mu\text{m}} = 0.581(f_{\text{measured}}^{70\mu\text{m}})^{1.13}, \quad (1)$$

derived from data presented by Gordon et al. (2008, in preparation), is applied to pixel values above a threshold of  $\sim 66 \text{ MJy sr}^{-1}$ . A small fraction of the pixels in a total of 40 LVL  $70 \mu\text{m}$  images require such a correction. The median correction to the global  $70 \mu\text{m}$  flux density for these 40 galaxies is only a few percent.

### 3.3. Archival *Spitzer* Data

Archival IRAC and MIPS data, with spatial coverage and sensitivity similar to or greater than that described in § 3.1 and § 3.2, are utilized for 78 (IRAC) and 57 (MIPS) galaxies. No new IRAC or MIPS observations were obtained for these subsets of the LVL sample. The data processing procedures for the archival data are the same as those followed for the new observations described above. Table 2 indicates for which galaxies we utilize archival *Spitzer* data.

## 4. Aperture Photometry

Table 2 presents the global flux densities for the entire LVL sample, for wavelengths spanning the near- to far-infrared. The data are corrected for Galactic extinction (Schlegel, Finkbeiner, & Davis 1998) assuming  $A_V/E(B - V) \approx 3.1$  and the reddening curve of Li & Draine (2001). The effect of airmass has been removed from the ground-based near-infrared fluxes. Below follows a description of the infrared data collected for the LVL program.

### 4.1. 2MASS Near-Infrared JHK<sub>s</sub> Photometry

The Two Micron All Sky Survey (2MASS) obtained data for the entire sky at 1.25, 1.65, and  $2.17 \mu\text{m}$  using two automated, ground-based 1.3 m telescopes (Skrutskie et al. 2006). Galaxy photometry is available from the 2MASS Extended Source Catalog for over a million galaxies and from the 2MASS Large Galaxy Atlas for several hundred galaxies larger than  $1'$  (Jarrett et al. 2003). Integrated fluxes for several LVL galaxies were adopted from the Large Galaxy Atlas, and these are generally consistent with expectations based on IRAC 3.6 and  $4.5 \mu\text{m}$  fluxes and simple stellar model extrapolations to 2MASS wavelengths. However, most LVL galaxies do not appear in the Large Galaxy Atlas, and for these systems many of the fluxes from the Extended Source Catalog are 0.5–2 mag low based on similar extrapolations from IRAC 3.5 and  $4.5 \mu\text{m}$  data. We find that when Extended Source Catalog fluxes appear unexpectedly faint, it is typically due to the comparatively small apertures used in the automated 2MASS extraction. Hence we have extracted 2MASS fluxes for the vast majority of the LVL sample using the same apertures and foreground star removals used to determine IRAC and MIPS fluxes, as discussed in the following section. Based on deep *H* band imaging of nearby galaxies with the 3.9 m Anglo-Australian Telescope, Kirby et al. (2008) likewise find that Extended Source Catalog extractions are 0.5–2 mag too faint.

## 4.2. *Spitzer* 3.6, 4.5, 5.8, 8.0, 24, 70, and 160 $\mu\text{m}$ Photometry

### 4.2.1. Foreground Star and Background Galaxy Removal

The presence of foreground stars and background galaxies can significantly affect the global infrared fluxes for some galaxies, particularly the fainter dwarfs and galaxies at low Galactic latitudes. Once identified, the foreground stars and background galaxies are removed through a simple interpolation of the local sky from the images using the IRAF task `IMEDIT`. Our procedure for identifying these sources relies on a multi-wavelength analysis (3.6, 8.0, 24  $\mu\text{m}$ , and  $\text{H}\alpha$ ), looking for objects  $\text{H}\alpha$ -rich or especially blue (foreground stars;  $f_\nu(3.6)/f_\nu(8.0) > 8$ ), or small red systems with galaxy-like morphologies. Archival *Hubble Space Telescope* imaging was also inspected for obvious background galaxy or foreground stellar identifications, when available. When uncertain about the identification of a particular source, we opted to err on the conservative side and allow such sources to remain in the global flux extraction. However, these sources of uncertain origin are typically very faint and negligibly impact global flux extractions. The median ratios of edited-to-unedited fluxes is [0.854, 0.846, 0.939, 0.971, 0.980, 1.00, 1.00] at [3.6, 4.5, 5.8, 8.0, 24, 70, 160]  $\mu\text{m}$ ; very few significant corrections are made at 24, 70, and 160  $\mu\text{m}$ .

The uncertainties provided in Table 2 include both calibration and statistical uncertainties. Calibration uncertainties are 5-10% for IRAC 3.6 and 4.5  $\mu\text{m}$  data, and 10-15% for IRAC 5.8 and 8.0  $\mu\text{m}$  data; 10% IRAC calibration uncertainties are used in Table 2. MIPS calibration uncertainties are 4%, 7%, and 12% respectively at 24, 70, and 160  $\mu\text{m}$ .

### 4.2.2. Aperture Corrections

For a given galaxy, the same aperture was used for extracting all IRAC and MIPS fluxes. Elliptical apertures for IRAC and MIPS photometry were based on capturing all the galaxy emission visible for all IRAC and MIPS images. Typically this means that the 3.6  $\mu\text{m}$  image was used to create the aperture, since *Spitzer* is most sensitive at 3.6  $\mu\text{m}$  and that is the *Spitzer* wavelength at which stars are brightest.

Since the IRAC flux calibration is based on point source photometry for a 12'' radius aperture, the fluxes for all extended sources and aperture radii  $\neq 12''$  need to have an additional correction applied. These corrections account for the “extended” emission due to the wings of the PSF and also for the scattering of the diffuse emission across the IRAC focal plane. As described in Dale et al. (2007), the IRAC extended source correction has been derived for a variety of source morphologies and extents. For an effective aperture radius  $r = \sqrt{ab}$  in arcseconds derived from the semi-major  $a$  and semi-minor  $b$  ellipse axes provided in Table 2, the IRAC extended source aperture correction is

$$f_{\text{true}}^{\text{IRAC}} / f_{\text{measured}}^{\text{IRAC}} = Ae^{-r^B} + C, \quad (2)$$

where  $A$ ,  $B$ , and  $C$  are listed in Table 3<sup>3</sup>. The median IRAC extended source aperture corrections are [0.914,0.941,0.826,0.756] at [3.6,4.5,5.8,8.0]  $\mu\text{m}$ .

Somewhat different from the situation for IRAC imaging, the main reason MIPS aperture corrections are needed is due to the smearing of light outside the aperture. MIPS aperture corrections are empirically determined from a comparison of fluxes from smoothed and unsmoothed 3.6  $\mu\text{m}$  imaging, an approximate proxy for tracing the MIPS galaxy morphologies. The aperture correction for a given MIPS flux is the ratio of the fluxes from the unsmoothed 3.6  $\mu\text{m}$  image to the flux from the 3.6  $\mu\text{m}$  image smoothed to the same PSF as the MIPS image in question. The median MIPS aperture corrections are [1.01,1.01,1.03,] at [24,70,160]  $\mu\text{m}$ , and the most significant corrections are [1.09,1.12,1.42] for CGCG 269-049.

### 4.3. Upper Limits

Many of the optically-faint galaxies in the sample are frequently undetected in the infrared, particularly at wavelengths of 5.8  $\mu\text{m}$  and longer. Upper limits are included in Table 2 for sources undetected by infrared imaging. The  $3\sigma$  upper limits for *Spitzer* imaging are derived according to

$$f_\nu(3\sigma \text{ upper limit}) = 3 \sigma_{\text{sky}} \Omega_{\text{pix}} \sqrt{N_{\text{pix}} + N_{\text{pix}}^2 / N_{\text{sky}}} \approx 3 \sigma_{\text{sky}} \Omega_{\text{pix}} \sqrt{2N_{\text{pix}}} \quad (3)$$

where  $\sigma_{\text{sky}}$  is the sky surface brightness fluctuation per pixel ( $\text{MJy sr}^{-1}$ ),  $\Omega_{\text{pix}}$  the solid angle subtended per pixel,  $N_{\text{pix}}$  the number of pixels in the galaxy aperture, and  $N_{\text{sky}}$  the number of pixels in the sky aperture. The parameter  $\sigma_{\text{sky}}$  is approximately 0.02, 0.03, 0.11, 0.12, 0.2, 0.9, 1.7  $\text{MJy sr}^{-1}$  at 3.6, 4.5, 5.8, 8.0, 24, 70, and 160  $\mu\text{m}$ , respectively (Lee et al. 2009). A similar computation for 2MASS near-infrared upper limits is carried out after converting that survey’s mean  $10\sigma$  point source sensitivities ( $\sim 16.4$ , 15.5, and 14.8 mag for  $J$ ,  $H$ , and  $K_s$ , respectively; Skrutskie et al. 2006) to  $3\sigma$  values and accounting for the difference in the  $4''$  radius 2MASS point source aperture and the LVL galaxy apertures.

## 5. Results

### 5.1. Detection Rate

The bottom panel of Figure 3 displays the detection rate as a function of  $B$  band apparent magnitude for the different *Spitzer* imaging channels. Nearly all galaxies are detected at all *Spitzer* wavelengths down to  $m_B \approx 14$  mag. Consistent with our pre-survey expectations, the  $m_B \sim 15.5$  mag cut-off for the outer tier of the sample that extends to 11 Mpc (see § 2) proved to be a useful sample selection criterion, as very few MIPS detections are available fainter than this

---

<sup>3</sup>See <http://ssc.spitzer.caltech.edu/irac/calib/extcal/>



magnitude limit. The inner tier/ANGST portion of the sample extends the sample to much fainter levels, as faint as  $m_B \approx 19$  mag in the cases of BK03N and M 81 Dwarf A. As expected for the optically-faint galaxies, the highest detection rates are found for the stellar-dominated 3.6 and 4.5  $\mu\text{m}$  channels, while the 70 and 160  $\mu\text{m}$  imaging proved to be far more challenging to convincingly detect cold dust emission.

## 5.2. Multi-Wavelength Spectral Energy Distributions

Figure 4 provides the ultraviolet-infrared spectral energy distributions for all 258 galaxies. The ultraviolet data are from Lee et al. (2009). The solid curve is the sum of a dust (dashed) and a stellar (dotted) model. The dust curve is a Dale & Helou (2002) model (least squares) fitted to ratios of the observed 24, 70, and 160  $\mu\text{m}$  fluxes, and then scaled to match the overall infrared brightness. The  $\alpha_{\text{SED}}$  listed within each panel parametrizes the distribution of dust mass as a function of heating intensity, as described in Dale & Helou (2002). To quantify the uncertainty on  $\alpha_{\text{SED}}$  displayed within each panel of Figure 4, 1,000 Monte Carlo simulations of the fit to each galaxy’s far-infrared fluxes are performed, utilizing the tabulated flux uncertainties to add a random (Gaussian deviate) flux offset at each MIPS wavelength. The  $\alpha_{\text{SED}}$  uncertainties reflect the standard deviations in the simulations. The stellar curve is a 1 Gyr continuous star formation, solar metallicity curve from Vazquez & Leitherer (2005) fitted to the 2MASS data. The initial mass function for this curve utilizes a double power law form, with  $\alpha_{1,\text{IMF}} = 1.3$  for  $0.1 < m/M_\odot < 0.5$  and  $\alpha_{2,\text{IMF}} = 2.3$  for  $0.5 < m/M_\odot < 100$  (e.g., Kroupa 2002). Though this stellar curve is not adjusted for internal extinction and may not be applicable to many galaxies, it is included as a “standard” reference against which deviations in the ultraviolet can be compared from galaxy to galaxy.

The spectral energy distributions for the LVL sample range widely. There are stellar-dominated (NGC 0404, UGC 05373, UGCA 0193) and comparatively dusty (IC 5256, NGC 6503) systems; for sources detected by MIPS, the infrared-to-far-ultraviolet ratio in the sample spans more than three orders of magnitude, from 0.1 to over 100 (§ 5.4). There are galaxies with far-infrared spectral energy distributions indicative of warm (UGCA 0281) and cold dust grains (NGC 5055). Compared to what would be expected based on their stellar and far-infrared emission, many galaxies show a dearth of emission from PAHs in the 8.0  $\mu\text{m}$  band (e.g., ESO 245-G005, UGC 01249, UGC 05272). The variations in global spectral energy distributions are discussed in more detail below.

## 5.3. Infrared Colors

The IRAC-MIPS infrared colors for the LVL sample are displayed in Panel a of Figure 5. The  $f_\nu(70\mu\text{m})/f_\nu(160\mu\text{m})$  ratio typically traces the temperature of large interstellar grains, while the  $f_\nu(8.0\mu\text{m})/f_\nu(24\mu\text{m})$  ratio has several influences. The flux at 24  $\mu\text{m}$  mostly represents emission from

very small grains (grains with effective radii of 15–40 Å; Draine & Li 2007), and the flux at 8.0  $\mu\text{m}$  can have contributions from stars, hot dust, PAHs, and AGN. Perhaps due to the diversity of emission mechanisms responsible for 8.0 and 24  $\mu\text{m}$  flux levels, the  $f_\nu(8.0\mu\text{m})/f_\nu(24\mu\text{m})$  ratio spans two orders of magnitude compared to the single factor of  $\sim 10$  stretch in the the  $f_\nu(70\mu\text{m})/f_\nu(160\mu\text{m})$  ratio. Since the LVL sample largely lacks “strong” AGN, loosely defined here as AGN that dominate a galaxy’s emission over substantial portions of the electromagnetic spectrum, it is unlikely that AGN contribute much to the scatter in Figure 5.

The far-infrared or total infrared, respectively commonly defined as the emission from 42–122  $\mu\text{m}$  (*FIR*) and 8–1000  $\mu\text{m}$  or 3–1100  $\mu\text{m}$  (*TIR*; Dale & Helou 2002), are frequently used as indications of the star formation rate in galaxies (Kennicutt 1998; Bell 2003). However, in many instances the far-infrared continuum is unavailable or not detected, so monochromatic infrared proxies for (*FIR*) or (*TIR*) are occasionally employed (e.g., Papovich & Bell 2002; Bavouzet et al. 2008). Hence, the tightness (dispersion) in monochromatic-to-bolometric ratios are of general interest. Five flavors of these ratios are displayed in the remaining panels of Figure 5, and a tabulation of median LVL infrared colors and monochromatic-to-bolometric infrared ratios can be found in Table 4 along with their dispersions. Panel b of Figure 5 shows the distribution of the 8.0  $\mu\text{m}$  emission with respect to the 3–1100  $\mu\text{m}$  total infrared, a distribution which exhibits a dispersion of 0.23 dex, similar to that for  $f_\nu(70\mu\text{m})/f_\nu(160\mu\text{m})$  and  $f_\nu(8.0\mu\text{m})/f_\nu(24\mu\text{m})$ . While it is evident that the LVL sample is distributed fairly evenly by morphology across  $f_\nu(70\mu\text{m})/f_\nu(160\mu\text{m})$  ratios, the bulk of the systems exhibiting relatively low  $f_\nu(8.0\mu\text{m})/f_\nu(24\mu\text{m})$  and  $\nu f_\nu(8.0\mu\text{m})/TIR$  ratios are from late-type spirals and irregulars.

The preponderance of late-type spirals and irregulars showing relatively low 8.0  $\mu\text{m}$  emission is amplified when “dust-only” 8.0  $\mu\text{m}$  emission is considered. Panel c of Figure 5 shows a plot similar to that in Panel b but with the stellar emission removed using the expression presented in Helou et al. (2004):

$$\nu f_\nu(8.0\mu\text{m})_{\text{dust}} = \nu f_\nu(8.0\mu\text{m}) - \eta^{8*} \nu f_\nu(3.6\mu\text{m}) \quad (4)$$

where  $\eta^{8*} = 0.232 \times 3.6/8.0$ . The dispersion (0.44 dex) and overall range are significantly larger when the dust-only 8.0  $\mu\text{m}$  emission is normalized to the total infrared. It is possible that a portion of these increases in dispersion and range are due to the inapplicability of Equation 4 to late-type spirals, but it should be noted that Equation 4 is based on a detailed analysis of NGC 300, a local system with an Sd morphological classification. Another possibility is that the late-type spirals and irregulars within LVL are on average less abundant in heavy metals, and thus either the formation of PAH molecules is starved or the relatively fragile PAHs are photo-dissociated in the hard radiation fields typically associated with low-metallicity environments (Engelbracht et al. 2005; Madden et al 2006; Wu et al. 2006; Dale et al. 2008; Sloan et al. 2008). Additional data and detailed follow-up utilizing LVL metallicities would be required to address this issue.

In contrast to the 8.0  $\mu\text{m}$ -to-*TIR* measures, the  $\nu f_\nu(24\mu\text{m})/TIR$  ratio (Panel d of Figure 5) shows a range less than an order of magnitude and a dispersion of 0.15 dex; the 70  $\mu\text{m}$ -to-*TIR* and 160  $\mu\text{m}$ -to-*TIR* ratios have even smaller dispersions (Panels e & f and Table 4). The implication

is that, compared to the  $8.0\ \mu\text{m}$  emission from galaxies, the infrared emission from very small grains at  $24\ \mu\text{m}$  and from large grains at  $70$  and  $160\ \mu\text{m}$  are far more tightly coupled to the bolometric infrared emission. Such a conclusion may naturally arise from inspection of the global spectral energy distributions in Figure 4, but it is nonetheless important to emphasize the differences between what is being emitted in the mid-infrared versus the far-infrared. This result conceptually follows work by Calzetti et al. (2007) and Kennicutt et al. (2007; 2009), who show that  $24\ \mu\text{m}$  and total infrared fluxes are more effective than  $8.0\ \mu\text{m}$  fluxes at tracing a galaxy’s current star formation rate (they also show that these infrared fluxes correlate even better with star formation, to within  $\sim 0.1$  dex, if they are coupled with  $\text{H}\alpha$  to capture the unobscured portion of star formation).

#### 5.4. The Infrared-to-Ultraviolet Ratio and Ultraviolet Spectral Slope

The infrared-to-ultraviolet ratio is a coarse measure of dust extinction in the ultraviolet, and thus should be related to the amount of reddening in ultraviolet spectra. Indeed, starbursting galaxies follow a tight correlation between the ratio of infrared-to-ultraviolet emission and the ultraviolet spectral slope (e.g., Calzetti et al. 1994; Calzetti et al. 1997; Meurer et al. 1999). Compared to the relation defined by starbursts, normal star-forming galaxies are offset to redder ultraviolet spectral slopes, exhibit lower infrared-to-ultraviolet ratios, and show significantly larger scatter (Buat et al. 2002, 2005; Bell 2002; Kong et al. 2004; Gordon et al. 2004; Burgarella et al. 2005; Calzetti et al. 2005; Seibert et al. 2005; Cortese et al. 2006; Boissier et al. 2007; Gil de Paz et al. 2007; Dale et al. 2007). These differences can be accentuated for systems lacking significant current star formation, such as elliptical galaxies, systems for which the luminosity is more dominated by a passively evolving older, redder stellar population. The LVL survey provides a unique population for exploring this relation, as it consists of a large sample of star-forming galaxies, approximately half of which are dwarf/irregular systems.

Figure 6 displays the LVL infrared-to-ultraviolet ratios as a function of the ultraviolet spectral slope. The total infrared is computed from the MIPS  $24$ ,  $70$ , and  $160\ \mu\text{m}$  fluxes (Equation 4 in Dale & Helou 2002), and the ultraviolet data are from *GALEX* (Lee et al. 2009). As expected, the well-known starbursts in the LVL sample lie close to the starburst curve: NGC 0253, NGC 4631, NGC 4449, NGC 1705, and NGC 4736, with the latter formally known as a post-starburst galaxy. Overall, the LVL population is broadly segregated in the infrared-to-ultraviolet ratio according to optical morphology, with Sb and earlier-type galaxies showing relatively high values, Sc/Sd/Sm systems exhibiting intermediate values, and irregulars appearing near the bottom of the diagram. To explore this distribution further, in Figure 7 we plot a version of the “birthrate parameter” as a function of the (perpendicular) distance to the starburst curve in Figure 7. Following Carlos-Muñoz et al. (2009), the ratio of far-ultraviolet-to-near-infrared luminosity is used as a proxy for the ratio of past-to-present star formation, sometimes referred to as the birthrate parameter (see also, for example, Boselli et al. 2001; Cortese et al. 2006). Here the far-ultraviolet emission is corrected for extinction using the infrared-to-ultraviolet-based recipe formulated in Buat et al. (2005).

There is a clear trend, suggesting that a galaxy’s star formation history plays an important role in determining its location within Figure 6. To more directly interpret these deviations from the starburst curve as a function of the age of the stellar population, the righthand axis of Figure 7 is quantified according to the age inferred from theoretical spectra. This comparison is accomplished by convolving *GALEX* far-ultraviolet and *Spitzer* 3.6  $\mu\text{m}$  filter transmission profiles with stellar spectra similar to those described in § 5.2 but for a wide range of ages (1 Myr to 10 Gyr). The ages for the respective simulated spectra are shown along the righthand axis at levels corresponding to the computed theoretical far-ultraviolet-to-near-infrared ratios along the lefthand axis. Assuming these theoretical spectra are broadly applicable to the LVL sample, the star formation timescales range from several million years up to a few billion years, with the oldest star formation episodes corresponding to the largest deviations from the starburst curve.

## 6. Summary

The Local Volume Legacy is a *Spitzer Space Telescope* legacy program built upon a foundation of *GALEX* ultraviolet and ground-based  $\text{H}\alpha$  imaging of 258 galaxies within 11 Mpc, nearly half of which are dwarf/irregulars. The proximity and nearly volume-limited nature of the survey are key aspects, enabling multi-wavelength analyses of star formation with high spatial resolution in a manner that is statistically representative of the nearby galaxy population. First results are reported based on infrared and ultraviolet fluxes. Whereas the far-infrared closely tracks the total-infrared emission, the mid-infrared-to-total-infrared ratios show large dispersions. The large scatter in comparing dust emission at 8.0  $\mu\text{m}$  and total dust emission is likely due to the notable deficiency of PAH emission from the low-metallicity galaxies prevalent in the LVL survey. The LVL sample shows a correlation between infrared-to-ultraviolet ratio and ultraviolet spectral slope, but it is shifted to redder colors than what is seen for starburst galaxies. Theoretical models are utilized to buttress the idea that deviations from the starburst relation correspond to the age of the stellar population.

Support for this work, part of the *Spitzer Space Telescope* Legacy Science Program, was provided by NASA through Contract Number XXX issued by the Jet Propulsion Laboratory, California Institute of Technology under NASA contract 1407. This research has made use of the NASA/IPAC Extragalactic Database which is operated by JPL/Caltech, under contract with NASA. This publication makes use of data products from the Two Micron All Sky Survey, which is a joint project of the University of Massachusetts and the Infrared Processing and Analysis Center/California Institute of Technology, funded by the National Aeronautics and Space Administration and the National Science Foundation. IRAF, the Image Reduction and Analysis Facility, has been developed by the National Optical Astronomy Observatories and the Space Telescope Science Institute. We gratefully acknowledge NASA’s support for construction, operation, and science analysis for the *GALEX* mission, developed in cooperation with the Centre National d’Etudes Spatiales of France

and the Korean Ministry of Science and Technology.

## REFERENCES

- Bavouzet, N., Dole, H., Le Floch, E., Caputi, K.I., Lagache, G., & Kochanek, C.S. 2008, *A&A*, 479, 83
- Bell, E.F. 2002, *ApJ*, 577, 150
- Bell, E.F. 2003, *ApJ*, 586, 794
- Boissier, S. et al. 2007, *ApJS*, 173, 524
- Boselli, A., Gavazzi, G., Donas, J., & Scodeggio, M. 2001, 121, 753
- Buat, V. et al. 2001, *ApJ*, 619, L51
- Buat, V., Boselli, A., Gavazzi, G., & Bonfanti, C. 2002, *A&A*, 383, 801
- Buat, V. et al. 2005, *ApJ*, 619, L51
- Burgarella, D., Buat, V., & Iglesias-Páramo, J. 2005, *MNRAS*, 360, 1413
- Calzetti, D. 1997, *AJ*, 113, 162
- Calzetti, D. et al. 2005, *ApJ*, 633, 871
- Calzetti, D. et al. 2007, *ApJ*, 666, 870
- Carlos-Muñoz, J. et al. 2009, in preparation
- Cortese, L., Boselli, A., Buat, V., Gavazzi, G., Boissier, S., Gil de Paz, A., Seibert, M., Madore, B.F., & Martin, C. 2006, *ApJ*, 637, 242
- Cortese, L., 2006, *ApJ*, 636, 242
- Dalcanton, J. et al. 2007, *BAAS*, 211, 7905
- Dale, D.A. et al. 2000, *AJ*, 120, 583
- Dale, D.A., Helou, G., Contursi, A., Silbermann, N.A., & Kolhatkar, S. 2001, *ApJ*, 549, 215
- Dale, D.A. & Helou, G. 2002, *ApJ*, 576, 159
- Dale, D.A. et al. 2007, *ApJ*, 655, 863
- Dale, D.A. et al. 2008, *ApJ*, submitted
- Draine, B.T., & Li, A. 2007, *ApJ*, 657, 810

- Engelbracht, C.W., Gordon, K.D., Rieke, G.H., Werner, M.W., Dale, D.A., & Latter, W.B. 2005, *ApJ*, 628, L29
- Fazio, G.G. et al. 2004, *ApJS*, 154, 10
- Gil de Paz, A. et al. 2007, *ApJS*, 173, 185
- Gil de Paz, A. et al. 2008, in preparation
- Gordon, K. et al. 2004, *ApJS*, 154, 215
- Gordon, K. et al. 2005, *PASP*, 117, 503
- Helou, G. et al. 2004, *ApJS*, 154, 253
- Hunter, D.A. et al. 2009, in preparation
- Jarrett, T.H., Chester, T., Cutri, R., Schneider, S.E., & Huchra, J.P. 2003, *AJ*, 125, 525
- Kennicutt, R.C. 1998, *ARA&A*, 36, 189
- Kennicutt, R.C. et al. 2003, *PASP*, 115, 928
- Kennicutt, R.C. et al. 2007, *ApJ*, 671, 333
- Kennicutt, R.C. et al. 2009, *ApJ*, in preparation
- Kennicutt, R.C., Lee, J.C., Funes, J.G., Sakai, S., & Akiyama, S. 2008, *ApJ*, in press
- Kirby, E.M., Jerjen, H., Ryder, S.D., & Driver, S.P. 2008, *ApJ*, in press
- Kong, X., Charlot, S., Brinchmann, J., & Fall, S.M. 2004, *MNRAS*, 349, 769
- Kroupa, P. 2002, *Science*, 295, 82
- Lee, J.C. 2006, Ph.D. thesis, University of Arizona
- Lee, J.C., Kennicutt, R.C., Funes, J.G., Sakai, S., & Akiyama, S. 2007, *ApJ*, 671, 113
- Lee, J.C. et al. 2009, in preparation
- Li, A. & Draine, B.T. 2001, *ApJ*, 554, 778
- Madden, S.C., Galliano, F., Jones, A.P., & Sauvage, M. 2006, *A&A*, 446, 877
- Meurer, G.R., Heckman, T.M., & Calzetti, D. 1999, *ApJ*, 521, 64
- Papovich, C. & Bell, E.F. 2002, *ApJ*, 579, L1
- Regan, M. et al. 2006, *ApJ*, 652, 1112

Rieke, G.H. et al. 2004, ApJS, 154, 25

Ryan-Weber, E. et al. 2002, AJ, 124, 1954

Schlegel, D.J., Finkbeiner, D.P., & Davis, M. 1998, ApJ, 500, 525

Seibert, M. et al. 2005, ApJ, 619, L55

Sloan, G.C., Kraemer, K.E., Wood, P.R., Zijlstra, A.A., Bernard-Salas, J., Devost, D., & Houck, J.R. 2008, ApJ, in press

Skrutskie, M.F. et al. 2006, AJ, 131, 1163

Wu, Y., Charmandaris, V., Hao, H., Brandl, B.R., Bernard-Salas, J., Spoon, H.W.W., & Houck, J.R. 2006, ApJ, 639, 157

Vazquez, G.A. & Leitherer, C. 2005, ApJ, 621, 695

Yan, L. et al. 2004, ApJS, 154, 60

Table 1. Galaxy Sample and Infrared Photometry Apertures

| Galaxy           | $m_B$<br>(mag) | $cz$<br>(km s <sup>-1</sup> ) | $D$<br>(Mpc) | $T$ | $E(B-V)$<br>(mag) | $\alpha_0$ & $\delta_0$<br>(J2000) | $2a$<br>( $''$ ) | $2b$<br>( $''$ ) | PA<br>( $^\circ$ ) |
|------------------|----------------|-------------------------------|--------------|-----|-------------------|------------------------------------|------------------|------------------|--------------------|
| WLM              | 11.03          | -116                          | 0.92         | 10  | 0.04              | 000158.9–152655                    | 672              | 340              | 0                  |
| NGC0024          | 12.19          | 554                           | 8.13         | 5   | 0.02              | 000955.9–245755                    | 301              | 216              | 225                |
| NGC0045          | 11.32          | 471                           | 7.07         | 8   | 0.02              | 001404.6–231101                    | 577              | 456              | 336                |
| NGC0055          | 8.42           | 129                           | 2.17         | 9   | 0.01              | 001508.2–391256                    | 2251             | 714              | 106                |
| NGC0059          | 13.12          | 382                           | 5.30         | -3  | 0.02              | 001525.8–212646                    | 256              | 180              | 302                |
| ESO410-G005      | 14.95          | ...                           | 1.90         | -1  | 0.01              | 001531.0–321048                    | 193              | 144              | 308                |
| Sculptor-dE1     | 17.78          | ...                           | 4.20         | 10  | 0.02              | 002351.6–244204                    | 160              | 103              | 0                  |
| ESO294-G010      | 15.52          | 117                           | 1.90         | -3  | 0.01              | 002633.7–415120                    | 165              | 102              | 0                  |
| IC1574           | 14.50          | 361                           | 4.92         | 10  | 0.02              | 004303.9–221444                    | 202              | 123              | 0                  |
| NGC0247          | 9.67           | 160                           | 3.65         | 7   | 0.02              | 004708.9–204456                    | 1476             | 581              | 352                |
| NGC0253          | 8.04           | 241                           | 3.94         | 5   | 0.02              | 004733.2–251734                    | 2050             | 808              | 50                 |
| ESO540-G030      | 16.46          | ...                           | 3.40         | -1  | 0.02              | 004920.8–180406                    | 168              | 148              | 0                  |
| UGCA015          | 15.38          | 301                           | 3.34         | 10  | 0.02              | 004949.1–210049                    | 150              | 78               | 28                 |
| ESO540-G032      | 16.55          | ...                           | 3.40         | -3  | 0.02              | 005024.6–195427                    | 100              | 91               | 0                  |
| UGC00521         | 15.31          | 659                           | 11.32        | 10  | 0.07              | 005112.2+120129                    | 107              | 107              | 90                 |
| SMC <sup>a</sup> | 2.70           | 158                           | 0.06         | 9   | 0.42              | ...                                | ...              | ...              | ...                |
| NGC0300          | 8.72           | 144                           | 2.00         | 7   | 0.01              | 005458.1–374054                    | 1507             | 1128             | 114                |
| UGC00668         | 9.88           | -234                          | 0.65         | 10  | 0.02              | 010450.5+020720                    | 682              | 547              | 60                 |
| UGC00685         | 14.20          | 157                           | 4.70         | 9   | 0.06              | 010723.2+164101                    | 179              | 147              | 122                |
| UGC00695         | 15.28          | 664                           | 10.20        | 6   | 0.03              | 010746.5+010347                    | 129              | 109              | 0                  |
| NGC404           | 11.51          | -48                           | 3.10         | -1  | 0.06              | 010927.7+354307                    | 234              | 229              | 0                  |
| UGC00891         | 14.72          | 643                           | 10.84        | 9   | 0.03              | 012118.9+122438                    | 194              | 118              | 42                 |
| UGC01056         | 14.87          | 595                           | 10.32        | 10  | 0.07              | 012847.6+164117                    | 125              | 117              | 0                  |
| UGC01104         | 14.41          | 686                           | 7.50         | 9   | 0.06              | 013242.5+181906                    | 166              | 103              | 0                  |
| NGC0598          | 6.27           | -179                          | 0.84         | 6   | 0.04              | 013350.8+303920                    | 4453             | 2762             | 12                 |
| NGC0625          | 11.71          | 405                           | 4.07         | 9   | 0.02              | 013504.4–412624                    | 499              | 256              | 90                 |
| NGC0628          | 9.95           | 657                           | 7.30         | 5   | 0.07              | 013641.8+154717                    | 721              | 717              | 338                |
| UGC01176         | 14.40          | 633                           | 9.00         | 10  | 0.06              | 014010.0+155426                    | 202              | 168              | 25                 |
| ESO245-G005      | 12.70          | 395                           | 4.43         | 10  | 0.02              | 014503.6–433528                    | 358              | 253              | 318                |
| UGC01249         | 12.07          | 338                           | 7.20         | 9   | 0.08              | 014729.0+271960                    | 524              | 290              | 331                |
| NGC0672          | 11.47          | 421                           | 7.20         | 6   | 0.08              | 014752.7+272550                    | 556              | 361              | 67                 |
| ESO245-G007      | 13.33          | 56                            | 0.44         | 10  | 0.02              | 015106.1–442647                    | 288              | 240              | 0                  |
| NGC0784          | 12.23          | 198                           | 5.19         | 8   | 0.06              | 020116.7+285005                    | 480              | 191              | 3                  |
| NGC855           | 13.30          | 595                           | 9.73         | -5  | 0.07              | 021403.9+275239                    | 190              | 171              | 68                 |
| ESO115-G021      | 13.34          | 513                           | 4.99         | 8   | 0.03              | 023746.8–612018                    | 332              | 147              | 221                |
| ESO154-G023      | 12.69          | 578                           | 5.76         | 8   | 0.02              | 025652.4–543359                    | 486              | 248              | 39                 |
| NGC1291          | 9.39           | 839                           | 9.37         | 0   | 0.01              | 031719.1–410632                    | 840              | 804              | 0                  |
| NGC1313          | 9.20           | 475                           | 4.15         | 7   | 0.11              | 031810.0–662908                    | 896              | 694              | 338                |
| NGC1311          | 13.18          | 571                           | 5.45         | 9   | 0.02              | 032006.9–521114                    | 300              | 141              | 36                 |
| UGC02716         | 14.64          | 379                           | 6.23         | 8   | 0.14              | 032407.9+174512                    | 174              | 123              | 90                 |
| IC1959           | 13.26          | 640                           | 6.06         | 9   | 0.01              | 033312.4–502445                    | 253              | 114              | 330                |
| NGC1487          | 12.34          | 848                           | 9.08         | 7   | 0.01              | 035545.5–422200                    | 391              | 260              | 63                 |
| NGC1510          | 13.47          | 913                           | 9.84         | -2  | 0.01              | 040332.7–432359                    | 126              | 122              | 0                  |
| NGC1512          | 11.13          | 896                           | 9.64         | 1   | 0.01              | 040355.0–432044                    | 491              | 288              | 55                 |
| NGC1522          | 13.93          | 905                           | 9.32         | 11  | 0.01              | 040607.6–524011                    | 151              | 99               | 37                 |



Table 1—Continued

| Galaxy                     | $m_B$<br>(mag) | $cz$<br>(km s <sup>-1</sup> ) | $D$<br>(Mpc) | $T$ | $E(B-V)$<br>(mag) | $\alpha_0$ & $\delta_0$<br>(J2000) | $2a$<br>( $''$ ) | $2b$<br>( $''$ ) | PA<br>( $^\circ$ ) |
|----------------------------|----------------|-------------------------------|--------------|-----|-------------------|------------------------------------|------------------|------------------|--------------------|
| IC2049                     | 15.19          | 869                           | 16.73        | 7   | 0.02              | 041204.2–583327                    | 119              | 106              | 0                  |
| ESO483-G013                | 14.18          | 823                           | 10.43        | –3  | 0.05              | 041240.9–230928                    | 205              | 147              | 322                |
| ESO158-G003                | 14.01          | 975                           | 9.96         | 9   | 0.01              | 044615.6–572044                    | 199              | 172              | 0                  |
| ESO119-G016                | 14.79          | 969                           | 9.84         | 10  | 0.02              | 045128.6–613905                    | 221              | 116              | 26                 |
| NGC1705                    | 12.77          | 628                           | 5.10         | 11  | 0.01              | 045413.5–532137                    | 167              | 120              | 220                |
| NGC1744                    | 11.60          | 748                           | 7.65         | 7   | 0.04              | 045957.8–260116                    | 410              | 225              | 349                |
| NGC1796                    | 12.86          | 987                           | 10.32        | 5   | 0.02              | 050242.8–610822                    | 256              | 205              | 99                 |
| ESO486-G021                | 14.47          | 865                           | 8.89         | 2   | 0.03              | 050319.9–252524                    | 115              | 99               | 90                 |
| MCG-05-13-004 <sup>b</sup> | 13.22          | 686                           | 6.63         | 9   | 0.01              | ...                                | ...              | ...              | ...                |
| NGC1800                    | 13.07          | 803                           | 8.24         | 9   | 0.01              | 050625.7–315715                    | 229              | 163              | 107                |
| UGCA106                    | 13.05          | 933                           | 9.77         | 9   | 0.02              | 051159.2–325817                    | 323              | 245              | 14                 |
| LMC <sup>a</sup>           | 0.91           | 278                           | 0.05         | 9   | 0.92              | ...                                | ...              | ...              | ...                |
| KKH037                     | 16.40          | –148                          | 3.39         | 10  | 0.07              | 064744.2+800723                    | 105              | 81               | 90                 |
| NGC2366                    | 11.43          | 100                           | 3.19         | 10  | 0.04              | 072850.9+691248                    | 501              | 298              | 31                 |
| UGCA133                    | 15.80          | ...                           | 3.20         | –3  | 0.04              | 073412.2+665313                    | 215              | 153              | 0                  |
| NGC2403                    | 8.93           | 131                           | 3.22         | 6   | 0.04              | 073655.0+653554                    | 1164             | 848              | 130                |
| NGC2500                    | 12.20          | 514                           | 7.63         | 7   | 0.04              | 080152.4+504405                    | 274              | 234              | 75                 |
| NGC2537                    | 12.82          | 447                           | 6.90         | 9   | 0.05              | 081314.7+455936                    | 211              | 199              | 0                  |
| UGC04278                   | 13.07          | 565                           | 7.59         | 7   | 0.05              | 081358.7+454445                    | 319              | 79               | 351                |
| UGC04305                   | 11.10          | 157                           | 3.39         | 10  | 0.03              | 081906.8+704309                    | 442              | 430              | 90                 |
| NGC2552                    | 12.56          | 524                           | 7.65         | 9   | 0.05              | 081920.0+500038                    | 312              | 205              | 54                 |
| M81dwA                     | 18.69          | 113                           | 3.55         | 10  | 0.02              | 082356.0+710145                    | 78               | 78               | 90                 |
| UGC04426                   | 15.00          | 397                           | 10.28        | 10  | 0.04              | 082828.4+415124                    | 206              | 145              | 10                 |
| UGC04459                   | 14.78          | 19                            | 3.56         | 10  | 0.04              | 083406.8+661036                    | 134              | 111              | 120                |
| UGC04483                   | 15.27          | 178                           | 3.21         | 10  | 0.03              | 083703.5+694632                    | 94               | 58               | 0                  |
| NGC2683                    | 10.64          | 411                           | 7.70         | 3   | 0.03              | 085241.0+332516                    | 822              | 420              | 41                 |
| UGC04704                   | 15.33          | 596                           | 7.75         | 8   | 0.03              | 085902.5+391223                    | 303              | 108              | 296                |
| UGC04787                   | 15.41          | 552                           | 6.53         | 8   | 0.02              | 090735.1+331638                    | 211              | 107              | 5                  |
| UGC04998                   | 14.72          | 623                           | 10.50        | 10  | 0.06              | 092512.9+682258                    | 187              | 162              | 71                 |
| NGC2903                    | 9.68           | 556                           | 8.90         | 4   | 0.03              | 093210.9+213005                    | 824              | 461              | 17                 |
| UGC05076                   | 15.21          | 571                           | 8.31         | 10  | 0.02              | 093236.5+515216                    | 165              | 139              | 90                 |
| CGCG035-007                | 15.46          | 574                           | 5.17         | 5   | 0.04              | 093444.9+062532                    | 126              | 96               | 63                 |
| UGC05139                   | 14.17          | 143                           | 3.84         | 10  | 0.05              | 094030.5+711033                    | 265              | 228              | 210                |
| IC0559                     | 14.82          | 513                           | 4.93         | 5   | 0.03              | 094443.9+093655                    | 135              | 124              | 63                 |
| F8D1                       | 16.14          | ...                           | 3.80         | –3  | 0.11              | 094447.1+672619                    | 254              | 254              | 90                 |
| [FM2000]1                  | 17.80          | ...                           | 3.40         | –3  | 0.08              | 094510.0+684547                    | 89               | 89               | 90                 |
| NGC2976                    | 11.24          | 3                             | 3.56         | 5   | 0.07              | 094715.9+675507                    | 457              | 312              | 322                |
| LEDA166101                 | 16.94          | ...                           | 3.50         | –3  | 0.14              | 095013.0+673037                    | 219              | 152              | 33                 |
| UGC05272                   | 15.41          | 520                           | 7.10         | 10  | 0.02              | 095023.1+312917                    | 196              | 96               | 112                |
| UGC05288                   | 14.32          | 557                           | 6.80         | 8   | 0.03              | 095116.9+074939                    | 164              | 141              | 331                |
| BK03N                      | 18.78          | –40                           | 4.02         | 10  | 0.08              | 095348.5+685808                    | 41               | 41               | 90                 |
| NGC3031                    | 7.89           | –34                           | 3.63         | 2   | 0.08              | 095531.8+690403                    | 1629             | 1123             | 154                |
| NGC3034 <sup>c</sup>       | 9.30           | 203                           | 3.53         | 7   | 0.16              | ...                                | ...              | ...              | ...                |
| UGC05340                   | 14.76          | 503                           | 5.90         | 10  | 0.02              | 095645.8+284932                    | 115              | 81               | 0                  |
| KDG061                     | 15.17          | –135                          | 3.60         | 8   | 0.07              | 095704.5+683536                    | 214              | 119              | 49                 |

Table 1—Continued

| Galaxy     | $m_B$<br>(mag) | $cz$<br>(km s <sup>-1</sup> ) | $D$<br>(Mpc) | $T$ | $E(B-V)$<br>(mag) | $\alpha_0$ & $\delta_0$<br>(J2000) | $2a$<br>( $''$ ) | $2b$<br>( $''$ ) | PA<br>( $^\circ$ ) |
|------------|----------------|-------------------------------|--------------|-----|-------------------|------------------------------------|------------------|------------------|--------------------|
| UGC05336   | 14.30          | 46                            | 3.70         | 10  | 0.08              | 095729.2+690250                    | 248              | 181              | 220                |
| Arp'sLoop  | 16.76          | 99                            | 3.90         | 10  | 0.08              | 095732.7+691700                    | 137              | 137              | 90                 |
| UGC05364   | 12.92          | 20                            | 0.69         | 10  | 0.02              | 095926.5+304458                    | 311              | 192              | 67                 |
| UGC05373   | 11.85          | 301                           | 1.44         | 10  | 0.03              | 095959.5+051957                    | 333              | 268              | 90                 |
| KKH057     | 17.95          | ...                           | 3.90         | -3  | 0.02              | 100014.6+631058                    | 73               | 53               | 45                 |
| UGCA193    | 14.84          | 662                           | 9.70         | 7   | 0.04              | 100236.4-060031                    | 284              | 69               | 14                 |
| NGC3109    | 10.39          | 403                           | 1.34         | 9   | 0.07              | 100307.6-260948                    | 900              | 334              | 90                 |
| NGC3077    | 10.61          | 14                            | 3.82         | 6   | 0.07              | 100319.2+684401                    | 576              | 483              | 64                 |
| AM1001-270 | 16.51          | 362                           | 1.30         | 10  | 0.08              | 100403.0-271948                    | 169              | 96               | 319                |
| BK05N      | 17.77          | ...                           | 3.80         | -3  | 0.06              | 100441.6+681526                    | 207              | 102              | 330                |
| UGC5428    | 15.95          | -129                          | 3.50         | 10  | 0.10              | 100507.5+663339                    | 196              | 168              | 90                 |
| UGC05423   | 15.20          | 350                           | 5.30         | 10  | 0.08              | 100531.3+702152                    | 107              | 70               | 140                |
| UGC5442    | 15.78          | -18                           | 3.70         | -3  | 0.05              | 100701.2+674938                    | 197              | 124              | 34                 |
| UGC05456   | 13.72          | 544                           | 3.80         | 5   | 0.04              | 100719.4+102151                    | 161              | 121              | 322                |
| IKN        | 17.31          | ...                           | 3.70         | -3  | 0.06              | 100805.9+682357                    | 180              | 156              | 180                |
| SextansA   | 11.86          | 324                           | 1.32         | 10  | 0.04              | 101100.8-044134                    | 285              | 258              | 0                  |
| [HS98]117  | 17.01          | -37                           | 4.00         | 10  | 0.12              | 102125.5+710652                    | 213              | 129              | 0                  |
| NGC3239    | 11.73          | 753                           | 8.29         | 9   | 0.03              | 102504.7+170856                    | 315              | 272              | 63                 |
| DDO078     | 15.84          | 55                            | 3.70         | -3  | 0.02              | 102627.4+673916                    | 141              | 141              | 90                 |
| UGC05672   | 15.14          | 531                           | 6.30         | 5   | 0.02              | 102820.9+223409                    | 289              | 104              | 340                |
| UGC05666   | 10.80          | 57                            | 4.02         | 9   | 0.04              | 102822.7+682448                    | 827              | 377              | 230                |
| UGC05692   | 13.71          | 180                           | 4.00         | 9   | 0.04              | 103036.4+703713                    | 306              | 211              | 0                  |
| NGC3274    | 13.21          | 537                           | 6.50         | 7   | 0.02              | 103216.6+274007                    | 186              | 135              | 90                 |
| BK06N      | 16.85          | ...                           | 3.80         | -3  | 0.01              | 103432.4+660036                    | 231              | 108              | 304                |
| NGC3299    | 14.11          | 641                           | 10.40        | 8   | 0.02              | 103623.8+124231                    | 264              | 207              | 0                  |
| UGC05764   | 15.21          | 586                           | 7.08         | 10  | 0.02              | 103643.1+313245                    | 150              | 85               | 44                 |
| UGC05797   | 15.00          | 713                           | 6.84         | 10  | 0.03              | 103925.4+014302                    | 141              | 138              | 0                  |
| UGC05829   | 13.73          | 629                           | 7.88         | 10  | 0.02              | 104241.6+342657                    | 270              | 204              | 57                 |
| NGC3344    | 10.45          | 586                           | 6.64         | 4   | 0.03              | 104332.3+245524                    | 396              | 394              | 0                  |
| NGC3351    | 10.53          | 778                           | 10.00        | 3   | 0.03              | 104357.5+114219                    | 586              | 457              | 10                 |
| NGC3368    | 10.11          | 897                           | 10.52        | 2   | 0.03              | 104645.5+114905                    | 511              | 349              | 346                |
| UGC05889   | 14.22          | 572                           | 9.30         | 9   | 0.03              | 104722.2+140416                    | 202              | 190              | 0                  |
| UGC05923   | 14.03          | 712                           | 7.16         | 0   | 0.03              | 104907.5+065504                    | 113              | 70               | 353                |
| UGC05918   | 15.22          | 340                           | 7.40         | 10  | 0.01              | 104936.5+653149                    | 140              | 113              | 65                 |
| NGC3432    | 11.67          | 616                           | 7.89         | 9   | 0.01              | 105232.7+363747                    | 476              | 187              | 38                 |
| KDG73      | 17.28          | -132                          | 3.70         | 10  | 0.02              | 105256.5+693317                    | 126              | 100              | 345                |
| NGC3486    | 11.05          | 681                           | 8.24         | 5   | 0.02              | 110023.2+285834                    | 495              | 389              | 83                 |
| NGC3510    | 14.30          | 705                           | 8.57         | 8   | 0.03              | 110343.6+285301                    | 310              | 136              | 345                |
| NGC3521    | 9.83           | 805                           | 8.03         | 4   | 0.06              | 110548.7-000222                    | 767              | 494              | 343                |
| NGC3593    | 11.86          | 628                           | 6.52         | 0   | 0.02              | 111436.7+124903                    | 373              | 211              | 86                 |
| NGC3623    | 10.25          | 807                           | 8.95         | 1   | 0.02              | 111856.0+130525                    | 663              | 331              | 352                |
| NGC3627    | 9.65           | 727                           | 10.05        | 3   | 0.03              | 112013.4+125927                    | 746              | 487              | 347                |
| NGC3628    | 10.28          | 843                           | 9.45         | 3   | 0.03              | 112014.8+133518                    | 1039             | 619              | 102                |
| UGC06457   | 15.00          | 963                           | 10.24        | 10  | 0.03              | 112712.4-005944                    | 150              | 111              | 19                 |
| UGC06541   | 14.40          | 249                           | 3.89         | 11  | 0.02              | 113328.1+491428                    | 124              | 87               | 316                |

Table 1—Continued

| Galaxy      | $m_B$<br>(mag) | $cz$<br>(km s <sup>-1</sup> ) | $D$<br>(Mpc) | $T$ | $E(B-V)$<br>(mag) | $\alpha_0$ & $\delta_0$<br>(J2000) | $2a$<br>( $''$ ) | $2b$<br>( $''$ ) | PA<br>( $^\circ$ ) |
|-------------|----------------|-------------------------------|--------------|-----|-------------------|------------------------------------|------------------|------------------|--------------------|
| NGC3738     | 11.97          | 229                           | 4.90         | 10  | 0.01              | 113548.6+543129                    | 220              | 175              | 343                |
| NGC3741     | 14.49          | 229                           | 3.19         | 10  | 0.02              | 113606.0+451709                    | 137              | 108              | 7                  |
| UGC06782    | 15.07          | 525                           | 14.00        | 9   | 0.03              | 114857.2+235016                    | 120              | 120              | 90                 |
| UGC06817    | 13.56          | 242                           | 2.64         | 10  | 0.03              | 115054.1+385259                    | 233              | 174              | 39                 |
| UGC06900    | 14.80          | 590                           | 7.47         | 10  | 0.02              | 115539.9+313106                    | 204              | 145              | 107                |
| NGC4020     | 13.82          | 760                           | 9.68         | 7   | 0.02              | 115856.5+302442                    | 222              | 136              | 18                 |
| NGC4068     | 13.02          | 210                           | 4.31         | 10  | 0.02              | 120402.8+523523                    | 255              | 178              | 22                 |
| NGC4080     | 14.28          | 567                           | 6.92         | 10  | 0.03              | 120451.8+265932                    | 153              | 131              | 312                |
| NGC4096     | 11.48          | 566                           | 8.28         | 5   | 0.02              | 120600.3+472847                    | 556              | 243              | 18                 |
| NGC4144     | 12.05          | 265                           | 9.80         | 6   | 0.01              | 120958.9+462730                    | 437              | 189              | 103                |
| NGC4163     | 13.75          | 165                           | 2.96         | 10  | 0.02              | 121208.9+361008                    | 213              | 164              | 4                  |
| NGC4190     | 13.90          | 228                           | 3.50         | 10  | 0.03              | 121344.6+363808                    | 210              | 164              | 45                 |
| ESO321-G014 | 15.63          | 610                           | 3.20         | 10  | 0.09              | 121349.3-381347                    | 171              | 105              | 22                 |
| UGC07242    | 14.65          | 68                            | 5.42         | 6   | 0.02              | 121408.4+660541                    | 157              | 85               | 0                  |
| UGCA276     | 15.70          | 284                           | 3.18         | 10  | 0.02              | 121459.9+361301                    | 161              | 143              | 301                |
| UGC07267    | 15.29          | 472                           | 7.33         | 8   | 0.02              | 121523.9+512104                    | 189              | 98               | 45                 |
| NGC4214     | 10.24          | 291                           | 2.92         | 10  | 0.02              | 121538.4+361943                    | 476              | 452              | 0                  |
| CGCG269-049 | 15.30          | 159                           | 3.23         | 10  | 0.02              | 121547.3+522315                    | 94               | 67               | 319                |
| NGC4236     | 10.05          | 0                             | 4.45         | 8   | 0.01              | 121635.9+692808                    | 1129             | 420              | 155                |
| NGC4244     | 10.88          | 244                           | 4.49         | 6   | 0.02              | 121729.8+374825                    | 1182             | 242              | 47                 |
| NGC4242     | 11.37          | 517                           | 7.43         | 8   | 0.01              | 121730.4+453710                    | 410              | 312              | 28                 |
| UGC07321    | 14.15          | 408                           | 20.00        | 7   | 0.03              | 121734.3+223225                    | 370              | 78               | 81                 |
| NGC4248     | 13.21          | 484                           | 7.24         | 3   | 0.02              | 121750.7+472432                    | 251              | 170              | 107                |
| NGC4258     | 9.10           | 448                           | 7.98         | 4   | 0.02              | 121854.9+471824                    | 1160             | 529              | 333                |
| ISZ399      | 14.72          | 900                           | 8.97         | 11  | 0.06              | 121959.5-172331                    | 132              | 102              | 314                |
| NGC4288     | 13.26          | 535                           | 7.67         | 7   | 0.01              | 122038.3+461737                    | 190              | 163              | 139                |
| UGC07408    | 13.35          | 462                           | 6.87         | 9   | 0.01              | 122115.5+454900                    | 220              | 192              | 90                 |
| UGC07490    | 13.05          | 465                           | 8.40         | 9   | 0.02              | 122424.6+701958                    | 226              | 220              | 0                  |
| NGC4395     | 10.64          | 319                           | 4.61         | 9   | 0.02              | 122552.2+333315                    | 1008             | 790              | 328                |
| UGCA281     | 15.36          | 281                           | 5.70         | 11  | 0.01              | 122616.7+482939                    | 87               | 73               | 81                 |
| UGC07559    | 14.20          | 218                           | 4.87         | 10  | 0.01              | 122706.1+370830                    | 154              | 108              | 336                |
| UGC07577    | 12.84          | 196                           | 2.74         | 10  | 0.02              | 122743.4+432926                    | 312              | 218              | 301                |
| NGC4449     | 9.99           | 207                           | 4.21         | 10  | 0.02              | 122810.4+440525                    | 473              | 354              | 57                 |
| UGC07599    | 14.88          | 278                           | 6.90         | 8   | 0.02              | 122828.2+371401                    | 92               | 70               | 312                |
| UGC07605    | 14.79          | 309                           | 4.43         | 10  | 0.01              | 122838.4+354301                    | 141              | 86               | 17                 |
| NGC4455     | 13.80          | 637                           | 7.75         | 7   | 0.02              | 122844.0+224918                    | 200              | 90               | 198                |
| UGC07608    | 13.67          | 538                           | 7.76         | 10  | 0.02              | 122845.2+431332                    | 156              | 138              | 0                  |
| NGC4460     | 12.78          | 490                           | 9.59         | -1  | 0.02              | 122845.9+445157                    | 338              | 147              | 37                 |
| UGC07639    | 13.99          | 382                           | 8.00         | 10  | 0.01              | 122953.3+473154                    | 231              | 140              | 334                |
| NGC4485     | 12.32          | 493                           | 7.07         | 10  | 0.02              | 123031.8+414202                    | 180              | 134              | 343                |
| NGC4490     | 10.22          | 565                           | 8.03         | 7   | 0.02              | 123034.4+413841                    | 418              | 232              | 121                |
| UGC07690    | 13.10          | 537                           | 7.73         | 10  | 0.03              | 123226.8+424225                    | 195              | 151              | 36                 |
| UGC07699    | 13.60          | 496                           | 6.85         | 6   | 0.01              | 123248.0+373718                    | 270              | 105              | 32                 |
| UGC07698    | 13.00          | 331                           | 6.10         | 10  | 0.02              | 123254.0+313218                    | 217              | 127              | 342                |
| UGC07719    | 15.33          | 678                           | 9.39         | 8   | 0.02              | 123400.6+390116                    | 158              | 86               | 347                |

Table 1—Continued

| Galaxy        | $m_B$<br>(mag) | $cz$<br>(km s <sup>-1</sup> ) | $D$<br>(Mpc) | $T$ | $E(B-V)$<br>(mag) | $\alpha_0$ & $\delta_0$<br>(J2000) | $2a$<br>( $''$ ) | $2b$<br>( $''$ ) | PA<br>( $^\circ$ ) |
|---------------|----------------|-------------------------------|--------------|-----|-------------------|------------------------------------|------------------|------------------|--------------------|
| UGC07774      | 15.02          | 526                           | 7.44         | 7   | 0.02              | 123622.8+400019                    | 201              | 57               | 100                |
| UGCA292       | 16.10          | 307                           | 3.10         | 10  | 0.02              | 123840.1+324601                    | 60               | 42               | 325                |
| NGC4594       | 8.98           | 1024                          | 9.33         | 1   | 0.05              | 123959.4–113714                    | 555              | 233              | 90                 |
| NGC4605       | 10.89          | 143                           | 5.47         | 5   | 0.01              | 123958.9+613628                    | 498              | 330              | 303                |
| NGC4618       | 11.22          | 544                           | 7.79         | 8   | 0.02              | 124133.3+410841                    | 335              | 267              | 22                 |
| NGC4625       | 12.92          | 609                           | 8.65         | 9   | 0.02              | 124152.3+411618                    | 198              | 191              | 140                |
| NGC4631       | 9.75           | 606                           | 8.05         | 7   | 0.02              | 124203.7+323205                    | 953              | 540              | 80                 |
| UGC07866      | 13.71          | 354                           | 4.57         | 10  | 0.02              | 124215.0+383020                    | 162              | 125              | 357                |
| NGC4656       | 10.96          | 646                           | 8.59         | 9   | 0.01              | 124356.2+320930                    | 719              | 255              | 220                |
| UGC07916      | 15.00          | 607                           | 8.21         | 10  | 0.02              | 124425.1+342312                    | 150              | 102              | 90                 |
| UGC07950      | 15.10          | 502                           | 7.91         | 10  | 0.02              | 124656.2+513649                    | 144              | 124              | 0                  |
| UGC07949      | 15.12          | 333                           | 9.90         | 10  | 0.02              | 124700.7+362850                    | 124              | 85               | 90                 |
| NGC4707       | 13.40          | 468                           | 7.44         | 9   | 0.01              | 124823.3+510952                    | 207              | 177              | 20                 |
| NGC4736       | 8.99           | 308                           | 4.66         | 2   | 0.02              | 125056.7+410706                    | 1033             | 825              | 100                |
| UGC08024      | 13.94          | 374                           | 4.30         | 10  | 0.01              | 125405.2+270854                    | 199              | 126              | 213                |
| NGC4826       | 9.36           | 408                           | 7.50         | 2   | 0.04              | 125642.8+214050                    | 723              | 449              | 113                |
| UGC08091      | 14.68          | 214                           | 2.13         | 10  | 0.03              | 125839.7+141306                    | 125              | 92               | 32                 |
| UGCA319       | 14.96          | 747                           | 7.40         | 9   | 0.08              | 130214.4–171417                    | 130              | 90               | 24                 |
| UGCA320       | 13.52          | 744                           | 7.24         | 9   | 0.08              | 130317.0–172529                    | 491              | 163              | 114                |
| UGC08188      | 12.40          | 321                           | 4.49         | 9   | 0.01              | 130550.8+373615                    | 379              | 326              | 90                 |
| UGC08201      | 12.80          | 37                            | 4.57         | 10  | 0.02              | 130625.0+674226                    | 268              | 150              | 90                 |
| MCG-03-34-002 | 14.79          | 922                           | 10.16        | 4   | 0.08              | 130756.6–164120                    | 130              | 80               | 320                |
| UGC08245      | 15.22          | 70                            | 3.64         | 10  | 0.03              | 130835.3+785612                    | 201              | 105              | 70                 |
| NGC5023       | 12.85          | 407                           | 5.40         | 6   | 0.02              | 131211.7+440221                    | 410              | 127              | 26                 |
| CGCG217-018   | 15.10          | 570                           | 8.21         | 10  | 0.01              | 131251.6+403232                    | 114              | 87               | 35                 |
| UGC08313      | 14.78          | 625                           | 8.72         | 5   | 0.01              | 131354.3+421231                    | 191              | 114              | 30                 |
| UGC08320      | 13.11          | 192                           | 4.33         | 10  | 0.02              | 131426.5+455527                    | 292              | 198              | 341                |
| UGC08331      | 14.31          | 260                           | 8.20         | 10  | 0.01              | 131529.6+473004                    | 236              | 115              | 323                |
| NGC5055       | 9.31           | 504                           | 7.55         | 4   | 0.02              | 131548.3+420142                    | 893              | 683              | 101                |
| NGC5068       | 10.70          | 673                           | 6.24         | 6   | 0.10              | 131855.4–210212                    | 613              | 593              | 90                 |
| IC4247        | 14.57          | 274                           | 4.97         | 2   | 0.06              | 132644.2–302143                    | 129              | 78               | 333                |
| NGC5204       | 11.73          | 201                           | 4.65         | 9   | 0.01              | 132936.0+582510                    | 338              | 211              | 351                |
| NGC5194       | 8.96           | 463                           | 8.00         | 4   | 0.04              | 132950.6+471307                    | 1699             | 1130             | 15                 |
| NGC5195       | 10.45          | 465                           | 8.00         | 2   | 0.04              | 132959.4+471556                    | 203              | 192              | 0                  |
| UGC08508      | 13.94          | 62                            | 2.69         | 10  | 0.02              | 133043.1+545436                    | 160              | 120              | 305                |
| NGC5229       | 14.18          | 364                           | 5.10         | 7   | 0.02              | 133402.9+475452                    | 279              | 102              | 347                |
| NGC5238       | 13.60          | 235                           | 5.20         | 8   | 0.01              | 133442.8+513650                    | 216              | 166              | 0                  |
| [KK98]208     | 14.30          | 381                           | 4.68         | 10  | 0.04              | 133635.5–293417                    | 360              | 150              | 57                 |
| NGC5236       | 8.20           | 516                           | 4.47         | 5   | 0.07              | 133700.8–295224                    | 1100             | 1055             | 0                  |
| ESO444-G084   | 15.48          | 587                           | 4.61         | 10  | 0.07              | 133720.2–280244                    | 84               | 78               | 0                  |
| UGC08638      | 15.10          | 274                           | 4.27         | 10  | 0.01              | 133919.4+244634                    | 179              | 132              | 73                 |
| UGC08651      | 14.45          | 201                           | 3.02         | 10  | 0.01              | 133953.5+404423                    | 194              | 140              | 59                 |
| NGC5253       | 10.87          | 404                           | 3.15         | 11  | 0.06              | 133956.1–313832                    | 351              | 193              | 44                 |
| NGC5264       | 12.60          | 478                           | 4.53         | 9   | 0.05              | 134136.0–295448                    | 268              | 226              | 66                 |
| UGC08760      | 14.45          | 193                           | 3.24         | 10  | 0.02              | 135051.3+380113                    | 216              | 113              | 29                 |

Table 1—Continued

| Galaxy      | $m_B$<br>(mag) | $cz$<br>(km s <sup>-1</sup> ) | $D$<br>(Mpc) | $T$ | $E(B-V)$<br>(mag) | $\alpha_0$ & $\delta_0$<br>(J2000) | $2a$<br>( $''$ ) | $2b$<br>( $''$ ) | PA<br>( $^\circ$ ) |
|-------------|----------------|-------------------------------|--------------|-----|-------------------|------------------------------------|------------------|------------------|--------------------|
| KKH086      | 16.99          | 287                           | 2.60         | 10  | 0.03              | 135433.8+041443                    | 131              | 83               | 0                  |
| UGC08837    | 13.71          | 144                           | 8.30         | 10  | 0.01              | 135444.0+535347                    | 364              | 148              | 17                 |
| UGC08833    | 15.15          | 228                           | 3.20         | 10  | 0.01              | 135448.4+355018                    | 121              | 115              | 0                  |
| NGC5457     | 8.31           | 241                           | 6.70         | 6   | 0.01              | 140312.2+542307                    | 1450             | 1039             | 37                 |
| NGC5474     | 11.82          | 273                           | 7.20         | 6   | 0.01              | 140459.9+533913                    | 386              | 335              | 210                |
| NGC5477     | 14.24          | 304                           | 7.70         | 9   | 0.01              | 140533.0+542732                    | 169              | 124              | 64                 |
| [KK98]230   | 17.84          | 62                            | 2.14         | 10  | 0.01              | 140710.4+350335                    | 67               | 49               | 0                  |
| UGC09128    | 14.46          | 154                           | 2.24         | 10  | 0.02              | 141556.8+230321                    | 127              | 88               | 36                 |
| NGC5585     | 11.20          | 305                           | 5.70         | 7   | 0.02              | 141948.4+564349                    | 392              | 266              | 38                 |
| UGC09240    | 13.31          | 150                           | 2.80         | 10  | 0.01              | 142443.4+443134                    | 222              | 182              | 90                 |
| UGC09405    | 14.57          | 222                           | 8.00         | 10  | 0.01              | 143524.0+571516                    | 199              | 136              | 333                |
| MRK475      | 15.46          | 583                           | 9.02         | 11  | 0.01              | 143905.5+364819                    | 72               | 71               | 196                |
| NGC5832     | 14.09          | 447                           | 8.74         | 3   | 0.03              | 145747.6+714056                    | 293              | 180              | 49                 |
| NGC5949     | 13.37          | 435                           | 8.53         | 4   | 0.02              | 152800.3+644548                    | 219              | 135              | 324                |
| UGC09992    | 14.86          | 427                           | 8.56         | 10  | 0.04              | 154147.9+671515                    | 156              | 109              | 340                |
| KKR25       | 16.53          | -139                          | 1.90         | 10  | 0.01              | 161347.6+542216                    | 94               | 87               | 0                  |
| NGC6503     | 10.91          | 60                            | 5.27         | 6   | 0.03              | 174927.5+700838                    | 394              | 217              | 120                |
| IC4951      | 13.91          | 794                           | 9.34         | 8   | 0.04              | 200931.8-615104                    | 225              | 92               | 355                |
| DDO210      | 14.14          | -137                          | 0.94         | 10  | 0.05              | 204651.6-125044                    | 155              | 72               | 103                |
| IC5052      | 11.79          | 598                           | 5.86         | 7   | 0.05              | 205206.0-691201                    | 450              | 168              | 323                |
| NGC7064     | 13.10          | 797                           | 9.86         | 5   | 0.01              | 212903.4-524605                    | 250              | 81               | 90                 |
| NGC7090     | 11.33          | 857                           | 10.41        | 5   | 0.02              | 213628.8-543320                    | 539              | 161              | 308                |
| IC5152      | 10.68          | 124                           | 1.97         | 10  | 0.03              | 220242.0-511741                    | 312              | 274              | 90                 |
| IC5256      | 14.58          | 950                           | 10.76        | 8   | 0.03              | 224945.4-684127                    | 124              | 76               | 22                 |
| UGCA438     | 14.67          | 62                            | 2.22         | 10  | 0.01              | 232627.4-322317                    | 189              | 163              | 0                  |
| ESO347-G017 | 14.41          | 690                           | 9.37         | 9   | 0.02              | 232655.9-372050                    | 212              | 129              | 90                 |
| UGC12613    | 12.50          | -183                          | 0.76         | 10  | 0.07              | 232833.7+144437                    | 461              | 269              | 113                |
| IC5332      | 11.21          | 706                           | 9.53         | 7   | 0.02              | 233427.6-360601                    | 645              | 573              | 0                  |
| NGC7713     | 11.51          | 689                           | 9.28         | 7   | 0.02              | 233615.4-375616                    | 370              | 227              | 345                |
| UGCA442     | 13.60          | 267                           | 4.27         | 9   | 0.02              | 234346.7-315724                    | 245              | 117              | 43                 |
| KKH098      | 17.22          | -137                          | 2.50         | 10  | 0.12              | 234534.1+384301                    | 126              | 79               | 5                  |
| ESO149-G003 | 15.04          | 594                           | 6.40         | 10  | 0.01              | 235202.4-523428                    | 249              | 100              | 332                |
| NGC7793     | 9.63           | 230                           | 3.91         | 7   | 0.02              | 235750.4-323530                    | 755              | 499              | 90                 |

Note. — The position angles in the above ellipse parameters are measured east of north.

<sup>a</sup>Infrared photometry for the Large and Small Magellanic Clouds will be provided by the SAGE (P.I. M. Meixner) and SAGE-SMC (P.I. K. Gordon) projects.

<sup>b</sup>NGC 1800 and MCG-05-13-004 spatially overlap so separate photometry for MCG-05-13-004 is not provided.

<sup>c</sup>The bright core of NGC 3034 (M 82) has rendered the *Spitzer* data extremely difficult to process; saturation effects severely limit our ability to extract reliable flux densities.

Table 2. Infrared Flux Densities

| Galaxy                   | 2MASS J<br>1.25 $\mu\text{m}$<br>(Jy) | 2MASS H<br>1.65 $\mu\text{m}$<br>(Jy) | 2MASS K <sub>s</sub><br>2.17 $\mu\text{m}$<br>(Jy) | IRAC<br>3.6 $\mu\text{m}$<br>(Jy) | IRAC<br>4.5 $\mu\text{m}$<br>(Jy) | IRAC<br>5.8 $\mu\text{m}$<br>(Jy) | IRAC<br>8.0 $\mu\text{m}$<br>(Jy) | MIPS<br>24 $\mu\text{m}$<br>(Jy) | MIPS<br>70 $\mu\text{m}$<br>(Jy) | MIPS<br>160 $\mu\text{m}$<br>(Jy) |
|--------------------------|---------------------------------------|---------------------------------------|--|-----------------------------------|-----------------------------------|-----------------------------------|-----------------------------------|----------------------------------|----------------------------------|-----------------------------------|
| WLM <sup>e f</sup>       | 2.45±0.24E-1                          | 3.13±0.31E-1                          | 1.17±0.12E-1                                       | 9.09±1.23E-2                      | 6.28±0.86E-2                      | 4.87±0.62E-2                      | 5.07±0.63E-2                      | 7.58±0.82E-2                     | 2.00±0.25E 0                     | 3.88±0.61E 0                      |
| NGC0024 <sup>e f</sup>   | 2.32±0.23E-1                          | 2.49±0.25E-1                          | 1.90±0.19E-1                                       | 1.04±0.14E-1                      | 7.06±1.01E-2                      | 8.81±1.16E-2                      | 1.28±0.16E-1                      | 1.30±0.07E-1                     | 2.23±0.19E 0                     | 7.00±1.05E 0                      |
| NGC0045                  | 2.08±0.21E-1                          | 2.29±0.23E-1                          | 1.67±0.17E-1                                       | 2.00±0.27E-1                      | 1.27±0.17E-1                      | 6.56±0.83E-2                      | 1.69±0.21E-1                      | 1.87±0.20E-1                     | 3.87±0.47E 0                     | 1.23±0.19E 0                      |
| NGC0055 <sup>e f</sup>   | 3.31±0.33E 0                          | 3.08±0.31E 0                          | 2.63±0.26E 0                                       | 2.03±0.27E 0                      | 1.40±0.19E 0                      | 1.50±0.19E 0                      | 2.28±0.28E 0                      | 6.29±0.68E 0                     | 1.20±0.15E 2                     | 2.53±0.40E 0                      |
| NGC0059                  | 8.48±0.85E-2                          | 1.13±0.11E-1                          | 6.36±0.64E-2                                       | 3.29±0.45E-2                      | 2.23±0.31E-2                      | 1.56±0.20E-2                      | 1.18±0.15E-2                      | 4.40±0.47E-2                     | 5.15±0.63E-1                     | 4.07±0.66E-1                      |
| ESO410-G005              | <6.18E-2                              | <9.05E-2                              | <1.11E-1   | 1.58±0.21E-2                      | 6.46±0.89E-3                      | 1.12±0.15E-2                      | 6.40±0.81E-3                      | 4.43±0.46E-3                     | 5.98±0.81E-2                     | 2.26±0.31E-1                      |
| Sculptor-dE1             | <3.66E-2                              | <5.35E-2                              | <6.59E-2   | <3.40E-4                          | <5.10E-4                          | <1.88E-3                          | <2.06E-3                          | <3.42E-3                         | <4.63E-2                         | <1.75E-1                          |
| ESO294-G010              | 1.73±0.17E-2                          | 2.12±0.21E-2                          | 1.35±0.14E-2                                       | 4.79±0.65E-3                      | 3.12±0.43E-3                      | <1.89E-3                          | <2.06E-3                          | <3.44E-3                         | <4.64E-2                         | <1.75E-1                          |
| IC1574                   | 1.96±0.20E-2                          | 2.18±0.22E-2                          | 1.55±0.16E-2                                       | 5.93±0.80E-3                      | 3.94±0.54E-3                      | 2.62±0.36E-3                      | 1.73±0.24E-3                      | <1.22E-3                         | <5.65E-2                         | <2.13E-1                          |
| NGC0247                  | 1.47±0.15E 0                          | 1.30±0.13E 0                          | 1.02±0.10E 0                                       | 8.54±1.15E-1                      | 5.89±0.81E-1                      | 6.12±0.77E-1                      | 8.48±1.06E-1                      | 9.89±1.06E-1                     | 1.57±0.19E 1                     | 6.88±1.07E 1                      |
| NGC0253 <sup>e</sup>     | 2.11±0.21E 1                          | 2.53±0.25E 1                          | 2.23±0.22E 1                                       | 1.23±0.17E 1                      | 8.25±1.13E 0                      | 1.94±0.24E 1                      | 3.86±0.48E 1                      | 8.00±0.86E 1                     | 1.18±0.14E 3                     | 1.87±0.29E 3                      |
| ESO540-G030              | <5.54E-2                              | <8.08E-2                              | <9.94E-2   | 2.17±0.29E-3                      | 1.58±0.22E-3                      | <1.66E-3                          | <1.81E-3                          | <3.42E-3                         | <4.07E-2                         | <1.53E-1                          |
| UGCA015                  | 6.42±0.64E-3                          | 9.01±0.90E-3                          | 4.27±0.43E-3                                       | 2.11±0.29E-3                      | 1.67±0.23E-3                      | 1.58±0.18E-3                      | 1.73±0.19E-3                      | <2.87E-3                         | <3.86E-2                         | <1.47E-1                          |
| ESO540-G032              | 4.75±0.48E-3                          | 1.15±0.12E-2                          | <3.64E-2   | 1.46±0.20E-3                      | 7.60±1.10E-4                      | <7.00E-4                          | <7.60E-4                          | <2.54E-3                         | <3.43E-2                         | <1.30E-1                          |
| UGC00521                 | 8.60±0.86E-3                          | 9.60±0.96E-3                          | 5.42±0.54E-3                                       | 3.01±0.41E-3                      | 2.24±0.31E-3                      | 1.04±0.14E-3                      | 1.16±0.15E-3                      | ...                              | ...                              | ...                               |
| SMC <sup>a e f</sup>     | ...                                   | ...                                   | ...  | ...                               | ...                               | ...                               | ...                               | ...                              | ...                              | ...                               |
| NGC0300                  | 3.26±0.33E 0                          | 3.27±0.33E 0                          | 2.52±0.25E 0                                       | 1.63±0.22E 0                      | 1.20±0.16E 0                      | 1.25±0.16E 0                      | 2.02±0.25E 0                      | 2.50±0.27E 0                     | 4.61±0.56E 1                     | 1.62±0.25E 1                      |
| UGC00668 <sup>e f</sup>  | 3.05±0.30E-1                          | 4.74±0.47E-1                          | 2.32±0.23E-1                                       | 1.24±0.17E-1                      | 9.09±1.25E-2                      | 3.34±0.42E-2                      | 7.13±0.89E-2                      | 8.63±0.93E-2                     | 2.46±0.30E 0                     | 5.99±0.94E 0                      |
| UGC00685                 | 4.20±0.42E-2                          | 2.28±0.23E-2                          | <1.04E-1   | 1.14±0.16E-2                      | 7.47±1.03E-3                      | 4.27±0.57E-3                      | 5.28±0.67E-3                      | ...                              | ...                              | ...                               |
| UGC00695                 | 9.45±0.95E-3                          | 9.99±1.00E-3                          | <5.51E-2   | 4.46±0.61E-3                      | 3.01±0.41E-3                      | 1.84±0.25E-3                      | 1.47±0.20E-3                      | ...                              | ...                              | ...                               |
| NGC0404 <sup>e</sup>     | 8.10±0.81E-1                          | 8.41±0.84E-1                          | 6.76±0.68E-1                                       | 4.72±0.64E-1                      | 2.53±0.35E-1                      | 2.29±0.30E-1                      | 1.57±0.20E-1                      | 1.46±0.16E-1                     | 2.84±0.35E 0                     | 3.52±0.55E 0                      |
| UGC00891                 | 2.43±0.24E-2                          | 1.34±0.13E-2                          | 1.55±0.16E-2                                       | 6.11±0.83E-3                      | 4.19±0.58E-3                      | 1.83±0.26E-3                      | 3.69±0.47E-3                      | ...                              | ...                              | ...                               |
| UGC01056                 | 1.77±0.18E-2                          | 2.60±0.26E-2                          | 2.91±0.29E-2                                       | 5.59±0.76E-3                      | 4.14±0.57E-3                      | 2.60±0.35E-3                      | 4.22±0.54E-3                      | ...                              | ...                              | ...                               |
| UGC01104                 | 2.02±0.20E-2                          | 2.11±0.21E-2                          | 1.58±0.16E-2                                       | 8.45±1.15E-3                      | 5.70±0.78E-3                      | 3.44±0.46E-3                      | 5.01±0.64E-3                      | ...                              | ...                              | ...                               |
| NGC0598 <sup>e f</sup>   | 2.12±0.21E 1                          | 2.12±0.21E 1                          | 1.67±0.17E 1                                       | 1.97±0.27E 1                      | 1.39±0.19E 1                      | 1.29±0.16E 1                      | 2.78±0.35E 1                      | 4.81±0.52E 1                     | 7.81±0.95E 2                     | 2.32±0.36E 2                      |
| NGC0625                  | 2.83±0.28E-1                          | 2.97±0.30E-1                          | 2.42±0.24E-1                                       | 1.23±0.17E-1                      | 8.83±1.21E-2                      | 9.22±1.17E-2                      | 1.37±0.17E-1                      | 8.79±0.95E-1                     | 6.49±0.79E 0                     | 8.52±1.33E 0                      |
| NGC0628 <sup>e f</sup>   | 1.66±0.17E 0                          | 1.67±0.17E 0                          | 1.32±0.13E 0                                       | 8.72±1.18E-1                      | 5.45±0.75E-1                      | 1.15±0.15E 0                      | 2.70±0.34E 0                      | 3.13±0.13E 0                     | 3.38±0.25E 1                     | 1.19±0.15E 1                      |
| UGC01176                 | <7.90E-2                              | <1.10E-1                              | <1.35E-1   | 8.28±1.12E-3                      | 6.22±0.85E-3                      | 4.43±0.59E-3                      | 4.37±0.56E-3                      | ...                              | ...                              | ...                               |
| ESO245-G005              | 5.02±0.50E-2                          | 5.90±0.59E-2                          | 4.14±0.41E-2                                       | 2.18±0.30E-2                      | 1.53±0.21E-2                      | 1.81±0.23E-2                      | 7.77±0.98E-3                      | 2.47±0.27E-2                     | 5.95±0.74E-1                     | 1.08±0.17E-1                      |
| UGC01249                 | 1.05±0.11E-1                          | 1.73±0.17E-1                          | 8.91±0.89E-2                                       | 6.19±0.84E-2                      | 3.86±0.53E-2                      | 3.79±0.48E-2                      | 1.94±0.24E-2                      | 9.50±1.03E-2                     | 1.87±0.23E 0                     | 4.25±0.66E 0                      |
| NGC0672                  | 3.59±0.36E-1                          | 3.66±0.37E-1                          | 2.96±0.30E-1                                       | 1.52±0.21E-1                      | 1.18±0.16E-1                      | 1.16±0.15E-1                      | 1.16±0.14E-1                      | 3.38±0.36E-1                     | 5.90±0.72E 0                     | 1.50±0.23E 0                      |
| ESO245-G007 <sup>f</sup> | 4.34±0.43E-2                          | 3.61±0.36E-2                          | <5.00E-2   | 1.72±0.23E-2                      | 1.25±0.17E-2                      | <4.32E-3                          | <5.45E-3                          | <6.98E-3                         | <9.41E-2                         | <3.55E-1                          |
| NGC0784                  | 1.03±0.10E-1                          | 1.02±0.10E-1                          | 7.22±0.72E-2                                       | 4.98±0.67E-2                      | 3.50±0.48E-2                      | 2.69±0.34E-2                      | 1.52±0.19E-2                      | 4.94±0.53E-2                     | 1.15±0.14E 0                     | 1.92±0.30E 0                      |

Table 2—Continued

| Galaxy                     | 2MASS J<br>1.25 $\mu\text{m}$<br>(Jy) | 2MASS H<br>1.65 $\mu\text{m}$<br>(Jy) | 2MASS K <sub>s</sub><br>2.17 $\mu\text{m}$<br>(Jy) | IRAC<br>3.6 $\mu\text{m}$<br>(Jy) | IRAC<br>4.5 $\mu\text{m}$<br>(Jy) | IRAC<br>5.8 $\mu\text{m}$<br>(Jy) | IRAC<br>8.0 $\mu\text{m}$<br>(Jy) | MIPS<br>24 $\mu\text{m}$<br>(Jy) | MIPS<br>70 $\mu\text{m}$<br>(Jy) | MIPS<br>160 $\mu\text{m}$<br>(Jy) |
|----------------------------|---------------------------------------|---------------------------------------|--|-----------------------------------|-----------------------------------|-----------------------------------|-----------------------------------|----------------------------------|----------------------------------|-----------------------------------|
| NGC0855 <sup>e f</sup>     | 9.07±0.91E-2                          | 9.78±0.98E-2                          | 7.97±0.80E-2                                       | 4.24±0.60E-2                      | 2.75±0.39E-2                      | 1.83±0.30E-2                      | 4.57±0.57E-2                      | 8.65±0.42E-2                     | 1.64±0.14E 0                     | 2.29±0.30E-1                      |
| ESO115-G021                | 5.85±0.58E-2                          | 6.67±0.67E-2                          | 4.17±0.42E-2                                       | 1.87±0.25E-2                      | 1.24±0.17E-2                      | 8.90±1.16E-3                      | 7.73±0.97E-3                      | 1.71±0.19E-2                     | 3.85±0.48E-1                     | 7.04±1.15E-1                      |
| ESO154-G023                | 1.32±0.13E-1                          | 1.41±0.14E-1                          | 1.05±0.10E-1                                       | 3.76±0.51E-2                      | 3.08±0.42E-2                      | 1.59±0.20E-2                      | 1.86±0.23E-2                      | 4.99±0.54E-2                     | 1.03±0.13E 0                     | 1.84±0.29E-1                      |
| NGC1291 <sup>e f</sup>     | 4.37±0.44E 0                          | 4.56±0.46E 0                          | 3.98±0.40E 0                                       | 2.11±0.28E 0                      | 1.27±0.18E 0                      | 9.47±1.22E-1                      | 6.35±0.80E-1                      | 5.60±0.24E-1                     | 6.17±0.46E 0                     | 2.76±0.30E-1                      |
| NGC1313                    | 9.81±0.98E-1                          | 1.04±0.10E 0                          | 7.41±0.74E-1                                       | 6.43±0.87E-1                      | 4.87±0.67E-1                      | 6.18±0.77E-1                      | 1.22±0.15E 0                      | 2.85±0.31E 0                     | 5.15±0.63E 1                     | 9.62±1.50E-1                      |
| NGC1311                    | 5.13±0.51E-2                          | 5.25±0.52E-2                          | 4.08±0.41E-2                                       | 2.37±0.32E-2                      | 1.68±0.23E-2                      | 1.27±0.16E-2                      | 1.23±0.16E-2                      | 2.90±0.31E-2                     | 7.20±0.88E-1                     | 1.16±0.18E-1                      |
| UGC02716                   | 2.53±0.25E-2                          | 2.56±0.26E-2                          | 2.22±0.22E-2                                       | 1.20±0.16E-2                      | 7.58±1.04E-3                      | 7.23±0.95E-3                      | 8.67±1.09E-3                      | 8.68±0.96E-3                     | 1.56±0.20E-1                     | 1.48±0.20E-1                      |
| IC1959                     | 3.45±0.34E-2                          | 3.54±0.35E-2                          | 2.77±0.28E-2                                       | 1.91±0.26E-2                      | 1.31±0.18E-2                      | 9.81±1.28E-3                      | 1.00±0.13E-2                      | 3.24±0.35E-2                     | 8.99±1.10E-1                     | 1.08±0.17E-1                      |
| NGC1487                    | 1.32±0.13E-1                          | 1.78±0.18E-1                          | 1.20±0.12E-1                                       | 7.10±0.96E-2                      | 4.61±0.63E-2                      | 7.63±0.98E-2                      | 1.37±0.17E-1                      | 2.94±0.32E-1                     | 4.68±0.57E 0                     | 7.60±1.19E-1                      |
| NGC1510                    | 3.77±0.38E-2                          | 3.71±0.37E-2                          | 3.09±0.31E-2                                       | 1.71±0.23E-2                      | 1.19±0.16E-2                      | 1.41±0.19E-2                      | 2.20±0.28E-2                      | 1.35±0.15E-1                     | 9.19±1.12E-1                     | 6.08±0.90E-1                      |
| NGC1512 <sup>e f</sup>     | 8.12±0.81E-1                          | 8.57±0.86E-1                          | 7.30±0.73E-1                                       | 3.88±0.53E-1                      | 2.43±0.34E-1                      | 2.64±0.34E-1                      | 4.37±0.55E-1                      | 4.38±0.21E-1                     | 6.34±0.48E 0                     | 2.24±0.29E-1                      |
| NGC1522                    | 2.61±0.26E-2                          | 2.28±0.23E-2                          | 1.99±0.20E-2                                       | 1.10±0.15E-2                      | 7.87±1.08E-3                      | 9.83±1.29E-3                      | 1.51±0.19E-2                      | 9.66±1.04E-2                     | 9.41±1.15E-1                     | 8.03±1.20E-1                      |
| IC2049                     | 1.08±0.11E-2                          | 1.26±0.13E-2                          | 8.79±0.88E-3                                       | 4.39±0.60E-3                      | 2.83±0.39E-3                      | 1.10±0.16E-3                      | 3.04±0.39E-3                      | 4.70±0.53E-3                     | 6.16±0.88E-2                     | 1.25±0.23E-2                      |
| ESO483-G013                | 3.93±0.39E-2                          | 3.85±0.39E-2                          | 3.37±0.34E-2                                       | 1.68±0.23E-2                      | 1.14±0.16E-2                      | 1.22±0.16E-2                      | 1.12±0.14E-2                      | 3.46±0.37E-2                     | 5.40±0.66E-1                     | 4.77±0.70E-1                      |
| ESO158-G003                | 3.84±0.38E-2                          | 3.54±0.35E-2                          | 2.74±0.27E-2                                       | 1.64±0.22E-2                      | 1.14±0.16E-2                      | 1.11±0.14E-2                      | 2.04±0.26E-2                      | 2.91±0.31E-2                     | 5.37±0.66E-1                     | 4.02±0.10E-1                      |
| ESO119-G016                | 1.89±0.19E-2                          | 2.21±0.22E-2                          | 1.51±0.15E-2                                       | 7.40±1.00E-3                      | 5.37±0.74E-3                      | 2.81±0.38E-3                      | 2.91±0.38E-3                      | 6.11±0.70E-3                     | 7.33±1.11E-2                     | 1.63±0.23E-2                      |
| NGC1705 <sup>e f</sup>     | 5.75±0.57E-2                          | 5.40±0.54E-2                          | 4.44±0.44E-2                                       | 2.57±0.36E-2                      | 1.79±0.25E-2                      | 1.01±0.19E-2                      | 1.68±0.20E-2                      | 5.45±0.22E-2                     | 1.26±0.10E 0                     | 1.44±0.23E-1                      |
| NGC1744                    | 1.12±0.11E-1                          | 1.13±0.11E-1                          | 8.94±0.89E-2                                       | 8.32±1.13E-2                      | 6.44±0.88E-2                      | 4.96±0.63E-2                      | 9.56±1.19E-2                      | 1.10±0.12E-1                     | 1.98±0.24E 0                     | 6.27±0.90E-1                      |
| NGC1796                    | 1.02±0.10E-1                          | 1.12±0.11E-1                          | 9.55±0.95E-2                                       | 5.51±0.75E-2                      | 3.76±0.52E-2                      | 8.48±1.09E-2                      | 1.91±0.24E-1                      | 2.22±0.24E-1                     | 3.38±0.41E 0                     | 6.86±1.07E-1                      |
| ESO486-G021                | 1.87±0.19E-2                          | 2.07±0.21E-2                          | 1.32±0.13E-2                                       | 6.57±0.89E-3                      | 4.25±0.58E-3                      | 4.96±0.66E-3                      | 6.12±0.78E-3                      | ...                              | ...                              | ...                               |
| MCG-05-13-004 <sup>b</sup> | ...                                   | ...                                   | ...  | ...                               | ...                               | ...                               | ...                               | ...                              | ...                              | ...                               |
| NGC1800                    | 8.96±0.90E-2                          | 1.03±0.10E-1                          | 8.34±0.83E-2                                       | 3.14±0.43E-2                      | 2.08±0.29E-2                      | 2.58±0.33E-2                      | 3.57±0.45E-2                      | 6.02±0.65E-2                     | 1.21±0.15E 0                     | 1.88±0.29E-1                      |
| UGCA106                    | 1.19±0.12E-1                          | 6.95±0.69E-2                          | 4.99±0.50E-2                                       | 2.69±0.37E-2                      | 1.93±0.26E-2                      | 1.75±0.22E-2                      | 2.51±0.31E-2                      | 5.05±0.55E-2                     | 8.88±1.09E-1                     | 2.36±0.37E-1                      |
| LMC <sup>a e f</sup>       | ...                                   | ...                                   | ...  | ...                               | ...                               | ...                               | ...                               | ...                              | ...                              | ...                               |
| kkh037                     | 5.43±0.54E-3                          | 6.24±0.62E-3                          | 6.43±0.64E-3                                       | 2.50±0.34E-3                      | 1.58±0.22E-3                      | 1.35±0.18E-3                      | 1.48±0.17E-3                      | 2.45±0.20E-3                     | 3.30±0.46E-2                     | 1.25±0.17E-2                      |
| NGC2366 <sup>e</sup>       | 1.45±0.15E-1                          | 1.47±0.15E-1                          | 1.10±0.11E-1                                       | 6.43±0.87E-2                      | 4.90±0.67E-2                      | 4.95±0.63E-2                      | 5.50±0.69E-2                      | 6.79±0.73E-1                     | 5.40±0.66E 0                     | 5.05±0.79E-1                      |
| UGCA133                    | 1.79±0.18E-2                          | 1.65±0.17E-2                          | 9.06±0.91E-3                                       | 4.09±0.55E-3                      | 3.10±0.43E-3                      | <2.65E-3                          | <2.89E-3                          | 4.81±0.44E-3                     | 6.48±1.23E-2                     | 2.45±0.30E-2                      |
| NGC2403 <sup>e f</sup>     | 2.94±0.29E 0                          | 2.91±0.29E 0                          | 2.39±0.24E 0                                       | 1.88±0.25E 0                      | 1.31±0.18E 0                      | 2.10±0.27E 0                      | 4.11±0.51E 0                      | 5.84±0.24E 0                     | 8.64±0.62E 1                     | 2.41±0.30E-1                      |
| NGC2500 <sup>e</sup>       | 1.71±0.17E-1                          | 1.80±0.18E-1                          | 1.39±0.14E-1                                       | 8.76±1.19E-2                      | 5.65±0.77E-2                      | 1.13±0.15E-1                      | 1.69±0.21E-1                      | 2.09±0.23E-1                     | 3.93±0.48E 0                     | 8.80±1.37E-1                      |
| NGC2537 <sup>e</sup>       | 1.93±0.19E-1                          | 1.95±0.19E-1                          | 1.60±0.16E-1                                       | 7.72±1.05E-2                      | 5.11±0.70E-2                      | 7.67±0.99E-2                      | 1.41±0.18E-1                      | 2.92±0.31E-1                     | 4.02±0.49E 0                     | 5.70±0.89E-1                      |
| UGC04278 <sup>e f</sup>    | 4.79±0.48E-2                          | 4.52±0.45E-2                          | 3.58±0.36E-2                                       | 2.18±0.30E-2                      | 1.57±0.22E-2                      | 1.65±0.22E-2                      | 1.56±0.20E-2                      | 3.80±0.41E-2                     | 8.96±1.10E-1                     | 1.58±0.23E-1                      |
| UGC04305 <sup>e f</sup>    | 1.66±0.17E-1                          | 2.91±0.29E-1                          | 2.16±0.22E-1                                       | 7.13±0.98E-2                      | 5.66±0.78E-2                      | 3.05±0.47E-2                      | 2.39±0.48E-2                      | 2.04±0.08E-1                     | 3.60±0.26E 0                     | 4.10±0.50E-1                      |
| NGC2552                    | 6.62±0.66E-2                          | 8.70±0.87E-2                          | 5.49±0.55E-2                                       | 3.35±0.45E-2                      | 2.27±0.31E-2                      | 2.17±0.28E-2                      | 1.78±0.22E-2                      | 5.77±0.62E-2                     | 9.79±1.20E-1                     | 2.35±0.37E-1                      |

Table 2—Continued

| Galaxy                   | 2MASS J<br>1.25 $\mu\text{m}$<br>(Jy) | 2MASS H<br>1.65 $\mu\text{m}$<br>(Jy) | 2MASS K <sub>s</sub><br>2.17 $\mu\text{m}$<br>(Jy) | IRAC<br>3.6 $\mu\text{m}$<br>(Jy) | IRAC<br>4.5 $\mu\text{m}$<br>(Jy) | IRAC<br>5.8 $\mu\text{m}$<br>(Jy) | IRAC<br>8.0 $\mu\text{m}$<br>(Jy) | MIPS<br>24 $\mu\text{m}$<br>(Jy) | MIPS<br>70 $\mu\text{m}$<br>(Jy) | MIPS<br>160 $\mu\text{m}$<br>(Jy) |
|--------------------------|---------------------------------------|---------------------------------------|--|-----------------------------------|-----------------------------------|-----------------------------------|-----------------------------------|----------------------------------|----------------------------------|-----------------------------------|
| M81dwA <sup>e f</sup>    | 3.77±0.38E-3                          | 3.88±0.39E-3                          | 2.92±0.29E-3                                       | 1.86±0.90E-3                      | 9.50±9.00E-4                      | <3.73E-3                          | <2.37E-3                          | <1.73E-2                         | <1.49E-1                         | <1.43E-1                          |
| UGC04426                 | 1.15±0.12E-2                          | 1.61±0.16E-2                          | 8.91±0.89E-3                                       | 4.58±0.62E-3                      | 3.29±0.45E-3                      | <2.53E-3                          | 3.22±0.42E-3                      | ...                              | ...                              | ...                               |
| UGC04459 <sup>e f</sup>  | 7.54±0.75E-3                          | 1.38±0.14E-2                          | 7.93±0.79E-3                                       | 4.71±1.00E-3                      | 3.88±1.00E-3                      | 2.65±0.90E-3                      | 7.32±1.00E-3                      | 2.81±0.11E-2                     | 3.48±0.34E-1                     | 3.41±1.11E-1                      |
| UGC04483 <sup>e</sup>    | 5.95±0.60E-3                          | 7.63±0.76E-3                          | 4.19±0.42E-3                                       | 1.84±0.25E-3                      | 9.60±1.30E-4                      | 6.40±1.00E-4                      | 1.13±0.15E-3                      | 7.05±0.77E-3                     | 1.05±0.13E-1                     | 2.01±0.25E-1                      |
| NGC2683                  | 2.16±0.22E 0                          | 2.46±0.25E 0                          | 2.10±0.21E 0                                       | 1.08±0.15E 0                      | 6.92±0.95E-1                      | 7.49±0.94E-1                      | 1.18±0.15E 0                      | ...                              | ...                              | ...                               |
| UGC04704                 | 2.11±0.21E-2                          | 2.76±0.28E-2                          | 2.63±0.26E-2                                       | 8.88±1.20E-3                      | 5.81±0.80E-3                      | 6.18±0.81E-3                      | 2.14±0.29E-3                      | ...                              | ...                              | ...                               |
| UGC04787                 | 2.59±0.26E-2                          | 2.40±0.24E-2                          | 1.93±0.19E-2                                       | 8.55±1.16E-3                      | 5.86±0.81E-3                      | 2.96±0.40E-3                      | 5.29±0.67E-3                      | ...                              | ...                              | ...                               |
| UGC04998                 | 2.55±0.26E-2                          | 3.08±0.31E-2                          | 1.77±0.18E-2                                       | 1.08±0.15E-2                      | 7.49±1.03E-3                      | 5.72±0.75E-3                      | 6.57±0.83E-3                      | <4.64E-3                         | <6.23E-2                         | <2.36E-1                          |
| NGC2903                  | 3.00±0.30E 0                          | 3.14±0.31E 0                          | 2.74±0.27E 0                                       | 1.61±0.22E 0                      | 1.09±0.15E 0                      | 2.20±0.28E 0                      | 5.11±0.64E 0                      | 7.00±0.75E 0                     | 7.26±0.89E 1                     | 1.82±0.28E-1                      |
| UGC05076                 | 1.62±0.16E-2                          | 1.26±0.13E-2                          | 9.06±0.91E-3                                       | 5.02±0.68E-3                      | 3.29±0.45E-3                      | 1.49±0.22E-3                      | 4.59±0.58E-3                      | ...                              | ...                              | ...                               |
| CGCG035-007              | 1.23±0.12E-2                          | 1.41±0.14E-2                          | 1.35±0.14E-2                                       | 4.27±0.58E-3                      | 2.89±0.40E-3                      | 1.83±0.25E-3                      | 2.03±0.26E-3                      | 4.46±0.50E-3                     | 1.18±0.15E-1                     | 1.00±0.18E-1                      |
| UGC05139 <sup>e f</sup>  | 3.09±0.31E-2                          | 3.97±0.40E-2                          | 1.60±0.16E-2                                       | 1.19±0.14E-2                      | 7.55±1.20E-3                      | 7.31±1.80E-3                      | 7.54±1.60E-3                      | 1.31±0.20E-2                     | 4.02±0.79E-1                     | 7.97±1.70E-1                      |
| IC0559                   | 1.92±0.19E-2                          | 1.72±0.17E-2                          | 2.37±0.24E-2                                       | 8.10±1.10E-3                      | 5.56±0.76E-3                      | 5.24±0.69E-3                      | 2.35±0.30E-3                      | 5.01±0.57E-3                     | 9.31±1.26E-2                     | 1.49±0.26E-1                      |
| F8D1                     | 2.96±0.30E-2                          | 7.01±0.70E-2                          | 1.88±0.19E-2                                       | 1.08±0.15E-2                      | 8.75±1.20E-3                      | <5.59E-3                          | <6.15E-3                          | <6.78E-3                         | <9.11E-2                         | <3.44E-1                          |
| [FM2000]1                | <1.85E-2                              | <2.56E-2                              | <3.14E-2   | <3.60E-4                          | <5.30E-4                          | <1.95E-3                          | <2.13E-3                          | <2.36E-3                         | <3.18E-2                         | <1.20E-1                          |
| NGC2976 <sup>e f</sup>   | 8.60±0.86E-1                          | 8.93±0.89E-1                          | 7.07±0.71E-1                                       | 4.34±0.59E-1                      | 2.84±0.39E-1                      | 5.04±0.65E-1                      | 1.02±0.13E 0                      | 1.38±0.06E 0                     | 1.99±0.14E 1                     | 4.83±0.64E-1                      |
| LEDA166101               | <8.21E-2                              | <1.12E-1                              | <1.35E-1   | 6.13±0.83E-3                      | 4.10±0.56E-3                      | <2.68E-3                          | <2.94E-3                          | <4.87E-3                         | <6.53E-2                         | <2.46E-1                          |
| UGC05272                 | 1.99±0.20E-2                          | 2.57±0.26E-2                          | 1.58±0.16E-2                                       | 7.36±1.00E-3                      | 5.12±0.70E-3                      | 3.78±0.50E-3                      | 1.84±0.24E-3                      | 1.31±0.14E-2                     | 3.09±0.38E-1                     | 3.09±0.50E-1                      |
| UGC05288                 | 2.91±0.29E-2                          | 2.34±0.23E-2                          | 2.44±0.24E-2                                       | 8.50±1.15E-3                      | 5.69±0.78E-3                      | 4.95±0.65E-3                      | 3.13±0.40E-3                      | 1.12±0.12E-2                     | 1.79±0.23E-1                     | 4.27±0.68E-1                      |
| BK03N                    | <3.81E-3                              | <5.29E-3                              | <6.48E-3   | <1.70E-4                          | <2.50E-4                          | <9.10E-4                          | <1.00E-3                          | <1.10E-3                         | <1.48E-2                         | <5.61E-2                          |
| NGC3031 <sup>e f</sup>   | 2.35±0.24E 1                          | 2.55±0.25E 1                          | 2.13±0.21E 1                                       | 1.09±0.15E 1                      | 6.53±0.90E 0                      | 5.88±0.75E 0                      | 8.04±1.00E 0                      | 5.09±0.20E 0                     | 8.52±0.60E 1                     | 3.56±0.43E-1                      |
| NGC3034 <sup>c e f</sup> | 9.29±0.93E 0                          | 1.08±0.11E 1                          | 1.01±0.10E 1                                       | ...                               | ...                               | ...                               | ...                               | ...                              | ...                              | ...                               |
| UGC05340 <sup>e</sup>    | 8.67±0.87E-3                          | 7.35±0.73E-3                          | <8.58E-3   | 2.54±0.35E-3                      | 1.61±0.22E-3                      | <1.41E-3                          | <1.54E-3                          | <2.60E-3                         | <3.51E-2                         | <1.32E-1                          |
| KDG061                   | 9.81±0.98E-3                          | 7.28±0.73E-3                          | 1.18±0.12E-2                                       | 4.66±0.63E-3                      | 2.89±0.40E-3                      | <2.33E-3                          | <2.56E-3                          | <4.25E-3                         | <7.05E-2                         | <2.66E-1                          |
| UGC05336                 | 2.47±0.25E-2                          | 2.05±0.20E-2                          | 1.47±0.15E-2                                       | 7.38±1.10E-3                      | 3.79±1.00E-3                      | <1.30E-2                          | <1.20E-2                          | <3.64E-2                         | <2.28E-1                         | <4.58E-1                          |
| ArpsLoop                 | <4.43E-2                              | <6.12E-2                              | <7.51E-2   | <3.70E-4                          | <5.50E-4                          | <2.01E-3                          | <2.20E-3                          | <3.66E-3                         | <4.91E-2                         | <1.85E-1                          |
| UGC05364 <sup>f</sup>    | <1.35E-1                              | <1.90E-1                              | <2.36E-1   | 1.95±0.26E-2                      | 1.36±0.19E-2                      | <7.13E-3                          | <7.77E-3                          | <6.49E-3                         | <8.75E-2                         | <3.30E-1                          |
| UGC05373 <sup>f</sup>    | 1.22±0.12E-1                          | 1.32±0.13E-1                          | 1.36±0.14E-1                                       | 4.97±0.67E-2                      | 3.61±0.50E-2                      | 1.51±0.19E-2                      | 1.55±0.19E-2                      | 2.10±0.23E-2                     | 1.21±0.19E-1                     | 1.88±0.39E-1                      |
| kkh057                   | <8.50E-3                              | <1.20E-2                              | <1.49E-2   | 6.00±0.80E-4                      | 2.20±0.30E-4                      | <4.60E-4                          | <5.00E-4                          | <1.65E-3                         | <2.23E-2                         | <8.30E-2                          |
| UGCA193                  | 1.58±0.16E-2                          | 1.21±0.12E-2                          | 1.91±0.19E-2                                       | 5.72±0.78E-3                      | 3.83±0.53E-3                      | 2.75±0.37E-3                      | 2.35±0.31E-3                      | 3.64±0.44E-3                     | 4.08±0.76E-2                     | 6.20±1.55E-1                      |
| NGC3109                  | 5.77±0.58E-1                          | 3.56±0.36E-1                          | 3.44±0.34E-1                                       | 2.34±0.32E-1                      | 1.73±0.24E-1                      | 1.10±0.14E-1                      | 1.20±0.15E-1                      | 2.56±0.28E-1                     | 6.75±0.82E 0                     | 1.21±0.19E-1                      |
| NGC3077 <sup>f</sup>     | 1.05±0.11E 0                          | 1.04±0.10E 0                          | 8.70±0.87E-1                                       | 5.54±0.75E-1                      | 3.75±0.51E-1                      | 4.34±0.55E-1                      | 8.11±1.01E-1                      | ...                              | ...                              | ...                               |
| AM1001-270 <sup>f</sup>  | <8.51E-3                              | <1.22E-2                              | <1.48E-2   | 3.26±0.44E-3                      | 2.25±0.31E-3                      | 2.80±0.29E-3                      | 3.08±0.33E-3                      | 3.41±0.30E-3                     | 4.58±0.74E-2                     | 1.73±0.25E-1                      |



Table 2—Continued

| Galaxy                  | 2MASS J<br>1.25 $\mu\text{m}$<br>(Jy) | 2MASS H<br>1.65 $\mu\text{m}$<br>(Jy) | 2MASS K <sub>s</sub><br>2.17 $\mu\text{m}$<br>(Jy) | IRAC<br>3.6 $\mu\text{m}$<br>(Jy) | IRAC<br>4.5 $\mu\text{m}$<br>(Jy) | IRAC<br>5.8 $\mu\text{m}$<br>(Jy) | IRAC<br>8.0 $\mu\text{m}$<br>(Jy) | MIPS<br>24 $\mu\text{m}$<br>(Jy) | MIPS<br>70 $\mu\text{m}$<br>(Jy) | MIPS<br>160 $\mu\text{m}$<br>(Jy) |
|-------------------------|---------------------------------------|---------------------------------------|--|-----------------------------------|-----------------------------------|-----------------------------------|-----------------------------------|----------------------------------|----------------------------------|-----------------------------------|
| BK05N                   | <4.85E-2                              | <6.74E-2                              | <8.30E-2   | 1.69±0.23E-3                      | 7.90±1.10E-4                      | <1.06E-3                          | <1.17E-3                          | <3.86E-3                         | <5.20E-2                         | <1.96E-1                          |
| UGC05428                | 1.41±0.14E-2                          | 1.28±0.13E-2                          | 1.03±0.10E-2                                       | 4.22±0.57E-3                      | 2.63±0.36E-3                      | <2.42E-3                          | <2.64E-3                          | <4.85E-3                         | <6.51E-2                         | <2.46E-1                          |
| UGC05423 <sup>e f</sup> | 1.20±0.12E-2                          | 1.37±0.14E-2                          | 1.36±0.14E-2                                       | 4.86±1.00E-3                      | 3.43±1.00E-3                      | 2.65±0.90E-3                      | 2.52±0.80E-3                      | 8.30±1.20E-3                     | 1.40±0.34E-1                     | 2.55±1.79E-1                      |
| UGC05442                | 1.51±0.15E-2                          | 1.46±0.15E-2                          | 1.33±0.13E-2                                       | 5.09±0.69E-3                      | 3.55±0.49E-3                      | 1.51±0.22E-3                      | 3.11±0.40E-3                      | 2.60±2.20E-4                     | <5.60E-2                         | <2.11E-1                          |
| UGC05456                | 3.80±0.38E-2                          | 5.01±0.50E-2                          | 3.10±0.31E-2                                       | 1.33±0.18E-2                      | 9.09±1.25E-3                      | 8.98±1.18E-3                      | 1.04±0.13E-2                      | 5.67±0.61E-2                     | 6.28±0.77E-1                     | 6.88±1.08E-1                      |
| IKN                     | <6.58E-2                              | <9.17E-2                              | <1.13E-1   | <2.20E-4                          | <3.30E-4                          | <1.22E-3                          | <1.34E-3                          | <4.45E-3                         | <6.00E-2                         | <2.27E-1                          |
| SextansA <sup>e f</sup> | <1.69E-1                              | <2.44E-1                              | <2.98E-1   | 3.24±0.44E-2                      | 2.18±0.30E-2                      | 2.66±0.34E-2                      | 1.77±0.22E-2                      | 3.05±0.33E-2                     | 7.05±0.87E-1                     | 9.76±1.55E-1                      |
| [HS98]117               | 5.42±0.54E-3                          | 6.82±0.68E-3                          | 9.03±0.90E-3                                       | 2.87±0.39E-3                      | 1.57±0.22E-3                      | <1.22E-3                          | <1.33E-3                          | <4.42E-3                         | <5.93E-2                         | <2.24E-1                          |
| NGC3239                 | 1.60±0.16E-1                          | 1.72±0.17E-1                          | 1.25±0.12E-1                                       | 7.42±1.00E-2                      | 4.97±0.68E-2                      | 7.47±0.96E-2                      | 8.72±1.09E-2                      | 3.58±0.39E-1                     | 4.95±0.60E 0                     | 7.40±1.16E 0                      |
| DDO078                  | <4.45E-2                              | <6.27E-2                              | <7.79E-2   | <1.90E-4                          | <2.80E-4                          | <1.03E-3                          | <1.12E-3                          | <3.74E-3                         | <5.04E-2                         | <1.91E-1                          |
| UGC05672                | 4.06±0.41E-2                          | 3.45±0.34E-2                          | 2.53±0.25E-2                                       | 1.19±0.16E-2                      | 7.71±1.06E-3                      | 7.16±0.94E-3                      | 6.96±0.88E-3                      | 8.49±0.95E-3                     | 7.49±1.16E-2                     | 3.93±0.63E-1                      |
| UGC05666 <sup>e f</sup> | 3.36±0.34E-1                          | 2.31±0.23E-1                          | 1.65±0.16E-1                                       | 1.51±0.21E-1                      | 9.05±1.27E-2                      | 6.48±0.87E-2                      | 6.63±0.89E-2                      | 2.74±0.13E-1                     | 5.19±0.43E 0                     | 1.05±0.15E 0                      |
| UGC05692                | 9.28±0.93E-2                          | 8.24±0.82E-2                          | 6.64±0.66E-2                                       | 2.69±0.36E-2                      | 1.77±0.24E-2                      | 1.66±0.21E-2                      | 1.12±0.14E-2                      | 1.12±0.13E-2                     | 2.98±0.38E-1                     | 6.14±0.98E-1                      |
| NGC3274                 | 4.24±0.42E-2                          | 4.15±0.41E-2                          | 3.59±0.36E-2                                       | 2.02±0.27E-2                      | 1.35±0.19E-2                      | 1.73±0.22E-2                      | 2.24±0.28E-2                      | 6.23±0.67E-2                     | 1.25±0.15E 0                     | 1.61±0.25E 0                      |
| BK06N                   | 8.54±0.85E-3                          | <1.16E-2                              | <1.23E-2   | 2.06±0.28E-3                      | 1.50±0.21E-3                      | <1.15E-3                          | <1.26E-3                          | <4.19E-3                         | <5.66E-2                         | <2.14E-1                          |
| NGC3299                 | 8.22±0.82E-2                          | 7.11±0.71E-2                          | 6.80±0.68E-2                                       | 2.99±0.40E-2                      | 2.04±0.28E-2                      | 1.83±0.24E-2                      | 2.83±0.35E-2                      | 2.48±0.27E-2                     | 3.03±0.38E-1                     | 1.03±0.16E 0                      |
| UGC05764                | 6.61±0.66E-3                          | 6.87±0.69E-3                          | 7.29±0.73E-3                                       | 2.66±0.36E-3                      | 1.89±0.26E-3                      | 1.25±0.18E-3                      | 1.02±0.14E-3                      | 3.45±0.40E-3                     | 6.03±0.87E-2                     | 8.71±1.67E-1                      |
| UGC05797                | 1.91±0.19E-2                          | 1.48±0.15E-2                          | 1.17±0.12E-2                                       | 6.48±0.88E-3                      | 4.08±0.56E-3                      | 3.74±0.50E-3                      | 3.01±0.39E-3                      | 4.29±0.50E-3                     | 1.11±0.15E-1                     | 2.27±0.37E-1                      |
| UGC05829                | 5.48±0.55E-2                          | 3.74±0.37E-2                          | 2.22±0.22E-2                                       | 1.36±0.18E-2                      | 9.20±1.26E-3                      | 5.90±0.77E-3                      | 6.46±0.82E-3                      | 3.16±0.34E-2                     | 7.17±0.88E-1                     | 9.06±1.43E-1                      |
| NGC3344 <sup>e</sup>    | 9.42±0.94E-1                          | 8.91±0.89E-1                          | 6.94±0.69E-1                                       | 4.01±0.54E-1                      | 2.49±0.34E-1                      | 4.74±0.60E-1                      | 9.74±1.21E-1                      | 1.18±0.13E 0                     | 1.51±0.18E 1                     | 5.12±0.80E 1                      |
| NGC3351 <sup>e f</sup>  | 1.68±0.17E 0                          | 1.77±0.18E 0                          | 1.54±0.15E 0                                       | 8.13±1.10E-1                      | 5.14±0.71E-1                      | 7.20±0.93E-1                      | 1.34±0.16E 0                      | 2.49±0.12E 0                     | 2.29±0.19E 1                     | 6.11±0.83E 1                      |
| NGC3368 <sup>e</sup>    | 2.29±0.23E 0                          | 2.52±0.25E 0                          | 2.11±0.21E 0                                       | 1.09±0.15E 0                      | 6.65±0.91E-1                      | 6.84±0.87E-1                      | 8.86±1.10E-1                      | 7.82±0.84E-1                     | 1.41±0.17E 1                     | 4.77±0.75E 1                      |
| UGC05889                | 3.39±0.34E-2                          | 3.91±0.39E-2                          | 3.03±0.30E-2                                       | 1.34±0.18E-2                      | 8.66±1.19E-3                      | 6.37±0.83E-3                      | 4.35±0.56E-3                      | 8.05±0.91E-3                     | <7.03E-2                         | <2.66E-1                          |
| UGC05923 <sup>e</sup>   | 2.63±0.26E-2                          | 2.92±0.29E-2                          | 2.18±0.22E-2                                       | 9.64±1.31E-3                      | 6.38±0.88E-3                      | 6.03±0.80E-3                      | 9.36±1.19E-3                      | 1.09±0.12E-2                     | 2.46±0.30E-1                     | 2.33±0.37E-1                      |
| UGC05918                | <3.53E-2                              | <4.00E-2                              | <4.97E-2   | 3.00±0.41E-3                      | 2.00±0.28E-3                      | <1.83E-3                          | <2.00E-3                          | <3.33E-3                         | <4.50E-2                         | <1.70E-1                          |
| NGC3432                 | 2.03±0.20E-1                          | 2.10±0.21E-1                          | 1.71±0.17E-1                                       | 1.02±0.14E-1                      | 7.38±1.01E-2                      | 1.36±0.17E-1                      | 2.29±0.29E-1                      | 5.99±0.65E-1                     | 9.67±1.18E 0                     | 1.85±0.29E 0                      |
| KDG073                  | <2.85E-2                              | <4.02E-2                              | <5.00E-2   | 1.94±0.26E-3                      | 6.10±0.80E-4                      | <8.20E-4                          | <9.00E-4                          | ...                              | ...                              | ...                               |
| NGC3486 <sup>e</sup>    | 4.80±0.48E-1                          | 5.82±0.58E-1                          | 4.47±0.45E-1                                       | 2.36±0.32E-1                      | 1.58±0.22E-1                      | 2.60±0.33E-1                      | 5.88±0.73E-1                      | 6.41±0.69E-1                     | 9.65±1.18E 0                     | 2.70±0.42E 0                      |
| NGC3510                 | 5.82±0.58E-2                          | 3.81±0.38E-2                          | 2.32±0.23E-2                                       | 2.07±0.28E-2                      | 1.45±0.20E-2                      | 1.52±0.20E-2                      | 2.31±0.29E-2                      | 5.34±0.58E-2                     | 1.18±0.14E 0                     | 1.82±0.28E 0                      |
| NGC3521 <sup>e f</sup>  | 3.74±0.37E 0                          | 4.22±0.42E 0                          | 3.50±0.35E 0                                       | 2.05±0.28E 0                      | 1.36±0.19E 0                      | 2.53±0.32E 0                      | 6.27±0.76E 0                      | 5.51±0.22E 0                     | 6.26±0.45E 1                     | 2.12±0.27E 1                      |
| NGC3593 <sup>e</sup>    | 7.76±0.78E-1                          | 9.45±0.94E-1                          | 7.66±0.77E-1                                       | 3.75±0.51E-1                      | 2.51±0.34E-1                      | 5.26±0.67E-1                      | 1.21±0.15E 0                      | 1.69±0.18E 0                     | 2.22±0.27E 1                     | 3.31±0.52E 1                      |
| NGC3623                 | 2.89±0.29E 0                          | 3.20±0.32E 0                          | 2.65±0.27E 0                                       | 1.27±0.17E 0                      | 7.95±1.09E-1                      | 7.43±0.94E-1                      | 7.67±0.96E-1                      | 5.55±0.60E-1                     | 7.01±0.86E 0                     | 3.57±0.56E 0                      |
| NGC3627 <sup>e f</sup>  | 3.34±0.33E 0                          | 3.73±0.37E 0                          | 3.17±0.32E 0                                       | 1.87±0.25E 0                      | 1.25±0.17E 0                      | 2.35±0.30E 0                      | 5.58±0.69E 0                      | 7.43±0.30E 0                     | 9.22±0.70E 1                     | 2.20±0.28E 1                      |

Table 2—Continued

| Galaxy                     | 2MASS J<br>1.25 $\mu\text{m}$<br>(Jy) | 2MASS H<br>1.65 $\mu\text{m}$<br>(Jy) | 2MASS K <sub>s</sub><br>2.17 $\mu\text{m}$<br>(Jy) | IRAC<br>3.6 $\mu\text{m}$<br>(Jy) | IRAC<br>4.5 $\mu\text{m}$<br>(Jy) | IRAC<br>5.8 $\mu\text{m}$<br>(Jy) | IRAC<br>8.0 $\mu\text{m}$<br>(Jy) | MIPS<br>24 $\mu\text{m}$<br>(Jy) | MIPS<br>70 $\mu\text{m}$<br>(Jy) | MIPS<br>160 $\mu\text{m}$<br>(Jy) |
|----------------------------|---------------------------------------|---------------------------------------|--|-----------------------------------|-----------------------------------|-----------------------------------|-----------------------------------|----------------------------------|----------------------------------|-----------------------------------|
| NGC3628                    | 2.43±0.24E 0                          | 2.98±0.30E 0                          | 2.66±0.27E 0                                       | 1.52±0.21E 0                      | 1.04±0.14E 0                      | 1.86±0.23E 0                      | 4.08±0.51E 0                      | 5.10±0.55E 0                     | 6.26±0.76E 1                     | 1.90±0.3                          |
| UGC06457                   | 1.52±0.15E-2                          | 1.65±0.17E-2                          | 1.18±0.12E-2                                       | 5.52±0.75E-3                      | 3.13±0.43E-3                      | 2.92±0.39E-3                      | 2.31±0.30E-3                      | 2.07±0.29E-3                     | 1.09±0.14E-1                     | 1.39±0.2                          |
| UGC06541 <sup>e</sup>      | 1.13±0.11E-2                          | 1.26±0.13E-2                          | 1.26±0.13E-2                                       | 5.28±0.72E-3                      | 3.88±0.53E-3                      | 1.98±0.27E-3                      | 2.29±0.30E-3                      | 6.57±0.72E-3                     | 1.95±0.24E-1                     | 7.30±1.4                          |
| NGC3738 <sup>e</sup>       | 1.32±0.13E-1                          | 1.40±0.14E-1                          | 1.04±0.10E-1                                       | 6.03±0.82E-2                      | 4.02±0.55E-2                      | 4.22±0.55E-2                      | 5.09±0.64E-2                      | 1.24±0.13E-1                     | 2.71±0.33E 0                     | 3.21±0.5                          |
| NGC3741                    | 1.13±0.11E-2                          | 1.83±0.18E-2                          | 1.12±0.11E-2                                       | 4.61±0.63E-3                      | 3.19±0.44E-3                      | 2.20±0.30E-3                      | 1.16±0.16E-3                      | 5.71±0.64E-3                     | 1.75±0.22E-1                     | 1.20±0.2                          |
| UGC06782                   | <3.29E-2                              | <4.63E-2                              | <5.74E-2   | 2.76±0.38E-3                      | 1.90±0.26E-3                      | 1.46±0.17E-3                      | 1.58±0.25E-3                      | 2.64±0.18E-3                     | 3.57±0.49E-2                     | 1.35±0.1                          |
| UGC06817                   | 2.33±0.23E-2                          | 2.62±0.26E-2                          | 2.15±0.22E-2                                       | 9.23±1.25E-3                      | 5.51±0.76E-3                      | 4.28±0.57E-3                      | 2.21±0.30E-3                      | 7.25±0.83E-3                     | 1.33±0.18E-1                     | 2.28±0.4                          |
| UGC06900                   | 2.38±0.24E-2                          | 1.82±0.18E-2                          | 1.81±0.18E-2                                       | 7.68±1.04E-3                      | 5.39±0.74E-3                      | 5.47±0.72E-3                      | 4.25±0.54E-3                      | 4.13±0.51E-3                     | <6.16E-2                         | <2.3                              |
| NGC4020                    | 6.58±0.66E-2                          | 5.44±0.54E-2                          | 5.91±0.59E-2                                       | 3.12±0.42E-2                      | 2.04±0.28E-2                      | 3.40±0.44E-2                      | 6.82±0.86E-2                      | 9.39±1.01E-2                     | 1.25±0.15E 0                     | 3.66±0.5                          |
| NGC4068                    | 5.05±0.50E-2                          | 4.16±0.42E-2                          | 3.72±0.37E-2                                       | 2.42±0.33E-2                      | 1.69±0.23E-2                      | 1.20±0.16E-2                      | 9.10±1.15E-3                      | 3.22±0.35E-2                     | 7.02±0.86E-1                     | 9.26±1.4                          |
| NGC4080                    | 5.25±0.52E-2                          | 5.12±0.51E-2                          | 3.45±0.34E-2                                       | 1.85±0.25E-2                      | 1.21±0.17E-2                      | 1.77±0.23E-2                      | 3.94±0.50E-2                      | 3.47±0.38E-2                     | 4.34±0.53E-1                     | 1.46±0.2                          |
| NGC4096                    | 5.58±0.56E-1                          | 6.22±0.62E-1                          | 5.35±0.54E-1                                       | 2.91±0.39E-1                      | 2.00±0.27E-1                      | 3.91±0.50E-1                      | 8.77±1.09E-1                      | 8.74±0.94E-1                     | 1.09±0.13E 1                     | 4.08±0.6                          |
| NGC4144 <sup>e</sup>       | 1.60±0.16E-1                          | 1.55±0.16E-1                          | 1.24±0.12E-1                                       | 7.01±0.95E-2                      | 4.81±0.66E-2                      | 4.45±0.57E-2                      | 6.14±0.77E-2                      | 1.13±0.12E-1                     | 2.37±0.29E 0                     | 5.12±0.8                          |
| NGC4163                    | 5.98±0.60E-2                          | 4.39±0.44E-2                          | 3.26±0.33E-2                                       | 1.73±0.23E-2                      | 1.15±0.16E-2                      | 7.26±0.95E-3                      | 5.64±0.71E-3                      | 1.24±0.14E-2                     | 1.78±0.23E-1                     | 2.38±0.4                          |
| NGC4190                    | 5.96±0.60E-2                          | 4.99±0.50E-2                          | 3.69±0.37E-2                                       | 1.83±0.25E-2                      | 1.20±0.16E-2                      | 9.91±1.29E-3                      | 5.83±0.74E-3                      | 1.78±0.19E-2                     | 5.65±0.69E-1                     | 6.94±1.1                          |
| ESO321-G014                | 1.18±0.12E-2                          | 9.34±0.93E-3                          | <7.33E-2   | 5.08±0.69E-3                      | 3.52±0.48E-3                      | 9.10±1.50E-4                      | 1.17±0.17E-3                      | 4.00±1.90E-4                     | <4.79E-2                         | <1.8                              |
| UGC07242                   | <2.97E-2                              | <4.19E-2                              | <4.96E-2   | <1.50E-4                          | <2.30E-4                          | <8.50E-4                          | <9.20E-4                          | <3.07E-3                         | <4.15E-2                         | <1.5                              |
| UGCA276                    | 1.24±0.12E-2                          | 7.66±0.77E-3                          | 4.49±0.45E-3                                       | 2.69±0.36E-3                      | 1.52±0.21E-3                      | <1.10E-3                          | <1.21E-3                          | <4.02E-3                         | <5.42E-2                         | <2.0                              |
| UGC07267                   | 2.50±0.25E-2                          | 1.98±0.20E-2                          | 1.75±0.18E-2                                       | 7.27±0.99E-3                      | 4.82±0.66E-3                      | 2.65±0.36E-3                      | 1.73±0.23E-3                      | 3.57±0.43E-3                     | 6.92±1.02E-2                     | 1.80±0.3                          |
| NGC4214 <sup>e</sup>       | 5.86±0.59E-1                          | 6.39±0.64E-1                          | 4.88±0.49E-1                                       | 3.11±0.42E-1                      | 2.14±0.29E-1                      | 3.27±0.41E-1                      | 5.43±0.68E-1                      | 2.00±0.22E 0                     | 2.20±0.27E 1                     | 3.79±0.5                          |
| CGCG269-049 <sup>e f</sup> | 4.91±0.49E-3                          | 6.62±0.66E-3                          | 3.31±0.33E-3                                       | 1.49±0.20E-3                      | 1.16±0.16E-3                      | 6.30±1.00E-4                      | 6.20±0.90E-4                      | 2.87±0.33E-3                     | 4.63±0.65E-2                     | <1.0                              |
| NGC4236 <sup>e f</sup>     | 6.35±0.63E-1                          | 8.31±0.83E-1                          | 5.70±0.57E-1                                       | 2.50±0.34E-1                      | 2.10±0.29E-1                      | 1.07±0.14E-1                      | 2.16±0.27E-1                      | 5.47±0.22E-1                     | 8.18±0.59E 0                     | 1.96±0.2                          |
| NGC4244 <sup>e f</sup>     | 6.73±0.67E-1                          | 6.86±0.69E-1                          | 5.78±0.58E-1                                       | 3.05±0.41E-1                      | 2.10±0.29E-1                      | 2.08±0.26E-1                      | 2.87±0.36E-1                      | 4.58±0.49E-1                     | 7.44±0.91E 0                     | 2.35±0.3                          |
| NGC4242 <sup>e</sup>       | 1.94±0.19E-1                          | 2.40±0.24E-1                          | 1.60±0.16E-1                                       | 1.03±0.14E-1                      | 6.15±0.84E-2                      | 6.34±0.81E-2                      | 9.90±1.23E-2                      | 1.07±0.12E-1                     | 1.98±0.24E 0                     | 7.00±1.0                          |
| UGC07321 <sup>e f</sup>    | 4.37±0.44E-2                          | 4.75±0.47E-2                          | 3.86±0.39E-2                                       | 2.28±0.31E-2                      | 1.46±0.20E-2                      | 1.71±0.22E-2                      | 2.37±0.30E-2                      | 2.98±0.32E-2                     | 5.87±0.72E-1                     | 1.99±0.3                          |
| NGC4248                    | 8.41±0.84E-2                          | 7.31±0.73E-2                          | 6.94±0.69E-2                                       | 4.13±0.56E-2                      | 2.50±0.34E-2                      | 2.43±0.31E-2                      | 3.09±0.39E-2                      | 3.43±0.37E-2                     | 4.95±0.61E-1                     | 1.28±0.2                          |
| NGC4258 <sup>e</sup>       | 5.03±0.50E 0                          | 5.50±0.55E 0                          | 4.63±0.46E 0                                       | 2.28±0.31E 0                      | 1.50±0.21E 0                      | 1.18±0.15E 0                      | 2.52±0.31E 0                      | 2.77±0.30E 0                     | 3.95±0.48E 1                     | 1.40±0.2                          |
| ISZ399                     | 3.54±0.35E-2                          | 3.99±0.40E-2                          | 3.45±0.34E-2                                       | 2.26±0.31E-2                      | 1.60±0.22E-2                      | 4.91±0.65E-2                      | 1.22±0.15E-1                      | 4.36±0.47E-1                     | 2.92±0.36E 0                     | 2.22±0.3                          |
| NGC4288                    | 5.35±0.54E-2                          | 6.46±0.65E-2                          | 3.25±0.33E-2                                       | 2.38±0.32E-2                      | 1.53±0.21E-2                      | 2.28±0.30E-2                      | 4.15±0.52E-2                      | 6.80±0.73E-2                     | 1.37±0.17E 0                     | 2.71±0.4                          |
| UGC07408                   | 4.48±0.45E-2                          | 3.67±0.37E-2                          | 3.29±0.33E-2                                       | 1.31±0.18E-2                      | 7.74±1.06E-3                      | 6.22±0.81E-3                      | 5.04±0.64E-3                      | <5.46E-3                         | <7.36E-2                         | <1.2                              |
| UGC07490                   | 7.21±0.72E-2                          | 8.07±0.81E-2                          | 6.83±0.68E-2                                       | 2.48±0.34E-2                      | 1.68±0.23E-2                      | 1.57±0.20E-2                      | 1.88±0.23E-2                      | 2.24±0.24E-2                     | 3.86±0.48E-1                     | 1.39±0.2                          |
| NGC4395                    | 4.68±0.47E-1                          | 4.45±0.44E-1                          | 3.20±0.32E-1                                       | 3.20±0.43E-1                      | 2.54±0.35E-1                      | 2.49±0.31E-1                      | 2.59±0.32E-1                      | 5.09±0.55E-1                     | 1.06±0.13E 1                     | 2.73±0.4                          |
| UGCA281 <sup>f</sup>       | 7.42±0.74E-3                          | 8.22±0.82E-3                          | 7.28±0.73E-3                                       | 3.64±0.50E-3                      | 2.64±0.36E-3                      | 1.79±0.25E-3                      | 1.77±0.23E-3                      | 6.12±0.66E-2                     | 4.47±0.55E-1                     | 1.73±0.2                          |

Table 2—Continued

| Galaxy                  | 2MASS J<br>1.25 $\mu\text{m}$<br>(Jy) | 2MASS H<br>1.65 $\mu\text{m}$<br>(Jy) | 2MASS K <sub>s</sub><br>2.17 $\mu\text{m}$<br>(Jy) | IRAC<br>3.6 $\mu\text{m}$<br>(Jy) | IRAC<br>4.5 $\mu\text{m}$<br>(Jy) | IRAC<br>5.8 $\mu\text{m}$<br>(Jy) | IRAC<br>8.0 $\mu\text{m}$<br>(Jy) | MIPS<br>24 $\mu\text{m}$<br>(Jy) | MIPS<br>70 $\mu\text{m}$<br>(Jy) | MIPS<br>160 $\mu\text{m}$<br>(Jy) |
|-------------------------|---------------------------------------|---------------------------------------|--|-----------------------------------|-----------------------------------|-----------------------------------|-----------------------------------|----------------------------------|----------------------------------|-----------------------------------|
| UGC07559                | 1.50±0.15E-2                          | 1.50±0.15E-2                          | 1.12±0.11E-2                                       | 5.95±0.81E-3                      | 3.78±0.52E-3                      | 2.13±0.29E-3                      | 1.83±0.24E-3                      | 6.45±0.72E-3                     | 1.51±0.19E-1                     | 1.74±0.29E-                       |
| UGC07577                | 7.76±0.78E-2                          | 7.78±0.78E-2                          | 4.19±0.42E-2                                       | 2.60±0.35E-2                      | 1.48±0.20E-2                      | 7.79±1.01E-3                      | 4.08±0.53E-3                      | 7.97±0.93E-3                     | 1.01±0.16E-1                     | 4.69±0.77E-                       |
| NGC4449 <sup>e</sup>    | 1.03±0.10E 0                          | 1.11±0.11E 0                          | 8.93±0.89E-1                                       | 4.81±0.65E-1                      | 3.14±0.43E-1                      | 6.32±0.80E-1                      | 1.35±0.17E 0                      | 3.21±0.35E 0                     | 4.49±0.55E 1                     | 8.43±1.32E                        |
| UGC07599                | 6.60±0.66E-3                          | 9.16±0.92E-3                          | 4.01±0.40E-3                                       | 2.71±0.37E-3                      | 1.49±0.21E-3                      | 2.35±0.24E-3                      | 2.56±0.26E-3                      | 2.13±0.15E-3                     | 2.88±0.40E-2                     | 1.09±0.15E-                       |
| UGC07605                | 1.39±0.14E-2                          | 1.11±0.11E-2                          | 6.09±0.61E-3                                       | 4.31±0.59E-3                      | 2.41±0.33E-3                      | 1.61±0.19E-3                      | 1.76±0.20E-3                      | 1.63±0.23E-3                     | 5.60±0.82E-2                     | 1.49±0.21E-                       |
| NGC4455                 | 5.22±0.52E-2                          | 5.47±0.55E-2                          | 4.28±0.43E-2                                       | 2.17±0.30E-2                      | 1.46±0.20E-2                      | 1.36±0.18E-2                      | 1.62±0.20E-2                      | 3.41±0.37E-2                     | 9.52±1.16E-1                     | 1.95±0.30E                        |
| UGC07608                | 2.12±0.21E-2                          | 1.55±0.15E-2                          | 1.49±0.15E-2                                       | 5.57±0.76E-3                      | 3.62±0.50E-3                      | 2.62±0.35E-3                      | 3.49±0.45E-3                      | 1.94±0.21E-2                     | 2.36±0.29E-1                     | 3.15±0.51E-                       |
| NGC4460 <sup>e</sup>    | 1.92±0.19E-1                          | 2.03±0.20E-1                          | 1.95±0.19E-1                                       | 8.35±1.13E-2                      | 5.62±0.77E-2                      | 7.77±1.00E-2                      | 1.24±0.16E-1                      | 3.05±0.33E-1                     | 3.71±0.45E 0                     | 5.42±0.85E                        |
| UGC07639                | 2.54±0.25E-2                          | 2.67±0.27E-2                          | 2.64±0.26E-2                                       | 1.14±0.15E-2                      | 7.69±1.06E-3                      | 4.53±0.60E-3                      | 3.29±0.42E-3                      | 5.57±0.65E-3                     | 1.19±0.16E-1                     | 1.19±0.24E-                       |
| NGC4485 <sup>e</sup>    | 9.47±0.95E-2                          | 9.93±0.99E-2                          | 6.95±0.69E-2                                       | 4.25±0.58E-2                      | 2.97±0.41E-2                      | 5.72±0.75E-2                      | 9.46±1.19E-2                      | 1.87±0.20E-1                     | 3.09±0.38E 0                     | 9.62±1.50E                        |
| NGC4490 <sup>e</sup>    | 9.34±0.93E-1                          | 9.35±0.93E-1                          | 8.14±0.81E-1                                       | 4.71±0.64E-1                      | 3.23±0.44E-1                      | 7.92±1.01E-1                      | 1.69±0.21E 0                      | 4.29±0.46E 0                     | 6.29±0.77E 1                     | 1.07±0.17E                        |
| UGC07690                | 4.76±0.48E-2                          | 5.26±0.53E-2                          | 2.77±0.28E-2                                       | 1.86±0.25E-2                      | 1.26±0.17E-2                      | 1.09±0.14E-2                      | 1.18±0.15E-2                      | 3.01±0.33E-2                     | 7.88±0.96E-1                     | 1.18±0.18E                        |
| UGC07699                | 5.39±0.54E-2                          | 7.75±0.77E-2                          | 5.35±0.54E-2                                       | 2.24±0.30E-2                      | 1.43±0.20E-2                      | 1.50±0.19E-2                      | 2.00±0.25E-2                      | 3.75±0.41E-2                     | 7.21±0.88E-1                     | 1.54±0.24E                        |
| UGC07698                | 2.61±0.26E-2                          | 2.58±0.26E-2                          | 2.11±0.21E-2                                       | 8.48±1.15E-3                      | 6.98±0.96E-3                      | 4.84±0.91E-3                      | 1.08±0.14E-2                      | 9.86±1.09E-3                     | 1.81±0.23E-1                     | 4.04±0.65E-                       |
| UGC07719                | 1.02±0.10E-2                          | 1.76±0.18E-2                          | 8.71±0.87E-3                                       | 4.66±0.63E-3                      | 3.10±0.43E-3                      | 1.71±0.24E-3                      | 1.22±0.17E-3                      | 1.34±0.14E-2                     | 2.20±0.27E-1                     | 1.31±0.23E-                       |
| UGC07774                | 2.03±0.20E-2                          | 2.81±0.28E-2                          | 1.48±0.15E-2                                       | 9.08±1.23E-3                      | 5.52±0.76E-3                      | 3.97±0.53E-3                      | 5.24±0.67E-3                      | 9.34±1.02E-3                     | 1.44±0.18E-1                     | 3.68±0.58E-                       |
| UGCA292 <sup>e f</sup>  | <5.69E-3                              | <8.04E-3                              | <1.00E-2   | 1.68±0.23E-3                      | 5.80±0.80E-4                      | <6.80E-4                          | 3.00±0.39E-3                      | <2.47E-3                         | 3.91±0.61E-2                     | <1.26E-                           |
| NGC4594 <sup>e f</sup>  | 8.07±0.81E 0                          | 9.20±0.92E 0                          | 7.56±0.76E 0                                       | 3.94±0.53E 0                      | 2.31±0.32E 0                      | 1.73±0.22E 0                      | 1.30±0.16E 0                      | 6.74±0.43E-1                     | 7.36±0.68E 0                     | 3.61±0.56E                        |
| NGC4605                 | 6.49±0.65E-1                          | 6.92±0.69E-1                          | 5.61±0.56E-1                                       | 3.25±0.44E-1                      | 2.27±0.31E-1                      | 3.88±0.49E-1                      | 7.36±0.92E-1                      | 1.05±0.11E 0                     | 2.04±0.25E 1                     | 3.74±0.58E                        |
| NGC4618 <sup>e</sup>    | 2.81±0.28E-1                          | 3.26±0.33E-1                          | 2.44±0.24E-1                                       | 1.58±0.21E-1                      | 1.04±0.14E-1                      | 1.72±0.22E-1                      | 3.27±0.41E-1                      | 4.01±0.43E-1                     | 7.89±0.96E 0                     | 1.73±0.27E                        |
| NGC4625 <sup>e f</sup>  | 9.82±0.98E-2                          | 1.13±0.11E-1                          | 8.98±0.90E-2                                       | 4.85±0.64E-2                      | 3.02±0.40E-2                      | 5.85±0.76E-2                      | 1.29±0.16E-1                      | 1.36±0.06E-1                     | 2.07±0.16E 0                     | 5.07±0.68E                        |
| NGC4631 <sup>e f</sup>  | 1.75±0.17E 0                          | 1.98±0.20E 0                          | 1.84±0.18E 0                                       | 1.26±0.17E 0                      | 8.36±1.15E-1                      | 2.45±0.31E 0                      | 5.86±0.73E 0                      | 8.15±0.33E 0                     | 1.30±0.10E 2                     | 2.76±0.35E                        |
| UGC07866                | 2.26±0.23E-2                          | 2.87±0.29E-2                          | 3.16±0.32E-2                                       | 8.46±1.15E-3                      | 5.12±0.70E-3                      | 2.53±0.34E-3                      | 2.86±0.37E-3                      | 6.76±0.76E-3                     | 2.42±0.30E-1                     | 2.35±0.39E-                       |
| NGC4656                 | 2.01±0.20E-1                          | 1.90±0.19E-1                          | 1.35±0.14E-1                                       | 9.54±1.29E-2                      | 7.05±0.97E-2                      | 7.65±0.97E-2                      | 1.02±0.13E-1                      | 5.41±0.58E-1                     | 9.23±1.13E 0                     | 1.23±0.19E                        |
| UGC07916                | <3.46E-2                              | <4.89E-2                              | <6.08E-2   | 2.51±0.34E-3                      | 1.71±0.24E-3                      | 9.50±1.30E-4                      | 1.06±0.14E-3                      | 6.33±0.69E-3                     | 6.98±0.91E-2                     | 8.10±1.42E-                       |
| UGC07950                | 3.63±0.36E-2                          | 4.17±0.42E-2                          | 3.19±0.32E-2                                       | 1.07±0.14E-2                      | 7.41±1.02E-3                      | 7.12±0.94E-3                      | 4.30±0.55E-3                      | 1.16±0.13E-2                     | 3.03±0.37E-1                     | 4.16±0.66E-                       |
| UGC07949                | 9.22±0.92E-3                          | 1.05±0.10E-2                          | 6.88±0.69E-3                                       | 3.24±0.44E-3                      | <8.20E-4                          | <1.51E-3                          | <1.64E-3                          | 2.19±0.28E-3                     | <3.68E-2                         | <1.39E-                           |
| NGC4707                 | 2.39±0.24E-2                          | 2.30±0.23E-2                          | 1.62±0.16E-2                                       | 1.09±0.15E-2                      | 6.28±0.86E-3                      | 5.09±0.67E-3                      | 4.30±0.55E-3                      | 1.11±0.12E-2                     | 2.28±0.29E-1                     | 4.67±0.75E-                       |
| NGC4736 <sup>e f</sup>  | 6.95±0.69E 0                          | 7.68±0.77E 0                          | 6.44±0.64E 0                                       | 3.60±0.49E 0                      | 2.32±0.32E 0                      | 2.72±0.35E 0                      | 5.17±0.64E 0                      | 5.65±0.23E 0                     | 9.39±0.73E 1                     | 1.74±0.21E                        |
| UGC08024 <sup>e f</sup> | 9.92±0.99E-3                          | 1.24±0.12E-2                          | 1.20±0.12E-2                                       | 4.07±1.00E-3                      | 2.99±1.00E-3                      | <5.81E-3                          | <3.99E-3                          | 7.40±1.10E-3                     | 5.70±5.02E-2                     | 2.62±1.25E-                       |
| NGC4826 <sup>e f</sup>  | 5.68±0.57E 0                          | 6.31±0.63E 0                          | 5.28±0.53E 0                                       | 2.52±0.34E 0                      | 1.57±0.22E 0                      | 1.64±0.21E 0                      | 2.35±0.29E 0                      | 2.52±0.15E 0                     | 5.07±0.51E 1                     | 8.70±1.27E                        |
| UGC08091 <sup>f</sup>   | 8.86±0.89E-3                          | 1.21±0.12E-2                          | 8.40±0.84E-3                                       | 3.06±0.42E-3                      | 2.29±0.32E-3                      | 1.57±0.22E-3                      | 1.47±0.20E-3                      | 4.29±0.49E-3                     | 1.56±0.20E-1                     | 1.48±0.25E-                       |
| UGCA319                 | 1.22±0.12E-2                          | 1.39±0.14E-2                          | 1.28±0.13E-2                                       | 5.50±0.75E-3                      | 3.51±0.48E-3                      | 2.50±0.34E-3                      | 5.15±0.65E-3                      | <2.55E-3                         | <3.43E-2                         | <1.30E-                           |

Table 2—Continued

| Galaxy                  | 2MASS J<br>1.25 $\mu\text{m}$<br>(Jy) | 2MASS H<br>1.65 $\mu\text{m}$<br>(Jy) | 2MASS K <sub>s</sub><br>2.17 $\mu\text{m}$<br>(Jy) | IRAC<br>3.6 $\mu\text{m}$<br>(Jy) | IRAC<br>4.5 $\mu\text{m}$<br>(Jy) | IRAC<br>5.8 $\mu\text{m}$<br>(Jy) | IRAC<br>8.0 $\mu\text{m}$<br>(Jy) | MIPS<br>24 $\mu\text{m}$<br>(Jy) | MIPS<br>70 $\mu\text{m}$<br>(Jy) | MIPS<br>160 $\mu\text{m}$<br>(Jy) |
|-------------------------|---------------------------------------|---------------------------------------|--|-----------------------------------|-----------------------------------|-----------------------------------|-----------------------------------|----------------------------------|----------------------------------|-----------------------------------|
| UGCA320                 | 3.51±0.35E-2                          | 4.67±0.47E-2                          | <3.27E-1   | 1.80±0.24E-2                      | 1.45±0.20E-2                      | 3.23±0.42E-3                      | 3.42±0.43E-3                      | 2.33±0.25E-2                     | 5.17±0.63E-1                     | 4.92±0.70E-1                      |
| UGC08188                | 1.18±0.12E-1                          | 1.70±0.17E-1                          | 1.22±0.12E-1                                       | 5.96±0.81E-2                      | 4.47±0.61E-2                      | 4.11±0.52E-2                      | 3.56±0.44E-2                      | 6.88±0.74E-2                     | 1.52±0.19E 0                     | 2.88±0.41E-1                      |
| UGC08201 <sup>e f</sup> | 3.20±0.32E-2                          | 4.69±0.47E-2                          | 3.73±0.37E-2                                       | 1.56±0.23E-2                      | 1.18±0.15E-2                      | 5.35±1.70E-3                      | 4.08±0.80E-3                      | 1.42±0.10E-2                     | 1.43±0.69E-1                     | 2.88±2.50E-1                      |
| MCG-03-34-002           | 1.72±0.17E-2                          | 1.78±0.18E-2                          | 2.22±0.22E-2                                       | 7.24±0.98E-3                      | 5.10±0.70E-3                      | 4.03±0.54E-3                      | 2.93±0.38E-3                      | 6.79±0.74E-3                     | 1.15±0.15E-1                     | 1.09±0.19E-1                      |
| UGC08245                | 1.78±0.18E-2                          | 1.67±0.17E-2                          | 1.39±0.14E-2                                       | 9.41±1.28E-3                      | 5.98±0.82E-3                      | 2.63±0.36E-3                      | 2.89±0.37E-3                      | 4.22±0.50E-3                     | 9.64±1.32E-2                     | 2.42±0.40E-1                      |
| NGC5023 <sup>e</sup>    | 9.86±0.99E-2                          | 1.04±0.10E-1                          | 8.98±0.90E-2                                       | 4.50±0.61E-2                      | 2.87±0.39E-2                      | 2.48±0.32E-2                      | 1.99±0.25E-2                      | 5.68±0.61E-2                     | 9.49±1.16E-1                     | 2.30±0.30E-1                      |
| CGCG217-018             | 1.60±0.16E-2                          | 2.13±0.21E-2                          | 1.62±0.16E-2                                       | 6.64±0.90E-3                      | 4.24±0.58E-3                      | 3.89±0.52E-3                      | 4.72±0.60E-3                      | 1.19±0.13E-2                     | 1.70±0.21E-1                     | 1.91±0.31E-1                      |
| UGC08313                | 1.81±0.18E-2                          | 2.88±0.29E-2                          | 2.41±0.24E-2                                       | 9.25±1.25E-3                      | 5.89±0.81E-3                      | 5.70±0.75E-3                      | 7.10±0.90E-3                      | 2.78±0.30E-2                     | 2.36±0.29E-1                     | 3.57±0.57E-1                      |
| UGC08320                | 5.83±0.58E-2                          | 6.20±0.62E-2                          | 5.02±0.50E-2                                       | 1.98±0.27E-2                      | 1.47±0.20E-2                      | 5.37±0.71E-3                      | 7.10±0.90E-3                      | 1.69±0.19E-2                     | 5.64±0.70E-1                     | 7.76±1.20E-1                      |
| UGC08331                | 2.18±0.22E-2                          | 2.33±0.23E-2                          | 1.58±0.16E-2                                       | 6.45±0.87E-3                      | 4.49±0.62E-3                      | 2.25±0.31E-3                      | 2.21±0.29E-3                      | 6.98±0.79E-3                     | 1.67±0.22E-1                     | 3.85±0.63E-1                      |
| NGC5055 <sup>e f</sup>  | 4.21±0.42E 0                          | 4.96±0.50E 0                          | 4.05±0.41E 0                                       | 2.38±0.32E 0                      | 1.55±0.21E 0                      | 2.63±0.34E 0                      | 5.64±0.70E 0                      | 5.74±0.23E 0                     | 7.27±0.52E 1                     | 2.95±0.37E-1                      |
| NGC5068                 | 8.64±0.86E-1                          | 8.12±0.81E-1                          | 7.10±0.71E-1                                       | 4.59±0.62E-1                      | 3.26±0.45E-1                      | 4.87±0.61E-1                      | 1.24±0.15E 0                      | 1.37±0.15E 0                     | 2.08±0.25E 1                     | 5.42±0.80E-1                      |
| IC4247                  | 1.85±0.19E-2                          | 1.57±0.16E-2                          | 1.39±0.14E-2                                       | 6.36±0.86E-3                      | 4.33±0.60E-3                      | 2.07±0.28E-3                      | 1.90±0.25E-3                      | ...                              | ...                              | ...                               |
| NGC5204 <sup>e</sup>    | 1.43±0.14E-1                          | 1.48±0.15E-1                          | 1.12±0.11E-1                                       | 6.80±0.92E-2                      | 4.59±0.63E-2                      | 5.04±0.65E-2                      | 8.22±1.03E-2                      | 1.78±0.19E-1                     | 4.01±0.49E 0                     | 7.36±1.11E-1                      |
| NGC5194 <sup>e f</sup>  | 4.99±0.50E 0                          | 5.89±0.59E 0                          | 4.52±0.45E 0                                       | 2.66±0.36E 0                      | 1.80±0.26E 0                      | 4.23±0.54E 0                      | 1.06±0.13E 1                      | 1.27±0.05E 1                     | 1.47±0.11E 2                     | 4.91±0.60E-1                      |
| NGC5195 <sup>e f</sup>  | 2.37±0.24E 0                          | 2.80±0.28E 0                          | 2.25±0.23E 0                                       | 8.34±1.13E-1                      | 5.11±0.70E-1                      | 4.62±0.61E-1                      | 6.46±0.81E-1                      | 1.39±0.27E 0                     | 1.55±0.33E 1                     | 1.34±0.30E-1                      |
| UGC08508                | 2.18±0.22E-2                          | 2.13±0.21E-2                          | 1.39±0.14E-2                                       | 8.43±1.14E-3                      | 5.10±0.70E-3                      | 3.91±0.52E-3                      | 4.27±0.54E-3                      | 6.27±0.70E-3                     | 1.46±0.19E-1                     | 1.95±0.33E-1                      |
| NGC5229                 | 3.60±0.36E-2                          | 4.76±0.48E-2                          | 4.23±0.42E-2                                       | 1.31±0.18E-2                      | 8.57±1.18E-3                      | 7.39±0.97E-3                      | 8.07±1.02E-3                      | 1.66±0.18E-2                     | 3.56±0.44E-1                     | 5.54±0.80E-1                      |
| NGC5238                 | 4.44±0.44E-2                          | 5.07±0.51E-2                          | 3.47±0.35E-2                                       | 1.23±0.17E-2                      | 8.72±1.20E-3                      | 8.29±1.08E-3                      | 5.30±0.67E-3                      | 1.63±0.18E-2                     | 4.01±0.50E-1                     | 7.38±1.10E-1                      |
| [KK98]208               | <2.20E-1                              | <3.19E-1                              | <3.91E-1   | <3.10E-4                          | <4.60E-4                          | <1.70E-3                          | <1.86E-3                          | ...                              | ...                              | ...                               |
| NGC5236 <sup>f</sup>    | 1.13±0.11E 1                          | 1.26±0.13E 1                          | 1.04±0.10E 1                                       | 6.23±0.84E 0                      | 4.11±0.56E 0                      | 9.49±1.18E 0                      | 2.41±0.30E 1                      | 3.96±0.43E 1                     | 3.50±0.43E 2                     | 7.93±1.20E-1                      |
| ESO444-G084             | <1.54E-2                              | <2.21E-2                              | <2.69E-2   | 2.79±0.38E-3                      | 1.76±0.24E-3                      | 1.59±0.22E-3                      | 6.30±0.90E-4                      | ...                              | ...                              | ...                               |
| UGC08638                | 1.32±0.13E-2                          | 2.29±0.23E-2                          | 1.52±0.15E-2                                       | 7.48±1.01E-3                      | 5.01±0.69E-3                      | 2.77±0.37E-3                      | 2.24±0.29E-3                      | 9.00±0.99E-3                     | 1.41±0.18E-1                     | 2.30±0.30E-1                      |
| UGC08651                | 2.09±0.21E-2                          | 1.59±0.16E-2                          | 1.59±0.16E-2                                       | 5.93±0.80E-3                      | 3.91±0.54E-3                      | 1.79±0.24E-3                      | 1.35±0.18E-3                      | 3.41±0.40E-3                     | 7.38±1.13E-2                     | 1.30±0.20E-1                      |
| NGC5253 <sup>e</sup>    | 4.40±0.44E-1                          | 4.44±0.44E-1                          | 3.54±0.35E-1                                       | 2.42±0.33E-1                      | 2.62±0.36E-1                      | 5.38±0.69E-1                      | 8.07±1.01E-1                      | ...                              | ...                              | ...                               |
| NGC5264                 | 1.50±0.15E-1                          | 1.15±0.12E-1                          | 1.08±0.11E-1                                       | 5.31±0.72E-2                      | 3.68±0.50E-2                      | 3.60±0.46E-2                      | 4.22±0.53E-2                      | ...                              | ...                              | ...                               |
| UGC08760                | 1.48±0.15E-2                          | 1.29±0.13E-2                          | 1.59±0.16E-2                                       | 6.10±0.83E-3                      | 4.36±0.60E-3                      | 2.08±0.28E-3                      | 1.35±0.18E-3                      | 1.19±0.14E-3                     | <5.58E-2                         | <2.10E-1                          |
| kkh086                  | <2.53E-2                              | <3.56E-2                              | <4.41E-2   | 1.29±0.18E-3                      | 7.20±1.00E-4                      | <7.60E-4                          | <8.30E-4                          | <2.76E-3                         | <3.72E-2                         | <1.40E-1                          |
| UGC08837                | 3.44±0.34E-2                          | 2.27±0.23E-2                          | 2.65±0.26E-2                                       | 1.56±0.21E-2                      | 1.00±0.14E-2                      | 7.17±0.94E-3                      | 1.06±0.13E-2                      | 1.90±0.21E-2                     | 2.86±0.36E-1                     | 7.69±1.20E-1                      |
| UGC08833                | 1.20±0.12E-2                          | 6.30±0.63E-3                          | 3.43±0.34E-3                                       | 2.45±0.33E-3                      | 2.05±0.28E-3                      | <1.73E-3                          | <1.89E-3                          | <3.14E-3                         | <4.24E-2                         | <1.60E-1                          |
| NGC5457 <sup>e f</sup>  | 4.38±0.44E 0                          | 5.04±0.50E 0                          | 4.41±0.44E 0                                       | 2.52±0.34E 0                      | 1.74±0.24E 0                      | 3.40±0.42E 0                      | 7.48±0.93E 0                      | 1.03±0.11E 1                     | 1.14±0.14E 2                     | 3.96±0.63E-1                      |
| NGC5474 <sup>e f</sup>  | 1.43±0.14E-1                          | 1.59±0.16E-1                          | 1.14±0.11E-1                                       | 1.04±0.14E-1                      | 7.34±1.02E-2                      | 7.59±1.01E-2                      | 1.17±0.15E-1                      | 1.84±0.08E-1                     | 3.72±0.27E 0                     | 9.87±1.20E-1                      |
| NGC5477 <sup>f</sup>    | 2.39±0.24E-2                          | 2.47±0.25E-2                          | 2.20±0.22E-2                                       | 7.41±1.01E-3                      | 5.16±0.71E-3                      | 4.19±0.56E-3                      | 2.60±0.34E-3                      | 1.72±0.19E-2                     | 4.25±0.52E-1                     | 4.38±0.70E-1                      |

Table 2—Continued

| Galaxy                 | 2MASS J<br>1.25 $\mu\text{m}$<br>(Jy) | 2MASS H<br>1.65 $\mu\text{m}$<br>(Jy) | 2MASS K <sub>s</sub><br>2.17 $\mu\text{m}$<br>(Jy) | IRAC<br>3.6 $\mu\text{m}$<br>(Jy) | IRAC<br>4.5 $\mu\text{m}$<br>(Jy) | IRAC<br>5.8 $\mu\text{m}$<br>(Jy) | IRAC<br>8.0 $\mu\text{m}$<br>(Jy) | MIPS<br>24 $\mu\text{m}$<br>(Jy) | MIPS<br>70 $\mu\text{m}$<br>(Jy) | MIPS<br>160 $\mu\text{m}$<br>(Jy) |
|------------------------|---------------------------------------|---------------------------------------|--|-----------------------------------|-----------------------------------|-----------------------------------|-----------------------------------|----------------------------------|----------------------------------|-----------------------------------|
| [KK98]230              | <7.67E-3                              | <1.08E-2                              | <1.35E-2   | 4.60±0.60E-4                      | 3.30±0.50E-4                      | <8.60E-4                          | <9.40E-4                          | <3.44E-3                         | <4.64E-2                         | <1.75E-1                          |
| UGC09128 <sup>e</sup>  | 1.30±0.13E-2                          | 9.19±0.92E-3                          | 9.25±0.93E-3                                       | 3.10±0.42E-3                      | 2.39±0.33E-3                      | <1.54E-3                          | <1.68E-3                          | <2.80E-3                         | <3.78E-2                         | <1.43E-1                          |
| NGC5585 <sup>e</sup>   | 1.45±0.14E-1                          | 1.57±0.16E-1                          | 1.12±0.11E-1                                       | 8.69±1.18E-2                      | 5.87±0.81E-2                      | 6.56±0.84E-2                      | 8.89±1.11E-2                      | 1.38±0.15E-1                     | 3.00±0.37E 0                     | 7.46±1.17E-1                      |
| UGC09240               | 4.80±0.48E-2                          | 4.17±0.42E-2                          | 3.32±0.33E-2                                       | 1.55±0.21E-2                      | 1.07±0.15E-2                      | 7.95±1.04E-3                      | 7.80±0.98E-3                      | 2.32±0.25E-2                     | 3.60±0.45E-1                     | 4.96±0.79E-1                      |
| UGC09405               | 1.51±0.15E-2                          | 2.01±0.20E-2                          | 1.29±0.13E-2                                       | 6.67±0.90E-3                      | 3.98±0.55E-3                      | 2.73±0.37E-3                      | 3.74±0.48E-3                      | 4.57±0.54E-3                     | 5.66±0.97E-2                     | 1.65±0.30E-1                      |
| MRK475                 | 2.26±0.23E-3                          | 2.00±0.20E-3                          | 1.42±0.14E-3                                       | 9.80±1.30E-4                      | 8.00±1.10E-4                      | 5.40±0.90E-4                      | 8.20±1.10E-4                      | 9.27±1.00E-3                     | 1.14±0.14E-1                     | 4.15±0.89E-1                      |
| NGC5832                | 1.07±0.11E-1                          | 1.09±0.11E-1                          | 9.68±0.97E-2                                       | 4.50±0.61E-2                      | 2.92±0.40E-2                      | 2.98±0.38E-2                      | 4.59±0.57E-2                      | 4.39±0.47E-2                     | 8.13±1.00E-1                     | 2.68±0.42E-1                      |
| NGC5949                | 1.39±0.14E-1                          | 1.47±0.15E-1                          | 1.21±0.12E-1                                       | 7.01±0.95E-2                      | 4.48±0.62E-2                      | 7.55±0.98E-2                      | 1.50±0.19E-1                      | 1.44±0.16E-1                     | 2.18±0.27E 0                     | 6.11±0.95E-1                      |
| UGC09992               | 1.14±0.11E-2                          | 9.90±0.99E-3                          | 9.72±0.97E-3                                       | 4.80±0.65E-3                      | 3.24±0.45E-3                      | 1.51±0.21E-3                      | 3.79±0.48E-3                      | 6.79±0.75E-3                     | 1.16±0.15E-1                     | 1.37±0.24E-1                      |
| KKR25 <sup>e f</sup>   | <1.89E-2                              | <2.68E-2                              | <3.34E-2   | <2.40E-4                          | <3.60E-4                          | <1.32E-3                          | <1.44E-3                          | <2.40E-3                         | <3.24E-2                         | <1.22E-1                          |
| NGC6503 <sup>e</sup>   | 9.49±0.95E-1                          | 1.05±0.10E 0                          | 8.60±0.86E-1                                       | 4.34±0.59E-1                      | 2.91±0.40E-1                      | 5.01±0.64E-1                      | 9.28±1.16E-1                      | 8.65±0.93E-1                     | 1.44±0.18E 1                     | 3.58±0.56E-1                      |
| IC4951                 | 3.47±0.35E-2                          | 3.60±0.36E-2                          | 3.44±0.34E-2                                       | 1.02±0.14E-2                      | 7.20±0.99E-3                      | 5.75±0.76E-3                      | 3.53±0.45E-3                      | ...                              | ...                              | ...                               |
| DDO210 <sup>f</sup>    | <2.59E-2                              | <3.75E-2                              | <4.59E-2   | 2.80±0.38E-3                      | 1.69±0.23E-3                      | <1.55E-3                          | <1.69E-3                          | <2.82E-3                         | <3.79E-2                         | <1.43E-1                          |
| IC5052 <sup>e</sup>    | 2.38±0.24E-1                          | 2.47±0.25E-1                          | 2.01±0.20E-1                                       | 1.24±0.17E-1                      | 8.65±1.19E-2                      | 9.01±1.16E-2                      | 1.39±0.17E-1                      | 3.82±0.41E-1                     | 4.56±0.56E 0                     | 8.52±1.33E-1                      |
| NGC7064                | 6.58±0.66E-2                          | 4.87±0.49E-2                          | 4.41±0.44E-2                                       | 2.37±0.32E-2                      | 1.54±0.21E-2                      | 1.12±0.15E-2                      | 1.19±0.15E-2                      | 3.24±0.35E-2                     | 1.01±0.12E 0                     | 1.98±0.21E-1                      |
| NGC7090 <sup>e</sup>   | 4.34±0.43E-1                          | 4.83±0.48E-1                          | 3.92±0.39E-1                                       | 2.18±0.30E-1                      | 1.45±0.20E-1                      | 2.49±0.32E-1                      | 4.87±0.61E-1                      | 6.53±0.70E-1                     | 1.03±0.13E 1                     | 2.84±0.44E-1                      |
| IC5152 <sup>d e</sup>  | 4.60±0.46E-1                          | 3.37±0.34E-1                          | 3.06±0.31E-1                                       | ...                               | 1.66±0.23E-1                      | ...                               | 2.27±0.28E-1                      | 2.09±0.23E-1                     | 4.86±0.59E 0                     | 1.13±0.18E-1                      |
| IC5256                 | 2.85±0.28E-2                          | 2.58±0.26E-2                          | 2.10±0.21E-2                                       | 8.08±1.10E-3                      | 5.37±0.74E-3                      | 8.82±1.17E-3                      | 1.75±0.22E-2                      | 1.88±0.20E-2                     | 2.79±0.34E-1                     | 6.06±0.95E-1                      |
| UGCA438                | 2.18±0.22E-2                          | 2.27±0.23E-2                          | 1.68±0.17E-2                                       | 9.02±1.22E-3                      | 6.34±0.87E-3                      | 3.85±0.51E-3                      | 4.23±0.53E-3                      | <4.66E-3                         | <6.29E-2                         | <2.38E-1                          |
| ESO347-G017            | 1.86±0.19E-2                          | 2.00±0.20E-2                          | 1.59±0.16E-2                                       | 8.80±1.19E-3                      | 5.68±0.78E-3                      | 3.21±0.43E-3                      | 2.94±0.38E-3                      | 8.51±0.95E-3                     | 2.77±0.35E-1                     | 2.91±0.48E-1                      |
| UGC12613 <sup>f</sup>  | 1.22±0.12E-1                          | 9.81±0.98E-2                          | 1.14±0.11E-1                                       | 5.55±0.75E-2                      | 3.31±0.46E-2                      | 1.84±0.24E-2                      | 2.63±0.33E-2                      | 2.57±0.28E-2                     | 3.48±0.45E-1                     | 1.21±0.19E-1                      |
| IC5332                 | 4.14±0.41E-1                          | 5.73±0.57E-1                          | 3.86±0.39E-1                                       | 2.38±0.32E-1                      | 1.64±0.23E-1                      | 1.85±0.23E-1                      | 2.93±0.37E-1                      | 3.34±0.36E-1                     | 4.61±0.56E 0                     | 1.98±0.31E-1                      |
| NGC7713                | 1.79±0.18E-1                          | 2.24±0.22E-1                          | 1.51±0.15E-1                                       | 1.00±0.14E-1                      | 6.85±0.94E-2                      | 8.53±1.09E-2                      | 1.40±0.17E-1                      | 2.84±0.31E-1                     | 5.69±0.69E 0                     | 1.09±0.17E-1                      |
| UGCA442                | 2.32±0.23E-2                          | 2.37±0.24E-2                          | 1.34±0.13E-2                                       | 1.12±0.15E-2                      | 7.51±1.03E-3                      | 3.81±0.51E-3                      | 2.63±0.34E-3                      | 1.01±0.11E-2                     | 1.20±0.16E-1                     | 2.63±0.44E-1                      |
| kkh098                 | 1.02±0.10E-2                          | 1.07±0.11E-2                          | 7.56±0.76E-3                                       | 2.42±0.33E-3                      | 1.56±0.22E-3                      | <1.46E-3                          | <1.60E-3                          | <2.65E-3                         | <3.56E-2                         | <1.34E-1                          |
| ESO149-G003            | 1.03±0.10E-2                          | 1.27±0.13E-2                          | <1.01E-1   | 3.55±0.48E-3                      | 2.59±0.36E-3                      | 6.90±1.00E-4                      | 8.40±1.10E-4                      | 8.90±1.60E-4                     | 5.59±0.82E-2                     | <2.14E-1                          |
| NGC7793 <sup>e f</sup> | 1.68±0.17E 0                          | 1.70±0.17E 0                          | 1.31±0.13E 0                                       | 7.71±1.04E-1                      | 4.69±0.64E-1                      | 1.02±0.13E 0                      | 1.85±0.23E 0                      | 2.03±0.08E 0                     | 3.33±0.24E 1                     | 1.17±0.15E-1                      |

Note. — See § 4 for corrections that have been applied to the data. The uncertainties include both statistical and systematic effects ( $\lesssim 10\%$  for the optical near-infrared data).

<sup>a</sup>Infrared photometry for the Large and Small Magellanic Clouds will be provided by the SAGE (P.I. M. Meixner) and SAGE-SMC (P.I. K. Gordon) projects.

<sup>b</sup>NGC 1800 and MCG-05-13-004 spatially overlap so separate photometry for MCG-05-13-004 is not provided.

<sup>c</sup>The bright core of NGC 3034 (M 82) has rendered the *Spitzer* data extremely difficult to process; saturation effects severely limit our ability to extract reliable flux densities.

<sup>d</sup>Only 4.5 and 8.0  $\mu\text{m}$  data were obtained for IC 5152.

<sup>e</sup>IRAC data taken from the archives.

<sup>f</sup>MIPS data taken from the archives.

Table 3. IRAC Aperture Correction Parameters

| $\lambda$         | A    | B     | C     |
|-------------------|------|-------|-------|
| 3.5 $\mu\text{m}$ | 0.82 | 0.370 | 0.910 |
| 4.5 $\mu\text{m}$ | 1.16 | 0.443 | 0.940 |
| 5.8 $\mu\text{m}$ | 1.49 | 0.207 | 0.710 |
| 8.0 $\mu\text{m}$ | 1.37 | 0.330 | 0.740 |

Note. — See § 4 and  
<http://ssc.spitzer.caltech.edu/irac/calib/extcal/>

Table 4. LVL Infrared Ratios and Dispersions

| Ratio  | Median | Dispersion<br>(dex) |
|--|--------|---------------------|
| $f_{\nu}(70\mu\text{m})/f_{\nu}(160\mu\text{m})$ | 0.84   | 0.22                |
| $f_{\nu}(8.0\mu\text{m})/f_{\nu}(24\mu\text{m})$ | 0.41   | 0.27                |
| $\nu f_{\nu}(8.0\mu\text{m})/TIR$                | 0.098  | 0.23                |
| $\nu f_{\nu}(8.0\mu\text{m})_{\text{dust}}/TIR$  | 0.19   | 0.44                |
| $\nu f_{\nu}(24\mu\text{m})/TIR$                 | 0.080  | 0.15                |
| $\nu f_{\nu}(70\mu\text{m})/TIR$                 | 0.60   | 0.11                |
| $\nu f_{\nu}(160\mu\text{m})/TIR$                | 0.31   | 0.12                |

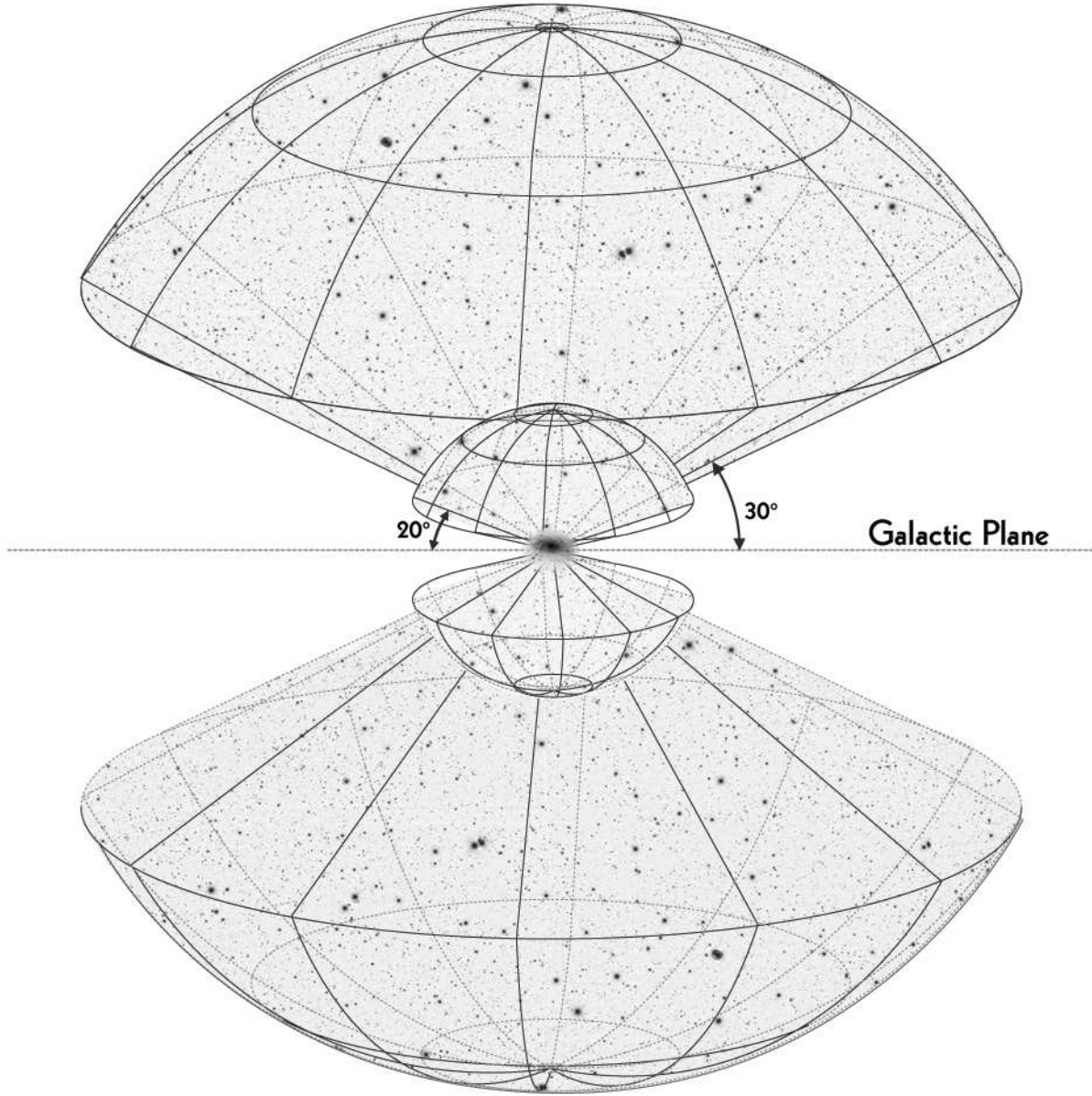


Fig. 1.— The tiered observing strategy includes *i*) all known galaxies in the inner cones, which begin beyond the Local Group and extend to 3.5 Mpc, and *ii*) magnitude-limited coverage to  $m_B = 15.5$  mag within the outer cones which extend to 11 Mpc.



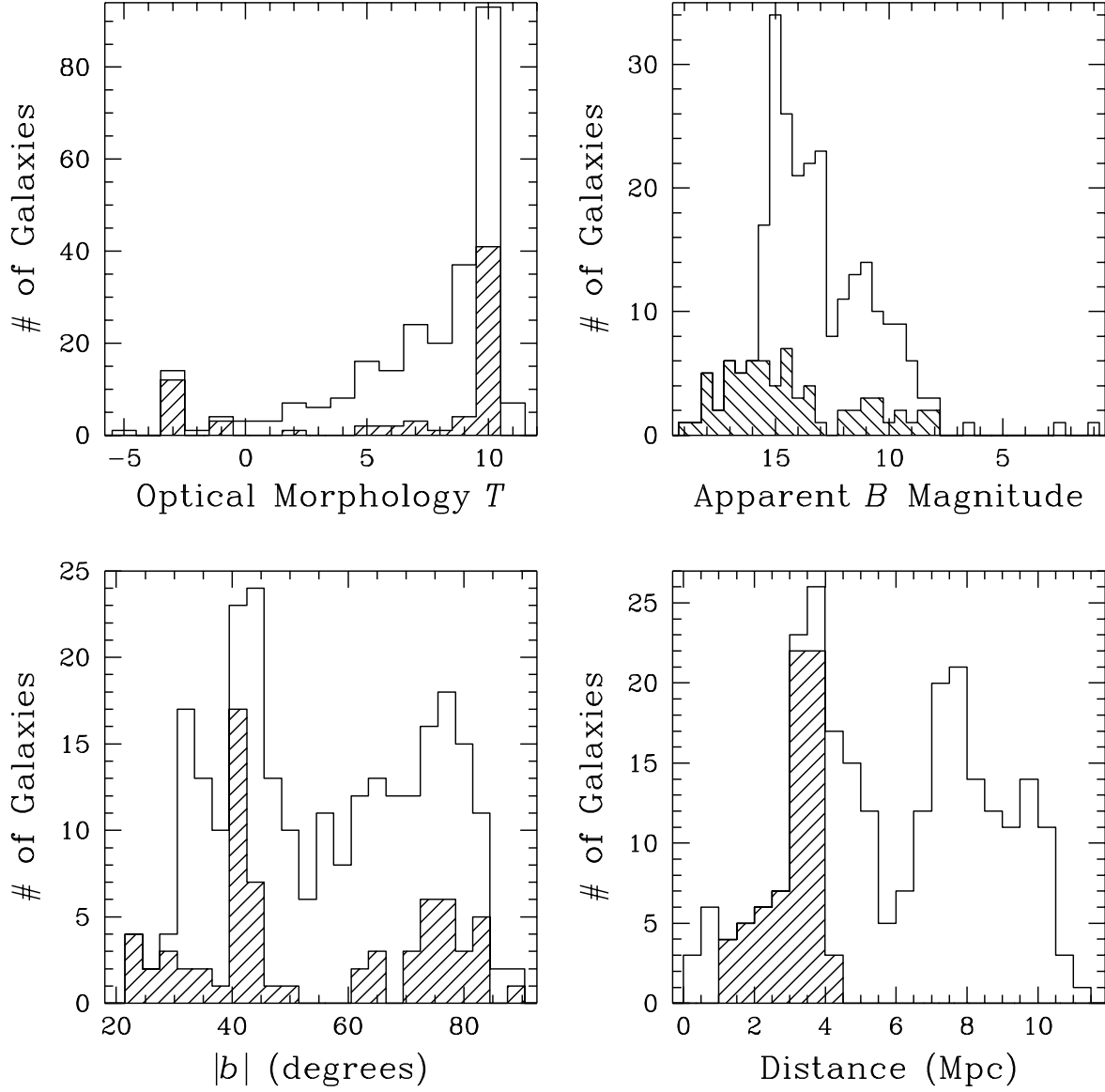


Fig. 2.— The sample of galaxies in the Local Volume Legacy survey. The shaded portions of the histograms portray the inner-tier, ANGST subsample.

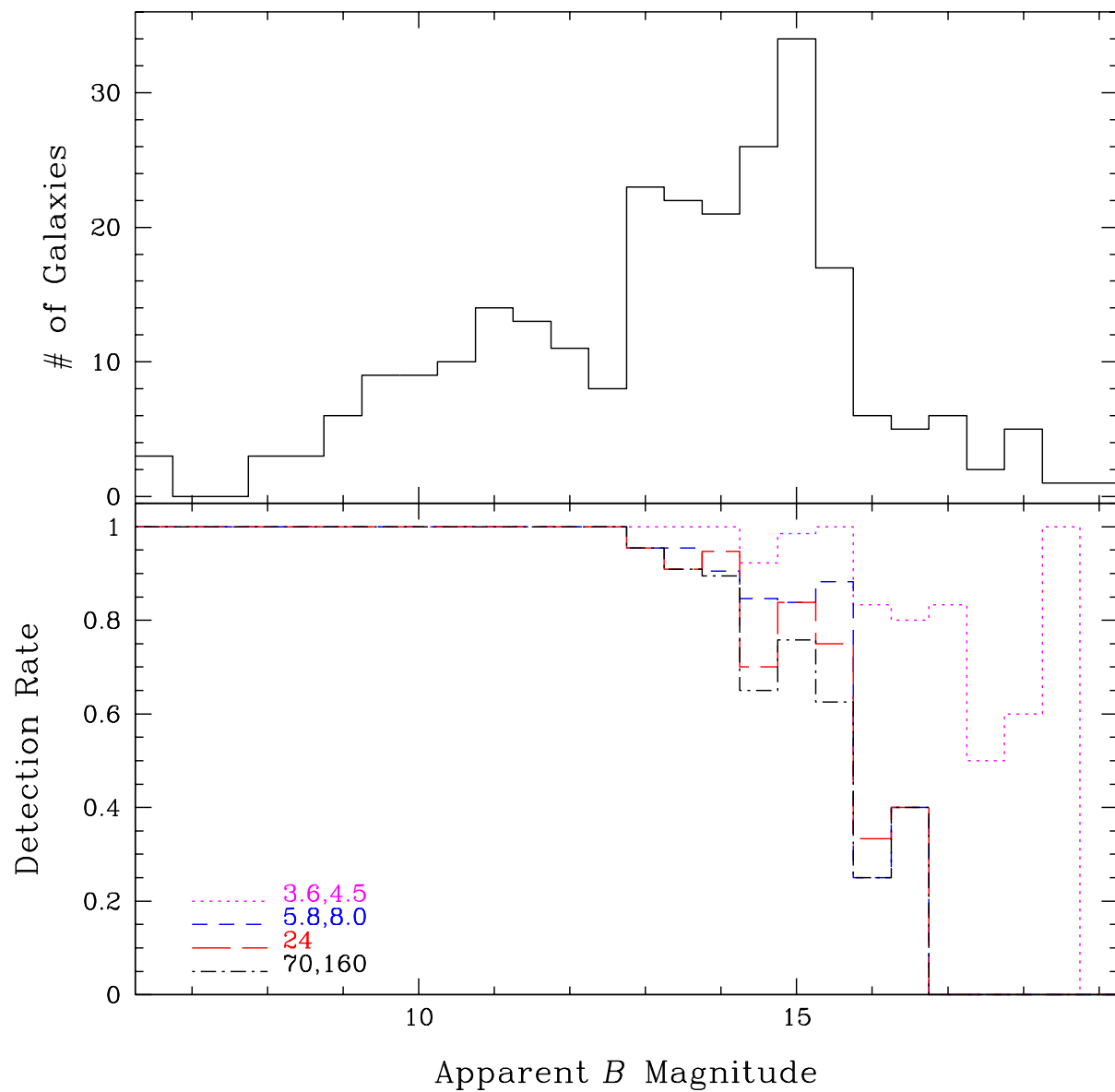


Fig. 3.— Top: The distribution of LVL galaxies as a function of apparent  $B$ -band magnitude. Bottom: The imaging detection rate for different *Spitzer* wavelengths.

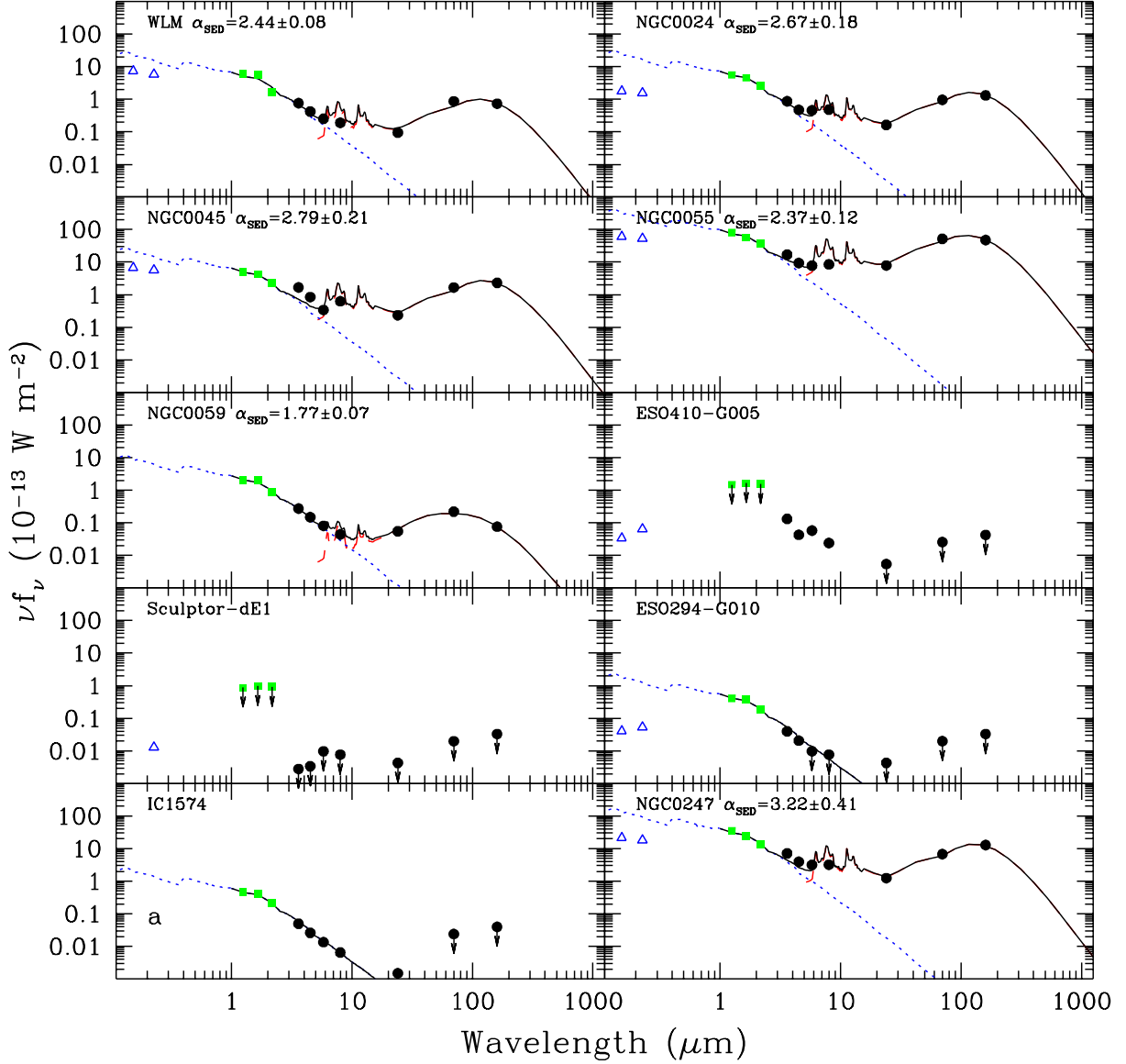


Fig. 4.— Globally-integrated 0.15-160  $\mu\text{m}$  spectral energy distributions for the LVL sample. *GALEX*, 2MASS, and *Spitzer* data are represented by open triangles, filled squares, and filled circles, respectively. Downward-pointing arrows, if present, indicate  $3\sigma$  upper limits. The solid curve is the sum of a dust (dashed) and a stellar (dotted) model. The dust curve is a Dale & Helou (2002) model fitted to the amplitude and ratios of the observed 24, 70, and 160  $\mu\text{m}$  fluxes; the  $\alpha_{\text{SED}}$  listed within each panel parametrizes the distribution of dust mass as a function of heating intensity, as described in Dale & Helou (2002). The stellar curve is a 1 Gyr continuous star formation, solar metallicity curve from Vazquez & Leitherer (2005) fitted to the 2MASS data (see § 5.2 for details).

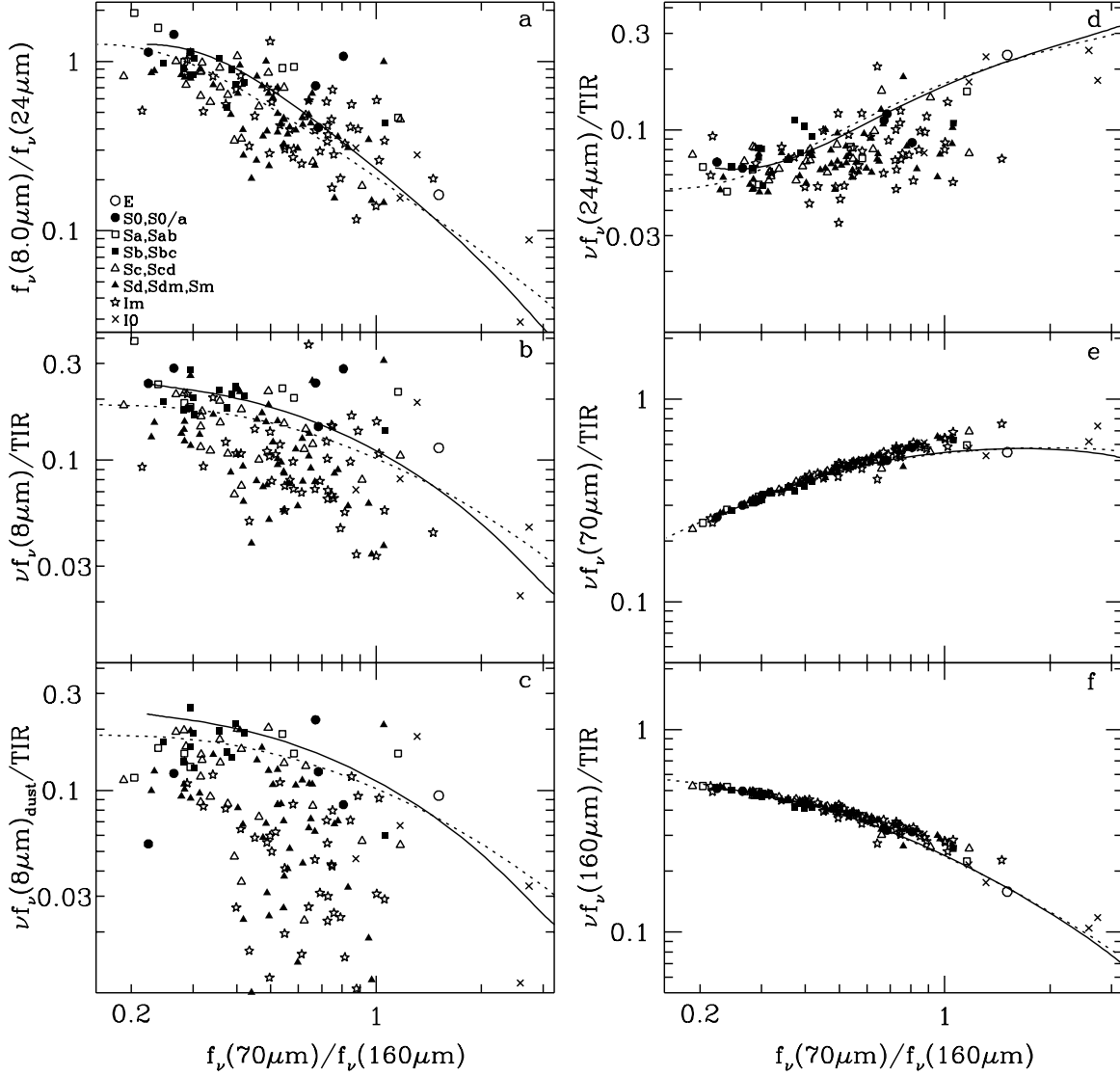


Fig. 5.— Top: The *Spitzer* infrared colors and monochromatic-to-bolometric infrared ratios for globally-integrated LVL data. The solid and dotted lines indicate the SED models of Dale & Helou (2002) and Dale et al. (2001), respectively, derived from the average global trends for a sample of normal star-forming galaxies observed by *ISO* and *IRAS*. The logarithmic ranges spanned by the  $x$ - and  $y$ -axes are the same for all panels, for ease of comparison.

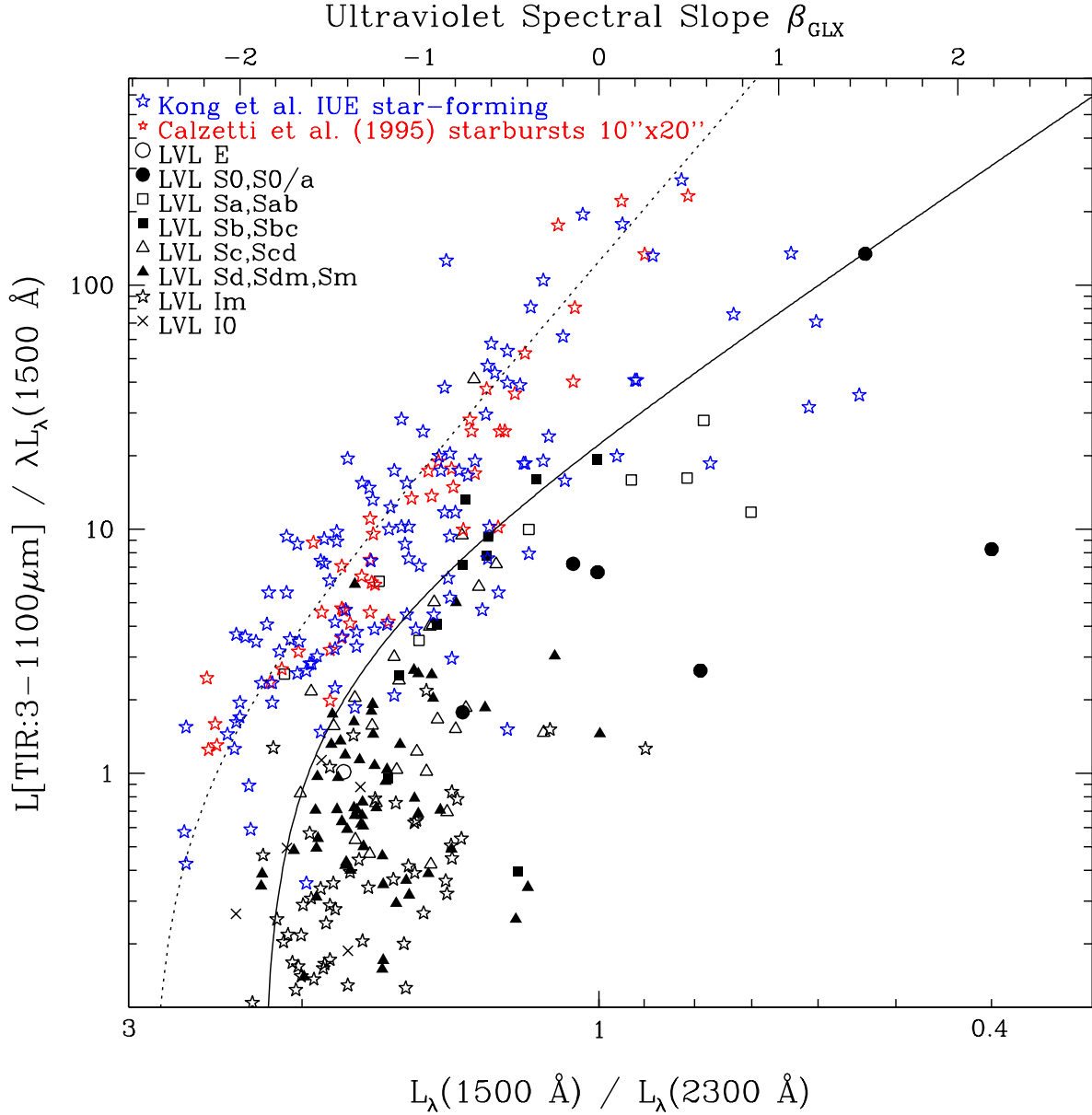


Fig. 6.— The infrared-to-far-ultraviolet ratio as a function of ultraviolet spectral slope. Normal star-forming and starbursting galaxies from Kong et al. (2004) and Calzetti et al. (1995) are plotted in addition to the LVL data points. The dotted curve is that for starbursting galaxies from Kong et al. (2004) and the solid curve is applicable to normal star-forming galaxies (Cortese et al. 2006).

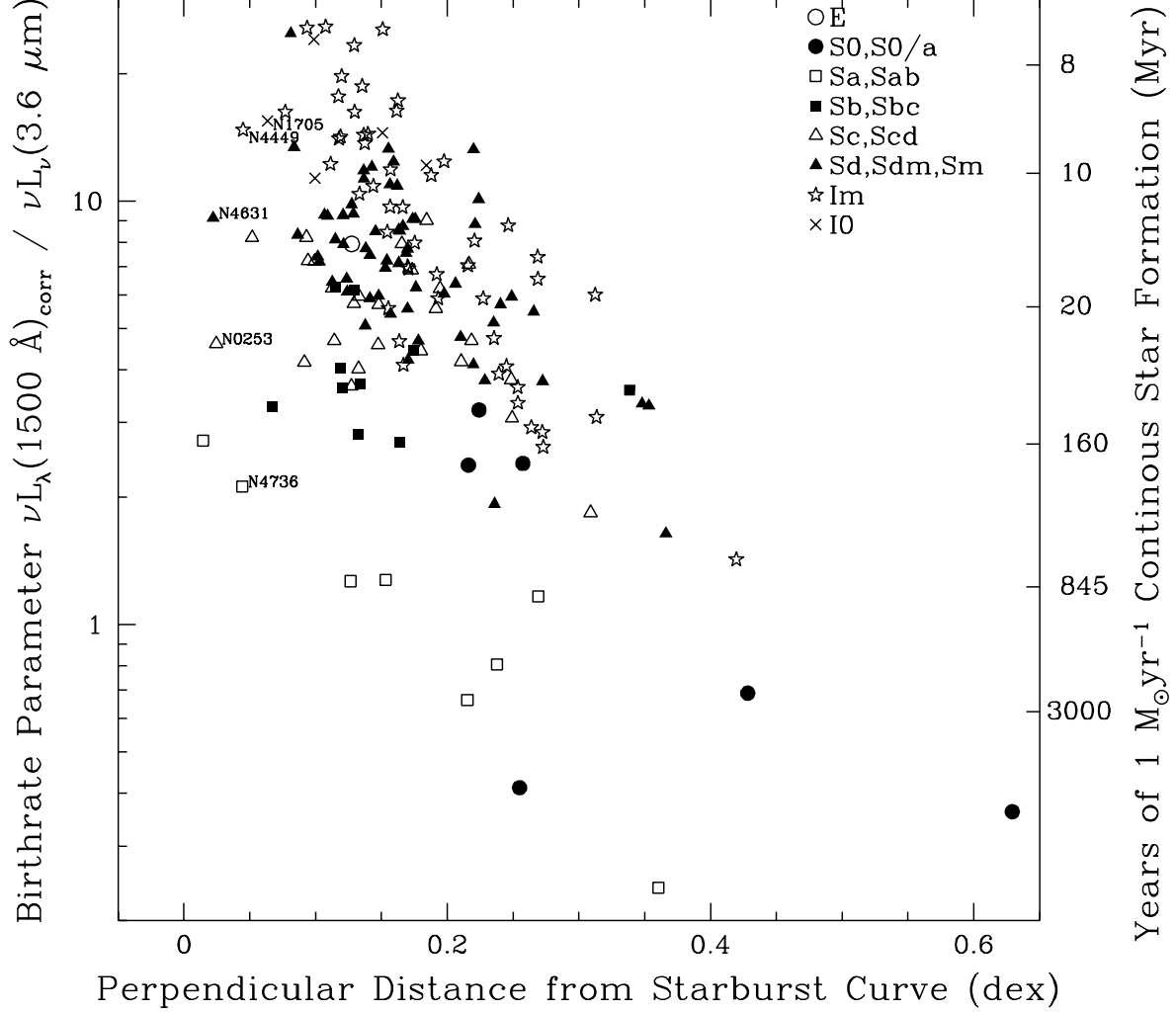


Fig. 7.— The dependence of galaxy star formation history as a function of distance from the starburst relation infrared-to-ultraviolet versus ultraviolet slope, as shown in Figure 6. The righthand axis shows the number of years (continuous) star formation has been occurring, as measured from theoretical spectra. The theoretical spectra utilized are solar metallicity,  $1 M_{\odot} \text{ yr}^{-1}$  continuous star formation curves assuming a double power law initial mass function, with  $\alpha_{1,\text{IMF}} = 1.3$  for  $0.1 < m/M_{\odot} < 0.5$  and  $\alpha_{2,\text{IMF}} = 2.3$  for  $0.5 < m/M_{\odot} < 100$  (Vazquez & Leitherer 2005).